U T O M N E S U N U M S I N T

The

SCHOOL OF MEDICINE and the DEPARTMENT OF BIOLOGY

of the

JOHANNES GUTENBERG-UNIVERSITY OF MAINZ

confer on

Alejandra Nacarino Martínez

born on *22.10.1976* in Cádiz (Spain)

in recognition of her dissertation

"Analysis of the influence of epitope flanking regions on MHC class I restricted antigen presentation"

and the successful examinations

the academic degree

„Doktor der Naturwissenschaften"

Mainz, *12.09.2007*

Dean Department of Biology

Day of the disputation: 07.12.2007

INDEX

1 Introduction

Immunology was born with the discovery of Edward Jenner (1796), when he discovered that cowpox (or vaccinia) induced protection against human smallpox. He injected the material from a pustule into the arm of an 8-year-old boy. When this boy was later intentionally inoculated with smallpox, the disease did not develop. This procedure was called vaccination (Latin: vaccinus, or from cows), which still remains to be the most effective method for preventing infections (Abul K.Abbas and Andrew H.Lichtman, 2003). Although it took almost two centuries for smallpox vaccination to become universal, the interest in this new science increased and with the help of the discoveries of further great scientists we have gained a remarkable knowledge in the understanding of the immune system and its functions.

1.1 The immune system

The immune system has evolved to protect against the continuous attack of viruses, bacteria, fungi and parasites. It is able to recognize and eliminate the pathogens. This defense against microbes is mediated by the early reactions of innate immunity and the later responses of adaptive (or specific) immunity (Abul K.Abbas and Andrew H.Lichtman, 2003).

1.2 The innate immune response

Innate immunity provides the early lines of defense against microbes. The principal components are physical and chemical barriers (e.g.: skin and antimicrobial substances produced at epithelial surfaces), phagocytic cells (neutrophils, macrophages), natural killer cells and proteins, like members of the complement system and cytokines that regulate and coordinate many activities of the cells of the innate immune response. Molecules produced during innate immune responses stimulate adaptive immunity and influence the nature of adaptive immune responses. For example, macrophages activated by microbes and interferon-gamma (IFN-γ) produce costimulators that enhance T cell activation.

The innate immune system uses pattern recognition receptors to recognize structures that are shared by microbes, but are not present on mammalian cells, and are often essential for survival of the microbes, thus limiting the capacity of microbes to evade detection.

1.3 The adaptive immune response

In contrast, adaptive immunity develops as a response to infection and adapts to the infection. It has the ability to "remember" and respond more vigorously to repeated exposures to the same pathogen. In addition, the adaptive immune system is able to recognize and react to a large number of microbial substances and has the capacity to distinguish among different, even closely related, microbes and molecules. For this reason it is also called specific immunity. The characteristics of adaptive immunity are specificity for different antigens, a diverse repertoire capable of recognizing a wide variety of antigens, memory for antigen exposure, specialized responses to different microbes, self-limitation and the ability to discriminate between foreign antigens and self antigens. An adaptive immune response is initiated by the recognition of foreign antigens by specific lymphocytes. Those respond by proliferating and by differentiating into effector cells, whose function is to eliminate the antigen, and into memory cells, which show enhanced responses on subsequent encounters with the antigen. The activation of lymphocytes requires antigen and additional signals that may be provided by microbes or by innate immune responses to microbes, the so called two-signal hypothesis. There are two types of adaptive immune responses, called humoral immunity and cell-mediated immunity, which are mediated by different components of the immune system and function to eliminate different types of microbes (Abul K.Abbas and Andrew H.Lichtman, 2003).

.

1.3.1 Humoral immunity

Humoral immunity is mediated by antibodies, which are produced by B lymphocyte derived plasma cells. Antibodies recognize microbial antigens, neutralize the infectivity of the microbes and target them for elimination by various effector mechanisms. There are different types of antibodies, which can activate different mechanisms. Some promote phagocytosis and others trigger the release of inflammatory mediators from leukocytes such as mast cells (Janeway et al., 2001).

1.3.2 Cell-mediated immunity

Cell-mediated immunity is mediated by T lymphocytes. Intracellular microbes, such as viruses and some bacteria, survive and proliferate inside phagocytes and other host cells, where they are inaccessible to circulating antibodies. Defense against such infections is a

function of cell-mediated immunity, which promotes the destruction of microbes residing in phagocytes or the killing of infected cells to eliminate reservoirs of infection. The detection of an infected cell is performed by T lymphocytes, which recognizes antigens on the cell surface of those cells (Janeway et al., 2001). The task of displaying cell-associated antigenic peptides for recognition by T cells is performed by specialized proteins that are encoded by genes in a locus called the major histocompatibility complex (MHC).

1.4 The MHC complex

The MHC was discovered as an extended locus containing highly polymorphic genes that determined the outcome of tissue transplants exchanged between individuals. These molecules are specialized peptide receptors and serve to display antigenic peptides on the cell surface for recognition by T lymphocytes. Usually, cells carry about 105 MHC molecules on their surface. There are a large number of genetic variants (alleles) at each genetic locus. Many of these alleles are represented at significant frequency (>1%) in the population, and in addition the alleles generally differ from one another by many (up to 30) amino acid substitutions. For example, in humans there are more than 200 alleles described at some MHC loci. Such a remarkable degree of polymorphism implies a selective pressure to establish and maintain it. One of the most important properties of every normal immune system is its ability to recognize, respond to, and eliminate non-self antigens while not reacting harmfully to self antigenic substances. This self-tolerance is maintained by several mechanisms that take place in the thymus, which is the organ where T lymphocytes mature. By encountering self antigens, these T lymphocytes are tested for being able to recognize and interact weakly to those (positive selection). Afterwards those lymphocytes interacting too strong and therefore inducing the self-reactive pathway are eliminated (negative selection) to protect cells presenting self-antigens (Abul K.Abbas and Andrew H.Lichtman, 2003). All these features of self, non-self and altered self can be distinguished with the help of molecules encoded by the MHC molecule. So to say, they serve as a passport for host cells.

The MHC genetic region (in humans on chromosome 6 and mice on chromosome 17) codes for class I and class II molecules as well as for other proteins, like the complement proteins, cytokines, the proteasome subunits LMP2 and LMP7, and several proteins involved in antigen processing. MHC class I molecules are expressed on all nucleated cells, whereas class II molecules are expressed mainly on specialized antigen-presenting cells, such as dendritic

cells, macrophages, and B lymphocytes, and a few other cell types, including endothelial cells and thymic epithelial cells. The expression of MHC gene products is enhanced by inflammatory and immune stimuli, particularly cytokines like IFN-γ, which stimulate the transcription of MHC genes.

1.4.1 Structure of MHC molecules

Both classes of MHC molecules are structurally similar and consist of an extracellular peptide-binding cleft, a non-polymorphic Ig-like region, a transmembran domain and a cytoplasmic region (Janeway et al., 2001). Class I molecules are composed of an α-chain (or heavy) in a covalent complex with a non-polymorphic polypeptide, ß2-microglobulin. The class II molecules contain two MHC-encoded polymorphic chains, an α- and a ß-chain. The peptide-binding cleft of MHC molecules has α-helical sides and an eight-stranded antiparallel ß-pleated sheet floor. The cleft of MHC class I molecules is formed by α1 and α2 segments of the α-chain and that of MHC class II molecules by the α1 and ß1 segments of the two chains. However, whereas the groove is open at both sides for MHC II molecules, it is closed for MHC I molecules (Bjorkman et al., 1987; Brown et al., 1993). As a result, MHC I can only accommodate peptides of 8-10 aa in length (Falk et al., 1991; Madden, 1995), whereas MHC II can bind peptides of up to 15-20 aa. In both cases, however, the ligand interacts with the surface of the binding groove only over a stretch of about 9 aa. Non-covalent (hydrophobic) interactions, electrostatic forces and hydrogen bonds fix the peptide to the MHC molecule. This is achieved by means of particular aa of the peptide, the so-called anchor-residues. The Ig-like domains of class I and II contain the binding sites for the co-receptors CD8 and CD4, respectively. Peptide antigens associated with class I molecules are recognized by CD8+ T lymphocytes, whereas class II-associated peptide antigens are recognized by CD4+ T lymphocytes.

1.4.2 Peptide binding on MHC molecules

MHC molecules show a broad specificity for peptide binding, and the fine specificity of antigen recognition resides largely in the antigen receptors of T lymphocytes. These molecules bind only one peptide at a time, and all the peptides that bind to a particular MHC molecule share common structural motifs. Peptide binding is of low affinity (Kd ~10-6 M), and the off-rate is very slow, so that complexes, once formed, persist for a sufficiently long time to be recognized by T cells. The polymorphic residues of MHC molecules are localized

in the peptide-binding cleft. Some of these polymorphic residues determine the binding specificities for peptides by forming structures, called pockets, which interact with complementary residues of the bound peptide, called anchor residues. Other polymorphic MHC residues and some residues of the peptide are not involved in binding to MHC molecules but instead form the structure recognized by T cells. Most MHC class I binding motifs require hydrophobic (aromatic and branched chain) aa in P9, i.e. at the C-terminus of the peptide. Peptides that bind to MHC II molecules have a conserved motif of 7 – 10 aa length with usually predominantly hydrophobic and aromatic amino acids. Thus, the binding motifs represent a strict selection criterion for peptide sequences to be presented by MHC molecules. There are three class I loci in humans, called HLA-A, B and C and in mice H-2K, H-2D, and H-2L. The class II loci are in humans, HLA-DR, -DQ and –DP and in mice H-2A and -2E. All MHC locus products are co-dominantly expressed, so that an individual may express up to six different MHC class I molecules.

1.5 MHC class I antigen processing pathway

1.5.1 The source of MHC class I peptides

The peptides that are presented bound to class I MHC molecules are derived from cytosolic proteins (Pamer and Cresswell, 1998; Princiotta et al., 2003; Yewdell, 2005). Most of these intracellular proteins are normal self proteins, which may be wrongly folded or no more needed. Foreign antigens in the cytosol may be the products of viruses or other intracellular microbes that infect such cells and synthesize their own proteins during their life cycle. In tumor cells, mutated self genes or oncogenes often produce peptide antigens that are recognized by class I-restricted CTLs. A further source for peptides presented by MHC class I molecules may also be derived from phagocytosed microbes. These are enclosed into endosomes and usually presented by MHC class II molecules. But through a process called cross presentation, those peptides are able to bind to the MHC class I molecules and thus be presented to CTLs for recognition. Recent work revealed that a large pool of nascent proteins was ubiquitinated and it was suggested, that it is composed mostly of defective ribosomal products (DRiPs) (Schubert et al., 2000; Turner and Varshavsky, 2000). This nascent protein pool appears to represent a further important source from which MHC class I epitopes are derived (Princiotta et al., 2003; Yewdell and Princiotta, 2004).

1.5.2 The ubiquitin-proteasome pathway

The degradation of most cellular proteins occurs by the ubiquitin-proteasome pathway (Goldberg et al., 2002; Goldberg, 2003; Rock et al., 2002). The first step in this pathway is the conjugation of the polypeptide cofactor ubiquitin to the ε amino group of lysines found in the protein substrate, and subsequently other ubiquitin molecules are linked to the first ubiquitin molecule. A chain of four or more ubiquitin molecules serves as a molecular "tag" that marks the protein for rapid degradation by the proteasome. The 26S proteasome is the macromolecular machine of the ubiquitin proteasome-dependent degradation pathway that is responsible for most of the nonlysosomal protein degradation in both the nucleus and cytosol (Wang et al., 2006). It is composed of a core cylinder, the 20S proteasome, which in cells it can be capped at both or just one end by the 19S complex (regulatory particle). The 19S complex performs various functions, including recognition and binding of polyubiquitin chains (Deveraux et al., 1994), release of free ubiquitin (Lam et al., 1997) and ATPase function (Rubin et al., 1998) as well as protein unfoldase function. Once in the 20S core, six peptidases sites act together to cleave the protein into many diverse oligopeptides (see below: 1.6 The proteasome).

1.5.3 Peptide trimming by cytosolic aminopeptidases

Proteasomal processing creates very large numbers of different peptides, depending on the length and sequence of the protein. *In vivo* experiments performed by York and Reits (Reits et al., 2004; York et al., 2002) make it clear that a substantial fraction of epitopes are generated as longer precursors, which usually would not fit into the MHC class I peptide binding groove. As proteasomes generate peptides in a length of 3–22 residues (Kisselev et al., 1999) are too long to bind stably to MHC class I molecules, an important question was whether cells can trim and present these extended peptides. To investigate this, in the labs of A. L. Goldberg and H. Schild the following experiments were performed: antigenic peptides with extra C- or N-terminal residues were injected into cells or were expressed from 'minigenes' in cells, and presentation of the mature epitope on MHC class I molecules was measured. Both C- and N-extended versions could be efficiently trimmed to the correct epitope and presented on MHC class I molecules. However, the addition of proteasome inhibitors completely blocked the presentation of peptides from constructs with even a single extra C-terminal residue, but did not affect the presentation of those constructs with the correct size or longer N-terminal extensions (Craiu et al., 1997b; Mo et al., 1999; Stoltze et al., 1998). These results

suggested that proteasomes are the only proteases in cells, which can generate the proper C terminus of these peptides from longer precursors. These results also indicate that the cytosol lacks carboxypeptidases, which remove extra residues from the C terminus of peptides, and indeed C-terminal trimming activity has yet not been detected in cell extracts (Beninga et al., 1998).

Now those N-terminal extended antigens can undergo further trimming by cytosolic aminopeptidases before entering into the endoplasmic reticulum (ER). Those aminopeptidases include the leucine aminopeptidase (Beninga et al., 1998), puromycin-sensitive aminopeptidase (Stoltze et al., 2000), bleomycin hydrolase (Stoltze et al., 2000), thimet oligopeptidase (Saric et al., 2001; York et al., 2003), and tripeptidyl aminopeptidase II, (Geier et al., 1999). Additionally, the insuline degrading enzyme (IDE) has been reported to play an important role in the regulation of essential biological functions (growth factor levels, insulin metabolism) by processing specific target proteins. This suggests a potential role in antigen presentation for IDE, despite this has not been well-investigated.

1.5.3.1 Leucine aminopeptidase (LAP)

In efforts to identify trimming aminopeptidases, leucine aminopeptidase (LAP) was first identified by Beninga and colleges (Beninga et al., 1998). It is stimulated by IFNγ and *in vitro* LAP generated the final antigen epitope SIINFEKL from the QLESIINFEKL precursor. So, taken together, it was concluded that LAP can contribute to the trimming process of antigenic peptide in the cytosol.

1.5.3.2 Puromycin sensitive aminopeptidase & bleomycin hydrolase

In an attempt to purify the enzyme responsible for the generation of the final epitope RGYVYQGL, from the precursor VSV-NP with N-terminal flanking 5 amino acids, SLSDLRGYVYQGL, Stolze and colleges identified the puromycin sensitive aminopeptidase (PSA) and bleomycin hydrolase (BH) from a cytosol fraction of a human EBV-transformed B cell line (Stoltze et al., 2000). PSA is a member of aminopeptidases belonging to the M1 family of metallopeptidases (Kisselev et al., 1999) and the first candidate in this group, which functions as a trimming enzyme of antigen peptides. It has been suggested that PSA is required for regulation of cell cycle, normal growth and behavior associated with anxiety and pain (Constam et al., 1995; Osada et al., 1999). However, physiological substrates are still

elusive. Another trimming peptidase, BH, is a cysteine protease and originally discovered as an enzyme that can inactivate the anticancer drug bleomycin (Sebti et al., 1989). Its expression level is associated with sensitivity to bleomycin in tumor cells. PSA and BH are widely distributed in many tissues and their gene structures are in common with housekeeping genes (Ferrando et al., 1997; Thompson et al., 1999).

1.5.3.3 Thimet oligopeptidase

THOP1 is a zinc-containing metalloendopeptidase of the M3 family with high similarity to neurolysin. This monomeric and highly conserved 78 kDa enzyme is present in all cells, but it is highly expressed in brain and testis and can be found as a secreted, cytosolic, and membrane-associated enzyme. It displays a preference for smaller peptides degrading them to a length of 6-17 residues long (Saric et al., 2004). This might be explained by the location of its catalytic site at the bottom of a deep narrow channel adapted to unstructured peptide substrates. Although THOP1 had previously been suggested to bind peptides and protect them from degradation (Portaro et al., 1999; Silva et al., 1999), Saric and colleagues (Saric et al., 2001) found that THOP1 inhibition protected peptides from degradation. THOP1 so far appears as an enzyme dedicated to peptide destruction in the cytosol. Additional studies by York and associates (York et al., 2003) demonstrated that peptide degradation by THOP1 limited antigen presentation by class I molecules. THOP1 overexpression reduced presentation of three model epitopes and total cell surface class I expression. Conversely, down-regulation of THOP1 enhanced presentation of the model epitope and increased total class I expression twofold.

1.5.3.4 Tripeptidyl peptidase II

Recently, several studies have also suggested an important role in antigen processing for tripeptidyl peptidase II (TPPII). This enzyme is a large (2–9 megadaltons) cytosolic peptidase that removes groups of three residues from the N terminus of peptide substrates (tripeptidyl exopeptidase activity) and has also been reported to have a weak endoprotease activity, preferentially cutting after arginine and lysine (Geier et al., 1999). Recent studies have suggested that TPPII may play two roles in MHC class I antigen presentation. One reported function is to make the endoproteolytic cleavages necessary to generate a presented peptide, as has been reported in the processing for HIV Nef73–82 (Seifert et al., 2003). However, it is unlikely that TPPII frequently generates the C-terminal residues, a function normally served

by proteasomes. Early studies had suggested that TPPII may even substitute for the proteasome in the degradation of cell proteins and generation of most antigenic peptides (Wang et al., 2000). However, these suggestions have not been substantiated. A second role proposed for TPPII is in trimming the N-terminal extensions from long precursor peptides (Levy et al., 2002). It has been suggested, based on studies in cultured cells with inhibitors, that among cytosolic peptides, only TPPII can trim peptides longer than ~16 aa (Reits et al., 2004), consistent with previous biochemical studies establishing that other cytosolic peptidases (e.g., thimet oligopeptidase (Reits et al., 2004) and various aminopeptidases (Levy et al., 2002) have little activity against peptides longer than 13–15 residues.

1.5.3.5 Insulin degrading enzyme (IDE)

Insulin-degrading enzyme (IDE, insulysin) is an 110-kDa thiol zinc-metalloendopeptidase located in cytosol, peroxisomes, endosomes, and on the cell surface (Duckworth et al., 1998b; Seta and Roth, 1997; Vekrellis et al., 2000) that cleaves small proteins of diverse sequence, many of which share a propensity to form ß-pleated sheet-rich amyloid fibrils under certain conditions [e.g., amyloid ß-protein (Aß), insulin, glucagon, amylin, atrial natriuretic factor, and calcitonin] (Bennett et al., 2000; Kurochkin, 2001). IDE is the major enzyme responsible for insulin degradation *in vitro* (Duckworth et al., 1998a), but the extent to which it mediates insulin catabolism *in vivo* has been controversial, with doubts expressed that IDE has any physiological role in insulin catabolism (Authier et al., 1996a; Authier et al., 1996b). Insulin, which is critical for glucose, lipid, and protein metabolism, as well as for cell growth and differentiation, is cleared mainly by the liver and kidney, but most other tissues also degrade the hormone. In addition to its putative role in insulin catabolism, IDE has been found to degrade Aß in neuronal and microglial cell cultures (Qiu et al., 1997; Qiu et al., 1998; Sudoh et al., 2002; Vekrellis et al., 2000), and to eliminate Aß's neurotoxic effects (Mukherjee et al., 2000). Although cerebral accumulation of Aß is believed to play a central role in Alzheimer's disease (AD) pathogenesis, in the vast majority of cases the underlying causes for this elevation are unknown. Furthermore, enzymes similar to IDE have been reported to be implicated in regulating growth factor levels (Stoppelli et al., 1988), muscle differentiation (Kayalar and Wong, 1989), and processing of insulin by antigen-presenting cells (Semple et al., 1989), suggesting that IDE has a multifaceted biological significance.

1.5.4 Transport into the ER

After degradation and trimming of proteins and peptides the question arises, how manage some of those peptides to escape complete degradation? Since more than 99% of these peptides are destroyed within 1 min after their generation and thus are lost for presentation at the cell surface (Reits et al., 2003). Some longer precursors have been found in cell extracts bound to heat shock proteins (HSPs), such as HSP70, HSP90, gp96 and group II chaperonin TRiC endoplasmic reticulum (ER), which might protect them from further proteolysis (Ishii et al., 1999; Srivastava, 2002). It is considered that the regulation of antigenic peptide degradation by these proteins is an important factor to determine the efficiency of antigen presentation. Indeed a small fraction of the peptides produced by proteasomes escape destruction in the cytosol and is transported by the transporter associated with antigen processing (TAP) into the ER lumen.

1.5.4.1 Transporter associated with antigen processing (TAP)

TAP is a heterodimeric ATP-binding cassette (ABC) transporter composed of TAP1 and TAP2 (Trowsdale et al., 1990). Both subunits can be subdivided into a transmembrane domain (TMD) that binds peptides and forms the translocation pore within the ER membrane, and a cytosolic nucleotide-binding domain (NBD), which energizes peptide translocation across the membrane by ATP hydrolysis (Gorbulev et al., 2001). Peptide binding, ATP hydrolysis and peptide transport are tightly coupled by large structural rearrangements within the transporter. The TMDs include 10 and 9 transmembrane segments (TMs) for TAP1 and TAP2, respectively. The unique N-terminal domains are important for binding to tapasin (Koch et al., 2004; Koch et al., 2005). The peptide-binding pocket is localized in the cytosolic loops between H4 and H5 of TAP1, H4 and H5 of TAP2, and a stretch of 15 amino acids C-terminal of H6 of TAP1 and TAP2, respectively (Nijenhuis et al., 1996; Nijenhuis and Hammerling, 1996). The single-particle electron microscopy (EM) analysis has demonstrated that the TAP1/2 complex has a diameter of approximately 10 nm with a central cavity of about 3 nm (Velarde et al., 2001). The ER-resident TAP represents a crucial checkpoint in the MHC class I-dependent pathway of antigen presentation of the adaptive immune system in vertebrates. Many of the proteasome-digested peptides are poor substrates for TAP-dependent translocation into the ER lumen since they are either too long or too short and therefore lost for ER translocation (Momburg et al., 1994). TAP preferentially binds peptides with a length of 8–16 amino acids, but transports peptides of 8–12 amino acids most efficiently

(Androlewicz and Cresswell, 1994; Uebel et al., 1995; van Endert et al., 1994), although longer peptides (up to 40 amino acids) or sterically restricted peptides can also be transported (Gromme and Neefjes, 2002; Koopmann et al., 1996; Neumann and Tampe, 1999).

By employing combinatorial peptide libraries, the peptide-binding motif of human TAP was deciphered (Uebel et al., 1997b; Uebel and Tampe, 1999). In addition to free N and C termini, the first three N-terminal and the C-terminal residues of the peptide are important for binding to TAP. Peptides with a hydrophobic or basic residue at the C terminus are favoured. Basic residues, particularly arginine, in the first three positions enhance binding. A proline residue in the second position very significantly impairs binding. Thus, TAP appears to concern itself, roughly speaking, with the ends of the peptide. Although peptide generation, transport, and loading are tightly regulated, the theoretical pool of peptides which might be displayed at the cell surface is enormous (>107), since the sequence between both termini of the peptide varies with respect to binding to TAP and MHC class I molecules. This concept of diversity and specificity is highly beneficial to the host since the cellular proteome can be monitored as a 'peptidome' displayed by MHC I molecules on the cell surface.

1.5.4.2 Transport into the ER by signal sequences

Secreted or membrane proteins are normally targeted to the ER by N-terminal signal sequences, which direct their transport through a transmembrane channel, the SEC61 complex, after which the signal sequence is usually removed by the ER enzyme signal peptidase (Anderson et al., 1991). Nevertheless, SEC61 can also act by translocating peptides from the ER back into the cytosol (Kopito, 1997; Werner et al., 1996).

1.5.5 Peptide trimming in the ER

Once in the ER peptides can undergo further trimming by the ER-luminal aminopeptidases 1 (ERAP1) (Saric et al., 2002) in human or ER-associated aminopeptidase (ERAAP) in rodents (Serwold et al., 2002), which is a zinc-containing metalloprotease ERAAP/ERAP1 is a 930 amino acid protein with a calculated molecular weight of 106 kDa and a native molecular weight of 130–150 kDa, due to addition of one or several N-linked oligosaccharides (Hattori et al., 1999; Schomburg et al., 2000). Although ERAAP/ERAP1 is expressed ubiquitously, expression is strongest in liver, lung, spleen, and thymus, paralleling expression of MHC class I molecules. In addition to that, its expression is increased in cells treated with IFN-γ, a potent stimulator of MHC class I presentation (Saric et al., 2002; Serwold et al., 2002; Stoltze et al.,

2000). In humans there are two aminopeptidases of this type in the ER, ERAP1 and 2. ERAP2 is a glycosylated protein with a native molecular weight of approximately 115 kDa and is highly homologous to ERAP1 (49% protein sequence identity). They seem likely to represent sister enzymes, both involved in peptide trimming in the human ER. Examination using confocal microscopy revealed that ERAAP and the human homologues, colocalize with several ER markers such as the KDEL receptor, calnexin, BiP, and gp96 (Saric et al., 2002; Saveanu et al., 2005; Serwold et al., 2002). Some studies have elucidated several aspects of the specificities of these aminopeptidases. As all M1 aminopeptidases are unable to cleave the X-Pro and Pro-X peptide bonds (Barrett et al., 1998), ERAP1 and ERAP2 do not cleave the X-Pro bond efficiently. ERAP1 displays a strong preference for substrates of 9 to 10 or more residues; consequently, peptides with a length adapted to HLA class I binding will be suboptimal or poor ERAP1 substrates. In contrast, ERAP2 differs from ERAP1 by breaking down 8-mer peptides efficiently. Savenau et. al. performed several cleavage studies in which ERAP1 preferentially removed large hydrophobic residues such as Leu, while ERAP2 showed a strong preference for the basic residues Arg and Lys (Hattori et al., 2000; Saveanu et al., 2005; Tanioka et al., 2003). They could show that ERAP1 and ERAP2 act in a concerted fashion to remove longer heterogeneous extensions from precursor peptides (Saveanu et al., 2005).

1.5.6 Peptide loading complex

After further trimming of the peptides translocated in the ER to a length of 8–11 residues (York et al., 2002), some are loaded onto MHC class I molecules, a complicated and tightly regulated process, which requires a macromolecular peptide-loading complex (PLC) comprised of TAP1/TAP2, tapasin, MHC class I heavy chain (HC), β2-microglobulin, calreticulin (CRT), calnexin (CNX) and ERp57 (Antoniou et al., 2002; Ortmann et al., 1997).
Tapasin, a type I membrane glycoprotein with a molecular mass of 48 kDa, is a central component of the PLC and has diverse functions such as: recruitment of ERp57 and MHC class I molecules to TAP (Bangia et al., 1999; Dick et al., 2002), stabilization of TAP (Garbi et al., 2003), increase in the efficiency of MHC class I surface presentation and the amount of MHC molecules associated with high-affinity peptides (Williams et al., 2002), exchange of high-koff by low-koff peptides in the binding groove of MHC class I molecules (Zarling et al., 2003), coordination and facilitation of peptide loading onto MHC class I molecules (Tan et al., 2002). As afore mentioned, the extra N-terminal domains of TAP are crucial for tapasin

binding and thus, for assembly of the PLC (Koch et al., 2004). The heterodimeric TAP complex binds four tapasin molecules and tapasin itself interacts with MHC class I through the C-terminal Ig domains in a ratio of 1:1 (Bangia et al., 1999; Bangia and Cresswell, 2005). So, Tapasin links TAP to peptide free MHC class I heavy-chain ß2-microglobulin dimers. Two other constituents of the complex, however, are 'housekeeping proteins'. These are the chaperone calreticulin and the thiol oxidoreductase ERp57, which normally assist in the folding of newly synthesized glycoproteins in the ER but which have been adapted to promote the assembly of MHC class I–peptide complexes. A cysteine within the ER luminal domain (C95) of tapasin is essential for the disulfide formation to ERp57, promoting retention of ERp57 in the PLC (Dick et al., 2002). Since discovery of ERp57 has been implicated in the control of the disulfide status of MHC class I molecules. The fully assembled PLC is essential for selection of high affinity peptides, and their transfer onto empty MHC class I molecules for later presentation to effector cells of the immune system.

Following peptide binding, MHC peptide complexes are released from the PLC and shuttled via the Golgi apparatus to the cell surface where they are scanned by CTLs, which may trigger an immune response.

1.6 The proteasome

The 26S proteasome complex is a multifunctional, proteolytic molecular machine found in both the cytosol and the nucleus, in which several enzymatic (proteolytic, ATPase, de-ubiquitinating) activities function together with the ultimate goal of protein degradation (Hough et al., 1986). Its functions include the removal of misfolded or abnormally assembled proteins like, the degradation of cyclins involved in the control of the cell cycle, the processing and degradation of transcription regulators, cellular-mediated immune responses and cell cycle arrest and apoptosis. These functions require both ubiquitin- and ATP-driven protein degradation pathways (Ciechanover et al., 2000; Young et al., 1998). The significance of the 26S proteasome in cell function is demonstrated by lethality of proteasome-less mutants in yeast, its existence in all three kingdoms of life, and by a number of clinical syndromes linked to abnormalities in regulated proteolysis (for example, Angelman's syndrome characterized by mental retardation and seizures).

1.6.1 Structure and composition of the eukaryotic proteasome

With a molecular mass of approximately 2.5 MDa, the 26S proteasome consists of the 20S core particle (CP) capped by the 19S regulatory complex at each end (also called CAP or PA700). The eukaryotic 20S proteasome is a large, cylinder-shaped protease with a molecular weight of about 700 kDa. Electron micrographs of 20S proteasomes revealed its molecular dimensions of about 160 A in length and 120 A in diameter (Groll et al., 1997; Groll et al., 2001). The complex is composed of 28 protein subunits (Fig. 1), which are arranged in four stacked rings, each comprising seven units with molecular masses of 21-34 kDa (Hegerl et al., 1991). These subunits can be divided into α and ß subfamilies, which assemble into four stacked heptameric rings following an α7ß7ß7α7 stoichiometry. Throughout evolution, the cylindrical structure of the 20S proteasome has been conserved, whereas its subunit composition has changed.

In the eukaryotic 20S proteasome, the α subunits forming the outer rings are catalytically inactive but are responsible for the assembly of the complex and its interactions with the regulatory complex, therefore controlling the access of the substrates to the catalytic chamber for degradation. The two inner rings, composed of β-subunits, harbour the catalytically active subunits, displaying their active sites on the inner surface of the central tunnel. Most β-subunits are generated from precursors that undergo N-terminal processing during proteasome assembly (Seemuller et al., 1996). Three of the mature subunits, called ß1(δ), ß2(Z), and ß5(MB1) form the so called constitutive proteasome (Fig. 1). They are proteollytically active and carry an amino-terminal threonine (Thr) residue as the catalytic nucleophile (Arendt and Hochstrasser, 1997; Fenteany et al., 1995; Groll et al., 1997; Heinemeyer et al., 1997). Some of these critical Thr residues can be covalently modified by the proteasome-specific inhibitor lactacystin (Fenteany et al., 1995).

1.6.2 Proteasomal activity

Experiments with fluorogenic substrates demonstrated that proteasomes carry at least five distinct cleavage preferences named chymotrypsin-like, trypsin-like, caspase-like (also called peptidylglutamylpeptide hydrolyzing (PGPH)) activities and branched chain amino acid preferring (BrAAP) and small neutral amino acid preferring (SNAAP) activity (Dick et al., 1998; Orlowski, 1993). All the active centers harbour an N-terminal threonine residue acting as the nucleophile, but the distinct preferences of the various active subunits were shown to be determined solely by the composition of the substrate binding pockets, which are termed as

S1, S2, S3…Sn and S1', S2', S3'…Sn' sites, depending on their proximity to the active centers (Groll et al., 1999; Groll and Huber, 2004). For example, the proteasomal specificity pocket S1 is formed by Arg45 of the corresponding ß-subunit, but the adjacent subunits in the ß-rings contribute to the architecture of the S1 pockets and modulate their character. The Arg45 in the S1 pocket of the ß1 subunit preferentially interacts with a glutamate residue in the P1 position and therefore provides for the caspase-like activity off this active site (Dick et al., 1998; Hilt and Wolf, 1996). The caspase-like activity implicates to cut after acid amino acids. However, experiments with proteolytic degradation of yeast enolase have revealed that subunit ß1 possesses beside its caspase-like also limited BrAAP activity (Cardozo et al., 1996; Vinitsky et al., 1994). Subunit ß2 has a glycine residue in position 45 and, consequently, a spacious S1 pocket confined at its bottom by Glu53. This subunit is well suited for accepting very large P1 residues of basic character and therefore exhibits tryptic like activity. The chymotryptic like activity is attributed to subunit ß5, which has its S1 pocket shaped in particular by Met45. This activity mainly cuts after hydrophobic amino acids. However, mutational analysis showed that subunit ß5 has also tendency to cleave after small neutral and branched side chains assigning additionally BrAAP and SNAAP activity to this subunit (Groll et al., 1999).

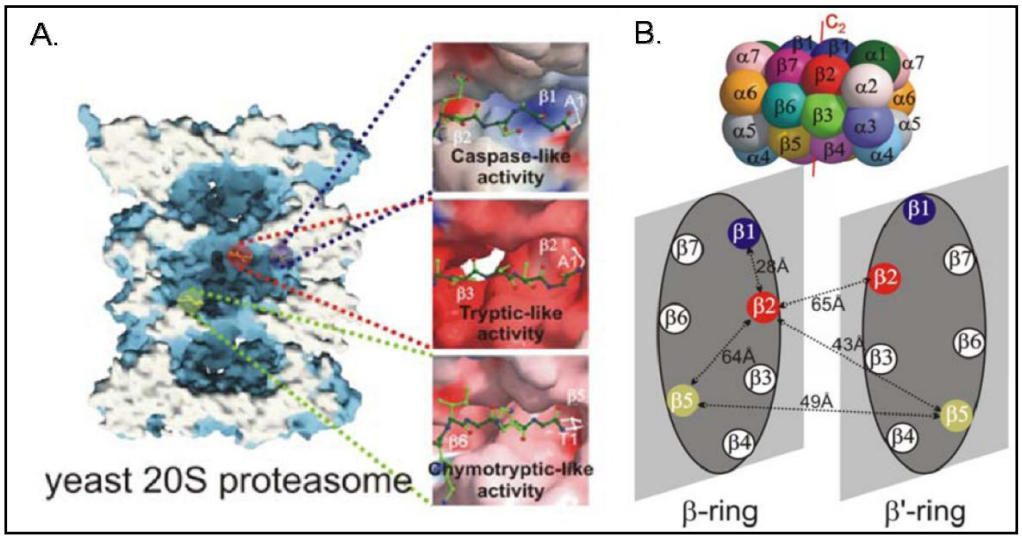

Fig. 1: Representation of the yeast 20S proteasome. A.: The three different proteolytic active centres are marked in a specific colour coding: subunit β1 in blue; subunit β2 in red; subunit β5 in green. Caspase-, tryptic- and chymotryptic-like active sites are zoomed and illustrated as surfaces; propeptides are presented as ball and stick models. B.: The composition of the constitutive proteasome. The 20S complex is composed of 28 protein subunits, which are arranged in four stacked rings, two outer α-rings and two inner ß-rings. Schematic representation of the central β and β'-rings of the yeast proteasome with selected distances between active sites according to the crystal structure (from Groll, 2004).

1.6.3 Conjugates of the 20S proteasome

Compared to the 20S core, which degrades small peptides and fully unfolded proteins in an ATP independent manner, protein degradation by the 26S proteasome generally requires not only ATP but also the presence of a polyubiquitin chain conjugated to the substrate protein (Verma et al., 2000). The 19S regulatory complex is composed of at least 18 different subunits, which are assembled into two main subcomplexes: a base that contains six ATPases and two non-ATPase subunits and abuts the proteasome α ring and a lid subcomplex containing at least 10 non-ATPase subunits that sit on top of the base (Schmidt et al., 2005; Voges et al., 1999). This 19S regulatory particle is responsible for recognition, unfolding and translocation of the selected susbtrates into the lumen of the 20S core particle. In contrast to the 20S core, the structure and function of the 19S regulatory complex are less understood. In addition to binding to the 19S regulatory complex, the 20S core can be capped by two other evolutionarily conserved activator protein complexes, PA28 (Hoffman et al., 1992) and PA200 (Ustrell et al., 2002), which can activate the proteolytic activity of the 20S proteasome against model peptide substrates. Different from the 26S proteasome, the resulting activated proteasome complexes do not recognize ubiquitinated protein substrates, and their activities and assembly are ATP-independent. There are three PA28 homologues, α, ß and γ. The PA28α and -ß subunits form a heteroheptameric complex to activate the 20S proteasome and are mainly cytoplasmic. This complex is highly abundant in immune tissues and can be induced by interferon-γ, suggesting that PA28αß is involved in the production of class I antigens for presentation (Rechsteiner et al., 2000). In comparison, the PA28γ subunit forms a homoheptameric activator complex and is localized in the nucleus. Although the function of PA28γ is not completely clear, genetic studies with mice and flies indicate that PA28γ may play a role in the cell cycle and apoptosis (Rechsteiner and Hill, 2005). Recent studies have suggested that either PA28 activators or PA200 can bind to one end of the 20S proteasome with the other end capped by a 19S complex to form a hybrid proteasome complex, possibly for immune response as well as in general intracellular proteolysis (Schmidt et al., 2005; Tanahashi et al., 2000).

1.6.4 The immunoproteasome

In mamalian, the cytokine IFN-γ induces the expression of three additional active proteasomal subunits, LMP7 (ß5i), LMP2 (ß1i), and MECL1 (ß2i), which replace their constitutive counterparts (Hisamatsu et al., 1996; Reidlinger et al., 1997; Savory et al., 1993). The

incorporation of the IFN-γ inducible subunits into the proteasome requires de novo assembly and depends of the cell development state and the tissue type (Schmidtke et al., 1996; Schmidtke et al., 1997). Those subunits are referred to as immuno subunits and allow cells to improve the generation of antigenic peptides presented by the MHC class I molecules on the cell surface (Brown et al., 1991; Ortiz-Navarrete et al., 1991). The introduction of the immuno subunits leads to an increase of the amount of generated oligopeptides, and to a higher binding affinity of some peptides to the MHC class I receptors (Boes et al., 1994; York and Rock, 1996). Antigenic peptides predominantly exhibit basic or hydrophobic C-terminal anchor residues, required for tight binding and stabilisation of MHC class I molecules (Engelhard, 1994; Silver et al., 1991). The specificity pockets of proteasomal chymotryptic- and tryptic-like active sites have suitable residue composition for producing antigenic peptides, but not the pocket of the caspase-like active site, located at subunit ß1. Interestingly, the immuno subunit (ß1i) shows two major differences in its primary sequence as compared to ß1. In ß1i Thr31 is changed to phenylalanine and Arg45 to leucine (Groll et al., 1997). Modelling experiments with wild type yeast proteasome showed that these two substitutions reduce the size of the pocket and suggest that the caspase-like activity of this subunit is altered to chymotryptic-like activity. Similar modelling of subunits ß2i and ß5i do not indicate substantial modifications in the arrangement and specificities of their pockets (Groll et al., 1997). However, *in vivo* experiments in mice show that mutants lacking these two immuno subunits have severe effect in MHC class I presentation (Fehling et al., 1994).

1.7 MHC class II antigen processing pathway

1.7.1 The source of MHC class II peptides

Antigens loaded on MHC-II are typically exogenous proteins internalized by the APC or endogenous proteins resident in the endosomal system. In fact, a fraction of the peptides bound to MHC-II are derived from proteins normally resident in the (Dongre et al., 2001; Engelhard, 1994; Rudensky et al., 1991). In principle, these cytosolic antigens could be recaptured as exogenous material by endocytosis of antigen liberated from apoptotic cells, or by phagocytosis of apoptotic bodies. A more likely source of peptides derived from cytosolic antigens is the transfer of material from the cytosol into lysosomes, or autophagy (Nimmerjahn et al., 2003). This implies that in principle, any protein can potentially be presented on MHC-I or MHC-II. The differences between MHC-I and MHC-II may thus be

distinguished more on the basis of their physiological role, binding characteristics and the mechanistic of peptide loading onto the MHC-II binding groove.

1.7.2 Antigen generation for MHC class II binding

The processing of antigens for presentation on MHC-II molecules occurs within the endocytic pathway. Work in B cell lines and monocytes showed that APCs contain specialized loading compartments, designated as MIIC (for MHC-II compartments). However, MHC-II-containing compartments in these APCs were found to represent conventional endosomes and lysosomes and are simply the sites to which the bulk of MHC-II and HLA-DM accumulate (Kleijmeer et al., 1997; Pierre et al., 1996).

A key question concerning antigen processing in the MHC-II pathway remains unresolved: Are peptides generated first and then loaded ("peptide capture"), as in the MHC-I pathway, or are peptides generated after binding of intact antigen to MHC-II molecules ("epitope capture")? In fact, examples can be found of proteins that apparently have to be cleaved before they can bind (Davidson et al., 1991). Although this may occur, intermediate proteolytic fragments are rare and short lived in the terminal degradative environment of lysosomes. An alternative model proposes that epitopes could be protected from destruction by binding as large proteins to MHC-II before lysosomal proteases have a chance to degrade them (Deng et al., 1993). The open binding groove in MHC-II allows the binding to whole proteins or long polypeptides, and the protruding ends unprotected by MHC-II could be trimmed by endo- and exopeptidases, while the peptides in the MHC-II groove are protected from degradation (Donermeyer and Allen, 1989; Mouritsen et al., 1992; Sette et al., 1989). A range of possible scenarios exists in which some proteins predominantly bind intact to MHC-II, others require fragmentation before they can bind to MHC-II, and still others experience a bit of both.

Processing of proteins for the MHC-II pathway is achieved by endopeptidases, exopeptidases and IFN-γ induced lysosomal thiol reductase (GILT). Several cysteine proteases have been linked to Ii and antigen processing (Musson et al., 2003), like the papain-like cathepsins S, L, B, F and H (in humans, cathepsins V), together with the asparagin endopeptidase (AEP), also known as mammalian legumain. The lysosomal proteases that have been implicated in the MHC-II pathway are not specific for immunological cells neither for tissues (Delamarre et al., 2005; Watts, 2004a). However, this reflects their primary role in catabolism.

1.7.3 Antigen loading onto MHC class II molecules

The MHC-II molecules, like the MHC-I molecules are synthetised in the ER. To protect MHC-II molecules from binding by peptides from the MHC-I pathway, a so called invariant chain (Ii) blocks the binding groove of the MHC-II molecule binding to it. The Ii is a trimer composed of three 30 kD subunits, each of which binds one newly synthesized class II αβ heterodimer forming a nonameric complex. After this MHC-II/Ii complex is released from the ER by vesicles, these can fuse with endosomes containing proteins and forming a MIIC compartment. The first step is the cleavage of the nonameric Ii-MHC-II complex, which is typically initiated in endosomes by the cleavage of Ii chain by AEP (legumain) or other unidentified proteases to yield a ~10 kD amino terminal Ii chain fragment termed p10. This fragment, which still contains the endosome/lysosome targeting signal, remains as a trimer and interacts with three αβ dimers of the MHC-II molecules. Further cleavage (involving various cathepsins including B, S, or L, depending on the cell types) results in a minimal class II–associated Ii-derived peptide (CLIP) bound to MHC-II. This cleavage is accompanied by the dissociation of the Ii chain-αβ nonamer to yield three αβ dimers. CLIP is subsequently exchanged for antigenic peptides, in a reaction favored by acidic pH and facilitated by the MHC-II-like chaperone HLA-DM. Furthermore, HLA-DM protein, whose function is modulated by HLA-DO in B cells, then catalyzes the dissociation of CLIP, stabilizes the empty MHC-II molecules and assists in peptide selection, supporting the strongest binding affinity (Gubler et al., 1998b; Pieters, 1997; Watts, 2004b).

1.8 Prediction of CTL epitopes

Cytotoxic T lymphocyte epitopes are potential candidates for vaccine design for various diseases. Reverse immunogenetic approaches attempt to optimize the selection of candidate epitopes, and thus minimize the experimental effort needed to identify new epitopes. Most of the existing T cell epitope prediction methods have a main focus on the highly specific MHC class I binding event. Nevertheless the generation of a CTL epitope includes not only the specific binding to the MHC class I molecules, but it also depends on the specificity of other processes like TAP transport and proteasomal cleavage (Larsen et al., 2005a). On this account, several approaches have been developed for predicting the antigen-processing steps preceding MHC class I binding, including proteasomal cleavage and TAP transport efficiency. Most of these algorithms for epitope prediction are based on the rules that are

characteristic for those intracellular processes. Not all details are known of those processes and still a lot of experimental studies have to be done. As a consequence, the accuracy of the algorithms used to find epitopes of target proteins still leave room for improvement. Anyway, one important aspect is missing completely in the prediction approaches, the non-proteasomal processing performed by cytosolic and ER aminopeptidases. The specificities of these peptidases are still not well known and therefore it is not possible to include their trimming information into any algorithm. Nevertheless, their role in antigen processing shouldn't be underestimated.

1.8.1 Prediction methods based on proteasomal cleavage

The first prediction algorithm published was based on the experimental proteasomal cleavage data of only seven naturally occurring peptides, compiled from different literature sources and thus comprising a small and heterogeneous data set (Holzhutter et al., 1999). Lately, a refined kinetic model, FragPredict was published by the same group (Holzhutter and Kloetzel, 2000). Based on *in vitro* proteasomal cleavages of the 436 aa protein enolase a further algorithm, PAProC was published (Kuttler et al., 2000) and set on the WWW for public use (Nussbaum et al., 2001). A further more precise program, NetChop was published 2002 by Kesmir and collegues. This neural network method was based on the enolase cleavage data and additionally used sequence information from MHC ligands. NetChop has also been made available for public access on the WWW.

1.8.2 Prediction methods based on TAP transport

Furthermore some algorithms were developed focused on TAP transport specificities. Mostly based on *in vitro* data of binding affinity
studies of combinatorial peptide libraries with TAP (Gubler et al., 1998a; Uebel et al., 1997a), Peters et al. published 2003 a prediction matrix, so called „stabilized matrix method" (SMM). The main difference to other systems is the aspect of including the TAP transport efficiency of N-terminal prolonged precursor peptides into the prediction criteria.

1.8.3 Prediction methods based on MHC class I binding

Nevertheless, as already mentioned above, most T cell epitope prediction algorithms have their main focus on the specific MHC peptide binding event. Those are based on structure

data and sequence information of MHC molecules or on the sequence information of the binding peptide. Furthermore there exist three different types of the generation of those algorithms: binding motifs, binding matrix and neural network. An example for a motif based algorithm that provides the prediction for more than 200 HLA alleles is SYFPEITHI (Rammensee et al., 1999). In contrast to other algorithms this database has been composed out of the information from naturally occurring MHC ligands, which have been experimentally verified.

1.8.4 Prediction methods merging all three events

Very few methods are based on the main three steps of MHC class I ligand generation: peptide generation by the proteasome, transport by TAP and binding on MHC class I molecules. Such a prediction model was first published by Tenzer and Peters in 2005, www.mhc-pathway.net. They developed a new matrix-based model for the differential prediction of c20S and i20S cleavages, which they found to be superior to all previously published prediction methods for proteasomal cleavages. By combining its predictions with TAP transportability, they were able to predict the relative amounts of peptides generated from a given protein that was available in the ER for binding to MHC class I molecules. Finally, we combined this with existing predictions of peptide binding to MHC class I molecules. The majority of the existing prediction models are based on *in vitro* data. In contrast, the new model of Tenzer and Peters consists on a dataset of 390 endogenously processed MHC class I ligands from cells with known proteasome composition. In this system they showed that the immunological advantage of switching from constitutive to immunoproteasomes lies in suppressing the creation of peptides in the cytosol that TAP can not transport. Nowadays, after being updated several times one of the best methods to perform epitope predictions is the NetCTL. The newest version includes the TAP transport specificity and has been trained with a database consisting of 1260 publicly available MHC class I ligands (Larsen et al., 2005b).

1.9 Aim of the Thesis Project

The aim of my thesis project is the analysis of the influence of the epitope flanking regions on MHC class I antigen presentation. As discussed before, epitopes require correct processing by cytosolic proteases for antigen presentation. The efficiency of epitope generation depends not only on the epitope itself but also on its flanking regions. In this project the influence of the

C-terminal region of the model epitope SIINFEKL from chicken ovalbumin (aa 257-264) has been investigated. This is a well characterized antigen presented on the murine MHC class I molecule H-2K^b. The target Flp-In HEK-293K^b (Tenzer, 2004) cell line was transfected with different constructs each enabling the expression of the SIINFEKL sequence with different defined C-terminal flanking regions. The constructs differed at the two first C-terminal positions after the SIINFEKL epitope, so called P1' and P2'. At these sites all 20 amino acids were exchanged consecutively and tested for their influence upon H-2K^b/SIINFEKL presentation on the cell surface of the Flp-In HEK-293K^b cells. The detection of this complex was performed by immunostaining and flow cytometry means.

Up to now, proteasomal cleavages were thought to be exclusively responsible for the generation of the final C terminus of CTL epitopes (Craiu et al., 1997c; Craiu et al., 1997a; Mo et al., 1999). With this background, the dependence of the SIINFEKL generation on proteasomal cleavage of the designed constructs was characterized using inhibitors against proteasomal active sites. Then the influence of an inhibited proteasome on epitope presentation was analyzed by detection of the H-2K^b/SIINFEKL on the cell surface. Further on, the possibility of other existing carboxypeptidases in the cytosol that could be involved in the correct trimming of the C terminus of antigenic peptides for MHC class I presentation was investigated, performing specific knockdowns and using inhibitors against the target peptidases.

2 Materials and Methods

2.1 Materials

2.1.1 Bacterial strains

The bacterial strains used for molecular cloning were *E. coli* Library Efficiency® DH5α Competent Cells (Invitrogene, Karlsruhe/Germany) and XL-1 blue (Stratagene, Heidelberg/ Germany).

2.1.2 Media for bacterial cells

All bacterial cell lines were grown in Luria Bertani (LB) medium and maintained on LB agar plates supplemented with suitable antibiotics wherever necessary. LB media contains 10 g Tryptone, 5 g Yeast extract and 10 g NaCl. These contents were dissolved in 1 l Millipore water. After autoclaving the LB-media it was cooled down to ~55°C prior to the addition of antibiotics.

2.1.3 Eukaryotic cell lines

Cell lines	Origin
Flp-In 293K^b:	Derived from the HEK-293 fibroblast cell line from human embryonic kidney. The Flp-In 293 cell line (Invitrogen, Karlsruhe/Germany), which carries a single specific FRT site, was transfected with a vector (pcDNA3-H-2K^b) coding for the murine H-2K^b molecule by Dr. Tenzer. This cell line was used for transfection of the SIINFEKL coding plasmid pEntry2.
LCL-721:	EBV-transformed human B cell line (Salter et al., 1985). This cell line was used for cytosolic purification and protease search.
25-D1.16:	Hybridoma cell line; produces an antibody, which recognizes the MHC class I-peptide complex of the murine H-2K^b and the Ovalbumin epitope SIINFEKL (Porgador et al., 1997).
Y-3:	Hybridoma cell line; produces an antibody, which recognizes the murine MHC class I molecule, H-2K^b.

2.1.4 Cell culture media

The eukaryotic cells were all cultured in DMEM (Vitromex, Geilenkirchen/ Germany) medium with penicillin/streptomycin (Serva, Heidelberg/ Germany). To the DMEM media 10% FCS (Vitromex, Geilenkirchen/ Germany) was added for the culture of the Flp-In 293K^b and the LCL721 and only 2% FCS for the hybridoma cell lines, 25-D1.16 or Y-3. To wash the cells 1x PBS was used. Both media were prepared in the lab. Trypsin/EDTA was purchased from Invitrogen, Karlsruhe/ Germany.

DMEM: 2 mM L-Glutamine; 1 mM Sodium pyruvate; HEPES (pH 7.4) 10 mM; 1x MEM

10x PBS: 1.4 M NaCl; 0.1 M NaH_2PO_4; pH 7.2

Selection medium for the Flp-In 293K^b before transfection: DMEM + 100 µg/ml Zeocin.

Selection medium for the Flp-In 293K^b after transfection with the pEntry2 plasmid coding for SIINFEKL: DMEM + 100-200 µg/ml Hygromycin B.

2.1.5 Plasmids

pBluescript II KS+ (MBI Fermentas, St. Leon-Rot/ Germany)

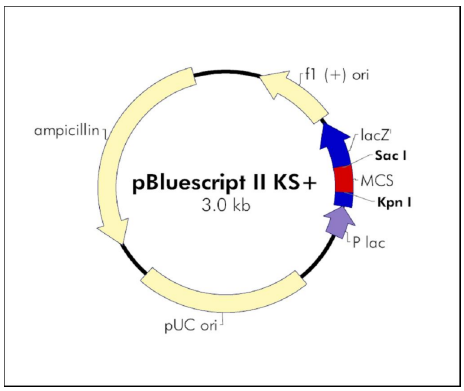

The pBluescript II KS+ has been used for the generation of the SIINFEKL constructs with the different amino acids. It is an advantage for successful mutagenesis to use small plasmids. The less a polymerase has to "read", the fewer mistakes can occur.

pOG44 (Invitrogen, Karlsruhe/ Germany)

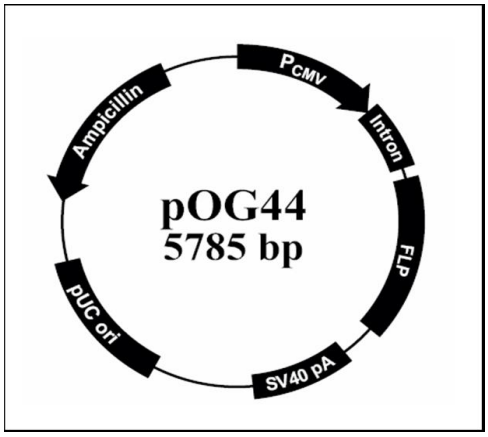

This vector is included in the Flp-In system kit. The pOG44 codes for the recombinase needed for the homologous recombination that leads to the insertion of the construct of interest. This has been always used for the cotransfection into the Flp-In293K^b cells with the pEntry2 vector carrying the SIINFEKL construct.

pEntry2 (Tenzer, 2004)

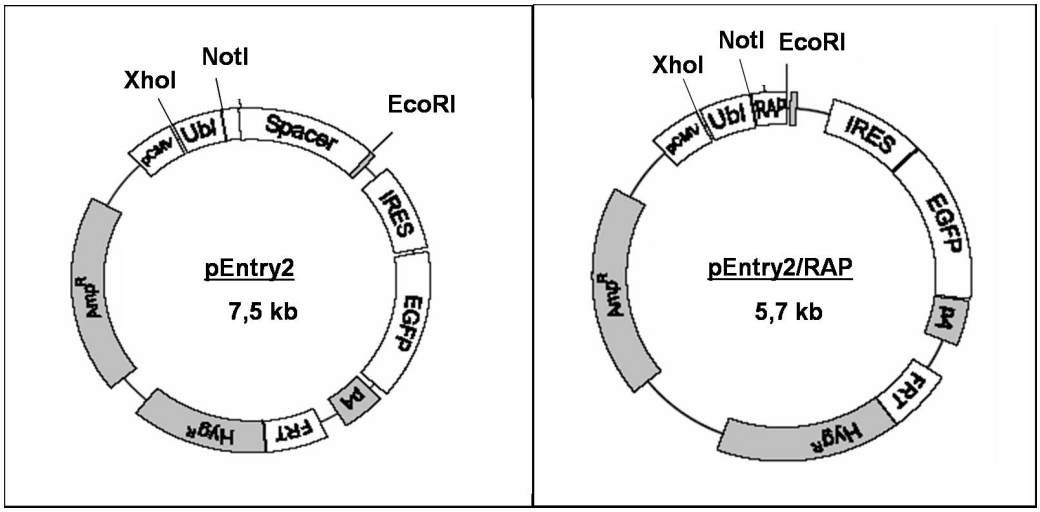

The plasmid pEntry2 was used for the cloning of the S8L constructs into the *Xho*I/*EcoR*I restriction sites and for further transfection into the target Flp-In 293K^b cells. The construct coding for SIINFEKL is also called RAP (reverse antigen processing). These have been generated by Dr. Tenzer from the pcDNA5/FRT provided in the Flp-In System-Kit from Invitrogen. Further information about the generation of the pEntry2 vector is found in the dissertation of Dr. Tenzer, 2004.

2.1.6 Constructs

The construct in which the amino acid exchanges were performed is the following:
Ubiquitin-RASNEMMETMLEQLE**SIINFEKL**TEWTSCYPYDVPDYASL-
The sequence LEQLE**SIINFEKL**TEWTS from the ovalbumin carries the SIINFEKL epitope presented by the H-2K^b molecule.

2.1.7 Restriction enzymes

For the cloning of the construct into the pEntry2 vector two restriction enzymes were used: *EcoR*I and *Xho*I. Both purchased by NEB labs, Ipswich/ USA.

2.1.8 Primer

Primers used for the amino acid exchange in the ovalbumin construct:

- Oligo annealing mutagenesis

Name		Sequence (5'-3')
5´P1	fw	CGAAAAGCTTNNBGAATGGACAAGTTGTTATCCATACGATGTACCAGACT ATGCAAGTTTATG
3´P1	rv	AATTCATAAACTTGCATAGTCTGGTACATCGTATGGATAACAACTTGTCCA TTCVNNAAGCTTTT
5´P1-Stop-A	fw	CGAAAAGCTTNDGTAATGGACAAGTTGTTATCCATACGATGTACCAGACT ATGCAAGTTTATG
3´P1-Stop-A	rv	AATTCATAAACTTGCATAGTCTGGTACATCGTATGGATAACAACTTGTCCA TTACHNAAGCTTTT
5´P1-Stop-B	fw	CGAAAAGCTTNNCTAATGGACAAGTTGTTATCCATACGATGTACCAGACT ATGCAAGTTTATG
3´P1-Stop-B	rv	AATTCATAAACTTGCATAGTCTGGTACATCGTATGGATAACAACTTGTCCA TTAGNNAAGCTTTT
5'P2-A	fw	CGA AAA GCT TGC CND GTG GAC AAG TTG TTA TCC ATA CGA TGT ACC AGA CTA TGC AAG TTT ATG
3'P2-A	rv	AAT TCA TAA ACT TGC ATA GTC TGG TAC ATC GTA TGG ATA ACA ACT TGT CCA CHN GGC AAG CTT TT
5'P2-B	rv	CGA AAA GCT TGC CNN CTG GAC AAG TTG TTA TCC ATA CGA TGT ACC AGA CTA TGC AAG TTT ATG
3'P2-B	rv	AAT TCA TAA ACT TGC ATA GTC TGG TAC ATC GTA TGG ATA ACA ACT TGT CCA GNN GGC AAG CTT TT
5'P2-Stop-A	fw	CGA AAA GCT TGC CND GTA AAC AAG TTG TTA TCC ATA CGA TGT ACC AGA CTA TGC AAG TTT ATG
3'P2-Stop-A	rv	AAT TCA TAA ACT TGC ATA GTC TGG TAC ATC GTA TGG ATA ACA ACT TGT TTA CHN GGC AAG CTT TT
5'P2-Stop-B	fw	CGA AAA GCT TGC CNN CTA AAC AAG TTG TTA TCC ATA CGA TGT ACC AGA CTA TGC AAG TTT ATG
3'P2-Stop-B	rv	AAT TCA TAA ACT TGC ATA GTC TGG TAC ATC GTA TGG ATA ACA ACT TGT TTA GNN GGC AAG CTT TT
5'P3-C	fw	CGA AAA GCT TGC CGC CND GAC AAG TTG TTA TCC ATA CGA TGT ACC AGACTA TGC AAG TTT ATG
3'P3-C	rv	AAT TCA TAA ACT TGC ATA GTC TGG TAC ATC GTA TGG ATA ACA ACT TGT CHN GGC GGC AAG CTT TT
5'P3-D	fw	CGA AAA GCT TGG CGC CNN CAC AAG TTG TTA TCC ATA CGA TGT ACC AGA CTA TGC AAG TTT ATG

5'P3-D2	fw	GCA AAA GCT TGC CGC CNN CAC AAG TTG TTA TCC ATA CGA TGT ACC AGA CTA TGC AAG TTT ATG
3'P3-D	rv	AAT TCA TAA ACT TGC ATA GTC TGG TAC ATC GTA TGG ATA ACA ACT TGT GNN GGC GGC AAG CTT TT
5'P3-Stop-A	fw	CGA AAA GCT TGC CGC CND GTA AAG TTG TTA TCC ATA CGA TGT ACC AGA CTA TGC AAG TTT ATG
3'P3-Stop-A	rv	AAT TCA TAA ACT TGC ATA GTC TGG TAC ATC GTA TGG ATA ACA ACT TTA CHN GGC GGC AAG CTT TT
5'P3-Stop-B	fw	CGA AAA GCT TGC CGC CNN CTA AAG TTG TTA TCC ATA CGA TGT ACC AGA CTA TGC AAG TTT ATG
3'P3-Stop-B	rv	AAT TCA TAA ACT TGC ATA GTC TGG TAC ATC GTA TGG ATA ACA ACT TTA GNN GGC GGC AAG CTT TT

Oligonucleotide IUB-Codes (Codes of the International Union of Biochemistry) for mixed (wobble) bases:

Coding for		**Coding for**	
either of two bases		**any of three bases possible**	
M	A and C	**V**	A and G and C
R	A and G	**H**	A and C and T
W	A and T	**D**	A and G and T
S	G and C	**B**	G and T and C
Y	C and T	**any of three bases possible**	
K	G and T	**N**	A and G and C and T

- Quick change mutagenesis

Name		**Sequence (5'-3')**
P1-B_Tyr/His	fw	ATA AAT TTC GAA AAG CTT YAC ATG TGG ACA AGT TGT TAT
P1-B_Tyr/His	rv	ATA ACA ACT TGT CCA CAT GTR AAG CTT TTC GAA ATT TAT
Cys/Trp	fw	ATA AAT TTC GAA AAG CTT TGS GAA TGG ACA AGT TGT TAT C
Cys/Trp	rv	GAT AAC AAC TTG TCC ATT CSC AAA GCT TTT CGA AAT TTA T
P2'Dori	fw	AAT TTC GAA AAG CTT GCC GAC TGG ACA AGT TGT TAT CCA

P2'Dori	rv	TGG ATA ACA ACT TGT CCA GTC GGC AAG CTT TTC GAA ATT
P2'Tori	fw	AAT TTC GAA AAG CTT GCC ACC TGG ACA AGT TGT TAT CCA
P2'Tori	rv	TGG ATA ACA ACT TGT CCA GGT GGC AAG CTT TTC GAA ATT
P2'Hori	fw	TTC GAA AAG CTT GCC CAC TGG ACA AGT TGT TAT
P2'Hori	rv	ATA ACA ACT TGT CCA GTG GGC AAG CTT TTC GAA
P2'H&	fw	AAT TTC GAA AAG CTT GCC CAC TAG ACA AGT TGT TAT CCA
P2'H&	rv	TGG ATA ACA ACT TGT CTA GTG GGC AAG CTT TTC GAA ATT
P2'I&	fw	TTC GAA AAG CTT GCC ATT TAG ACA AGT TGT TAT
P2'I&	rv	ATA ACA ACT TGT CTA AAT GGC AAG CTT TTC GAA
P3-A_Glu	fw	TTC GAA AAG CTT GCC GCC GAG ATG AGT TGT TAT CCA TAC
P3-A_Glu	rv	GTA TGG ATA ACA ACT CAT CTC GGC GGC AAG CTT TTC GAA
P'RRori	fw	ATA AAT TTC GAA AAG CTT AGG AGG TGG ACA AGT TGT TAT
P'RRori	rv	ATA ACA ACT TGT CCA CCT CCT AAG CTT TTC GAA ATT TAT
P'RR&	fw	TTC GAA AAG CTT AGG AGG TAG ACA AGT TGT TAT
P'RR&	rv	ATA ACA ACT TGT CTA CCT CCT AAG CTT TTC GAA
P'RRRori	fw	T TC GAA AAG CTT AGG AGG AGG ACA AGT TGT TAT
P'RRRori	rv	ATA ACA ACT TGT CCT CCT AAG CTT TTC GAA
P'RRR&	fw	TTC GAA AAG CTT AGG AGG AGG TAG AGT TGT TAT
P'RRR&	rv	ATA ACA ACT CTA CCT CCT CCT AAG CTT TTC GAA
P'LLori	fw	TTC GAA AAGCTT CTTCTT TGG ACA AGT TGT TAT
P'LLori	rv	ATA ACA ACT TGT CCA AAG AAG AAG CTT TTC GAA
P'LL&	fw	TTC GAA AAG CTT CTT CTT TAG ACA AGT TGT TAT
P'LL&	rv	ATA ACA ACT TGT CTA AAG AAG AAG CTT TTC GAA
P'LA&	fw	TTC GAA AAG CTT CTT GCC TAG ACA AGT TGT TAT
P'LA&	rv	ATA ACA ACT TGT CTA GGC AAG AAG CTT TTC GAA

Primers used for the detection of the protease knockdowns by real-time PCR including the control primers for the housekeeping gene EF1α:

Proteases	**Primers (5'-3')**	**Purchased from**
IDE for	AAA AAG AGG CGA CAC CAT ACC	Metabion
IDE rev	AGG TAC AAA TAG GCC ATG TT	Metabion
ThOP1 for	Quantitec primers	Qiagen
ThOP1 rev	Quantitec primers	Qiagen
TPPII for	CAT TGT GAC CAG TGG AGG AGC	Metabion

TPPII rev	TGG CCA GTG AGT TGC TTC TCC	Metabion
EF1α for	GATTACAGGGACATCTCAGGCTG	Metabion
EF1α rev	TATCTCTTCTGGCTGTAGGGTGG	Metabion

2.1.9 siRNA oligonucleotides

Targeted protease	**Direction**	**siRNA sequence (5'-3')**	**Purchased from**
TPPII	sense	r(AAG CAA CUC ACU GGC CAA A)dTd T	Qiagen
TPPII	antisense	r(UUU GGC CAG UGA GUU GCU U)dTdT	Qiagen
ThOP1	sense	r(AGU UGA AGG UCA CCC UCA A)dTdT	Qiagen
ThOP1	antisense	r(UUG AGG GUG ACC UUC AAC U)dTdT	Qiagen
IDE* Duplex 1	sense	r(UCAAAGGGCUGGGUUAAUAUU)dTdT	Prof. van Endert
	antisense	r(UAUUAACCCAGCCCUUUGAUU)dTdT	Prof. van Endert
IDE* Duplex 2	sense	r(ACACUGAGGUUGCAUAUUUUU)dTdT	Prof. van Endert
	antisense	r(AAAUAUGCAACCUCAGUGUUU)dTdT	Prof. van Endert
IDE* Duplex 3	sense	r(GAACAAAGAAAUACCCUAAUU)dTdT	Prof. van Endert
	antisense	r(UUAGGGUAUUUCUUUGUUCUU)dTdT	Prof. van Endert
IDE* Duplex 4	sense	r(GAAGUUACGUGCAGAAGGAUU)dTdT	Prof. van Endert
	antisense	r(UCCUUCUGCACGUAACUUCUU)dTdT	Prof. van Endert

* The IDE siRNA used for the knockdowns was a mixture of the four duplex siRNAs listed above.

SC: Scramble Control, randomized siRNA (only control) from Ambion.

2.1.10 Antibodies

Primary antibodies:

25-D1.16 a mouse IgG1 monoclonal antibody specific for SIINFEKL peptide associated with H-2K^b (Porgador *et al*., 1997)

Y-3 a mouse IgG2b monoclonal antibody which recognizes the H-2K^b (heavy chain) (Jones and Janeway, 1981)

Both primary antibodies produced from hybridoma supernatants and used in a working solution of 1:100, diluted with FACS-buffer.

Secondary antibodies:

Goat anti-mouse IgG(H+L) F(ab)2-fragment, APC conjugated, Dianova GmbH, Deutschland. Working solution: 1:200, diluted in FACS-buffer

2.1.11 Proteins

Proteasome 20S	purification in our lab by Dr. Tenzer
TPPII	purification in our lab by Dr. Tenzer

2.1.12 Inhibitors

All inhibitors listed were diluted in pure distilled water.

Inhibitor Molecular weight	**Stock solution**	**Working solution**	**Inhibited proteases**	**Purchased from**
Butabindide oxalate	10 mM	200-100 µM	TPPII	Tocris, UK
Epoxomicin	100 µM	2-1 µM	Proteasome (Chymotrypsin subunit)	Biomol, Germany
Lactacystin	10 mM	50 µM	Proteasome (Chymotrypsin subunit)	Calbiochem, Germany
AAF-CMK	10 mM	50 µM	TPPII	Bachem/Sigma
Cpp-AAF-pAb	10 mM	300 µM	ThOP1	Bachem

2.1.13 Chemicals & buffers

Standard chemicals were purchased from Sigma-Aldrich, Fluka, or Roth:
Acetonitrile, acrylamid:bis-acrylamid 29:1, agarose (electrophoresis grade, ultra pure), ammonium chloride, ammonium peroxodisulfate, ampicillin, beta-mercaptoethanol, bovines serum albumin (BSA) fraction V, calcium chloride, DMSO, DTT, EDTA, acetic acid, ethanol, glycerol, HEPES, potassium acetat, potassium chloride, L-Glutamine, methanol, $MgCl_2$, sodium acetat, sodium chloride, NaOH, Na_2HPO_4, NaH_2PO_4, penicillin/streptomycin, 2-propanol, roti-nanoquant, hydrochloric acid, TEMED, trifluor acetic acid.

DNA ladder 1kb Plus	MBI Fermentas
Prestained Protein Marker Broad Range (6-175) kDa	MBI Fermentas
TRIzol reagent	MBI Fermentas
Fluorogenic peptide substrates	Bachem
Pfu DNA-Polymerase	Stratagene
Triton X-100	Serva
Hygromycin B	Invitrogen
G418	PAA Laboratories
Zeocin	Invitrogen
dNTPs (10 mM stock in water)	MBI Fermentas
Oligo(dT)n (working solution 100ng/ml)	Roche Diagnostics

2.1.14 Plastic materials and equipment

Centrifuges:	Sorvall RC5C, Sorvall Instruments (rotor GS-3)
	Heraeus Biofuge Fresco, Kendro
	5415 R, Eppendorf AG
Electrophoresis:	Agarose electrophoresis chamber, Biorad
Electroporation machine:	Gene Pulser II, Bio-Rad
Flow cytometer:	FACS Canto BD
Geldocumentation system:	GelDoc, Biorad
Liquid chromatography:	ÄKTA-FPLC Explorer 10, Pharmacia
	SMART-HPLC, Pharmacia
Mass spectrometry:	nanoACQUITY UPLC™,Waters

	Q-Tof Premier™, Waters
Micro pipettes:	Eppendorf AG and Biohit
Thermocycler:	Primus PCR, MWG Biotech
	iCycler machine, BioRad
UV-Spectrometer:	SpectraFluor Plus, Tecan GmbH
	BioMate 3, Thermo Spectronic
Ultracenrifuge:	CENTRIKON T-1065, Kontron Instruments
Scale:	BC210S Sartorius GmbH

Centrifugal filter devices from Millipore:
- Amicon Ultra-4 (5 kD)
- Amicon Ultra-15 (10 kD)
- Amicon Ultra 100 kD
- ZipTips® for 96-well-plates

Reagenzgefäße, diverse Größen:
Falcon® bezogen über: Becton Dickinson GmbH, Germany
Cell culture flasks and plastic:
Greiner Holding AG and Falcon, Becton Dickinson GmbH

2.2 Methods

2.2.1 Molecular cloning methods

2.2.1.1 Plasmid preparation (Mini)

The plasmid DNA was isolated from transformed *E. coli* (DH5α) using the PEQLab mini prep kit. An overnight culture was setup by inoculating a randomly selected colony in 4 ml LB medium with appropriate antibiotics and grown at 37°C at 230 rpm. The next morning, cells were pelleted in Eppendorf tubes for 2 minutes at 12.000 rpm. The supernatant was removed and bacterial cells were resuspended in 250 µl buffer I. 250 µl lysis buffer II were added, the tube gently inverted and kept for 5 min. After that 350 µl neutralising buffer III were added and mixed without vortexing. The Eppendorf tube was centrifuged at 12.000 rpm for 10 min. The supernatant was taken out and applied to a HiBind® spin column by pipetting. The spin column was centrifuged for 1 min at 12.000 rpm. The flow-through was discarded and the

column was washed with 750 µl buffer HB and wash buffer according to the protocol. Plasmid DNA was eluted with 50 µl destilled water.

2.2.1.2 Plasmid preparation (Maxi)

For large scale plasmid DNA preparation, commercially available kits (Qiagen, Germany) based on a modified alkaline lysis procedure were used. From a 500 ml overnight bacterial culture was the cells were pelleted down in 400 ml bottles for 10 min at 5000 rpm in a Heraeus centrifuge (rotor GS-3). The supernatant was removed and bacterial cells were resuspended in 10 ml buffer P1 and after that 10 ml P2 alkaline lysis solution were added. The tube was gently inverted and kept for another 5 min. After that 10 ml P3 buffer were added and mixed without vortexing. The supernatant obtained from the treatment of cell pellet with alkaline lysis solutions was allowed to bind to an anion-exchange resin under appropriate low-salt and pH conditions. RNA, proteins and other impurities were removed by a medium-salt wash. Plasmid DNA was eluted in a high-salt buffer and desalted by isopropanol precipitation.

2.2.1.3 DNA sequencing

The DNA sequencing was performed by the sequencing service of the Nano+Bio-Center, TU Kaiserslautern, Germany.

2.2.1.4 Nucleic acid quantification

The DNA was quantitated spectrophotometrically (BioMate 3, Thermo Spectronic) by measuring absorbance at 260 nm. The purity of DNA was confirmed by measuring the OD260/OD280 ratio. Purified DNA had an OD260/OD280 ratio of ~1.8.

2.2.1.5 Agarose gel electrophoresis

DNA fragments were separated on 1.0% agarose gels. 6x gel loading buffer was added to DNA samples at a final concentration of 1x prior to loading onto the gel. Electrophoresis was carried out in 1x TAE buffer at 10 V/cm. Ethidium bromide (0.5 µg/ml) was supplemented in the agarose gel for visualizing DNA on an UV transilluminator. DNA ladder 1kb Plus (MBI

Fermentas) was used as a molecular size marker to assess the size of DNA fragments from their relative mobility.

2.2.1.6 Purification of DNA fragments from agarose gels

After electrophoresis, DNA was visualized using a UV transilluminator (Biorad). Agarose blocks containing the desired DNA fragment(s) were excised and weighed. DNA was extracted using a gel extraction kit Nucleospin® Extract II (Macherey-Nagel, Germany). Briefly, 3 volumes of solubilization and binding buffer were added to 1 volume of the agarose gel slice. The contents were incubated at 50°C till complete dissolution of the agarose gel. The suspension was then pipetted onto a spin column to allow the adsorption of DNA on a silica-gel membrane. Impurities were washed away with ethanol-containing buffer. DNA was finally eluted in Millipore water.

2.2.1.7 DNA ligation

For the ligation of DNA fragments the T4-DNA-ligase kit (NEB) was used, containing the T4 DNA Ligase and an optimized buffer system. The molar ratio between vector and insert was 1:3. The ligation reaction was incubated overnight at 16°C.

2.2.1.8 Transformation of competent bacteria

Bacterial transformation is the process by which competent bacterial cells take up DNA molecules. The different *E. coli* strains (Invitrogen) were transformed according to the manufacturer's protocol, performing a heat shock at 42°C. All vectors for bacterial cloning used carry the ampicilin resistance gene. Thus after transformation the cells were plated onto LB-Ampicillin plates for selection and incubated over night at 37°C.

2.2.1.9 Sitespecific mutagenesis by quickchange PCR

The QuikChange site-directed mutagenesis kit (Stratagene) is used to make point mutations, switch amino acids, and delete or insert single or multiple amino acids. The QuikChange site-directed mutagenesis method is performed using the proof-reading PfuTurbo® DNA polymerase, which replicates both plasmid strands with high fidelity and without displacing the mutant oligonucleotide primers. The basic procedure utilizes a supercoiled double-

stranded DNA (dsDNA) vector with an insert of interest and two synthetic oligonucleotide primers containing the desired mutation (see section *2.1.8*). The oligonucleotide primers used are each complementary to opposite strands of the vector. Following temperature cycling, the product is treated with *Dpn* I. The *Dpn* I endonuclease (target sequence: 5′-Gm6ATC-3′) is specific for methylated and hemimethylated DNA and is used to digest the parental DNA template and to select for mutation-containing synthesized DNA. The nicked vector DNA containing the desired mutations is then transformed into XL1-Blue supercompetent cells. The small amount of starting DNA template required performing this method, the high fidelity of the PfuTurbo DNA polymerase, and the low number of thermal cycles contributes to the high mutation efficiency and decreased potential for generating random mutations during the reaction. This method was used to exchange the amino acids at specific positions in the construct carrying the SIINFEKL epitope. The reaction was performed according to the manufacturer's protocol. The cycle conditions were the following:

Denaturation step at 95°C 30 seconds
18 cycles:
1. 95°C 30 seconds
2. 55°C 1 minute
3. 68°C 5 minute
Store at 4°C

2.2.1.10 Mutagenesis by annealing of oligonucleotides

A further method for mutagenesis of genes is the insertion of synthetic gene fragments carrying at their ends corresponding restriction sites that fit into the construct of interest. In this work, different constructs coding for the SIINFEKL epitope but carrying different amino acids at specific positions at the C-terminus of this antigen have been generated. Therefore 100 pmol oligonucleotides (see section *2.1.8*) of each complementary strand of the region of interest were annealed in 100 µl annealing buffer for 5 min at 95°C incubated and cooled down very slowly (~0.5°C/min) to room temperature. This annealing-mix was used for the ligation into the corresponding cleaved vector.
Annealing buffer: 10 mM Tris-HCl pH 8.0, 50 mM NaCl, 10 mM $MgCl_2$, 1 mM DTT

2.2.2 Cell culture methods

The given cell lines were maintained in monolayer/suspension cultures in DMEM medium supplemented with 10% heat inactivated (1 h by 56°C) fetal calf serum (FCS) with 2 mM L-glutamine, 1 mM Na-pyruvat, 100 U/ml Penicillin and 100 µg/ml Streptomycin. The hybridoma cell lines 25-D1.16 and Y-3 were maintained with only 2-3% FCS. The cells were grown in the incubator in a humidified atmosphere with 10% CO_2 and 37°C.

For passaging cell lines they were first washed with 1x PBS to remove traces of FCS and then trypsinized with trypsin/EDTA (Invitrogen). After 5 minutes incubation the cells were removed from the cell culture flask with the same quantity of fresh media as trypsin. Then a centrifugation step (3 min at 1800 rpm) follows and the resulting pellet is resuspended in fresh DMEM media. The cells were then seeded in a ratio of 1:10 into a new tissue culture flask.

2.2.2.1 Long-term storage

Growing cells were trypsinized, pelleted and washed thoroughly with 1x PBS to remove traces of trypsin and medium. Cells were then resuspended in freezing buffer (90% FCS: 10% DMSO), at a density of 2-3 million cells/ml, and aliquoted into cryovials (Nalgene™). Vials were placed in a cell freezing box (Nalgene™) and left at -80°C for gradual freezing. Frozen cell vials were then transferred to liquid nitrogen for long term storage.

2.2.2.2 Thawing and repropagating cells

The cells are thawed at 37 °C in a water bath, resuspended in 20 ml of DMEM/10 % FCS previously warmed at 37 °C, and then centrifuged at 1500 rpm for 3 minutes. Supernatant is then aspirated and the cell pellet resuspended in culture medium and then distributed in a serial of 1:3 into a 6 well-plate.

2.2.2.3 Trypan blue exclusion

Trypanblue was added to the cell suspension. 5 µl of the stained cell suspension was given into a “Neubauer” counting chamber and the viable cells of 2-3 squares were counted excluding the blue dead cells.

Cells per ml = counted cells/square x dilution factor x 10^4

2.2.2.4 Transfection with Fugene

The adherent Flp-In 293K^b cells were transfected with the pEntry2 plasmid using Fugene (Roche Diagnostics GmbH, Mannheim/Germany) according to the manufacturer's instruction. The day before transfection, 8x 10^5 cells/ well were seeded into 6-well plates. Next day cells were washed with 1x PBS (pH 7.2) to remove the serum and 1 ml DMEM serum free medium was added to each well. DNA-Fugene complexes were made at a 1:3 ratio of DNA:Fugene. For one well of a 6 well-plate 12 µl of Fugene were diluted into 88 µl of DMEM serum free medium separately. After 5 min incubation 4 µg DNA diluted in DMEM serum free medium was added to the Fugene dilution and mixed together. After 20 min incubation at room temperature the DNA-Fugene complex was dropwise added to the 6-well plate.

2.2.3 Acid wash analysis

The stably transfected Flp-In 293K^b cell lines with the pEntry2 vector, carrying the SIINFEKL epitope with the amino acid exchanges were analyzed for SIINFEKL presentation on the cell surface using the acid wash method. The acid solution dissociates the peptides bound to the MHC molecules and thus empties the MHC molecules on the cell suface. First the transfectants were washed with 1x PBS (pH 7.2) and removed from the plate bottom with EDTA (not trypsin). After centrifugation of the cell suspension 2 min at 1800 rpm, the pellet is resuspended in 500 µl (for 1x 10^6 cells) isotonic acid-wash buffer (pH 3.0) and incubated for 1.5 min. To stop the reaction 1 ml of the stop-solution was added. After this incubation, cells were washed 2 times with full medium. The cells were allowed to recover in the presence or absence of inhibitors at 37°C for 6-8 h taking each 2 or 3 h aliquots for FACS analysis.

Composition of the buffers:

1) Acid wash solution: Mix 1:1 0.263 M citric acid and 0.132 M NaH_2PO_4
2) Stop solution: 0.15 M. $NaHPO_4$ pH 7.5

2.2.3.1 Inhibition assays for acid wash analysis

To assess the role of the proteasome and TPPII, the transfectants were treated with the corresponding inhibitors (section *2.1.13*). For *in vivo* inhibitor assays like the acid wash assay the cells were incubated with the medium containing the corresponding inhibitor for 45 min at 37°C before starting the acid wash. Then the cells were stripped with the acid solution and

incubated with the medium containing the corresponding inhibitor for the rest of the kinetic as described above.

2.2.4 Flow cytometry analysis

Flow cytometry analysis was performed for the detection of the SIINFEKL/H-2K^b complex on the cell surface of the transfectants. The monoclonal murine 25-D1.16 primary antibody recognizes this complex, and was used in combination with the secondary goat anti-mouse APC conjugated antibody.

Flow cytometry was performed using a FACSCanto flow cytometer (Becton Dickinson). Single cell suspensions were washed twice with FACS buffer. Staining was done as follows: 3x 10^5 cells were incubated in 96-well round bottom plates for 30 min with the primary antibody diluted in FACS buffer at 4°C. After the incubation, cells were centrifuged for 3 min at 1800 rpm and were washed two times with FACS buffer. Afterwards, cells were incubated with fluorochrome-conjugated secondary antibody for 30 minutes at 4°C in the dark, subsequently washed 3 times in FACS buffer and finally resuspended in 100 µl of FACS buffer. If necessary the cells can be fixed with PfA buffer, so they can be stored by 4 °C in the dark up to one week before being measured by FACS.

FACS buffer: 1% BSA und 0.05% sodium azid in 1x PBS

PfA buffer: 1% paraformaldehyd in 1x FACS buffer

2.2.5 siRNA mediated gene silencing in Flp-In 293K^b transfectants

Small interfering RNA (siRNA) are duplexes of about 21 nt with 3'-overhangs, which mediate sequence-specific mRNA degradation. In mammalian cells siRNA molecules are capable of specifically silencing gene expression without induction of the unspecific interferon response pathway. An effective strategy to deliver siRNAs to target cells in cell culture includes electroporation.

2.2.5.1 Electroporation

To asses the function of TPPII, ThOP1 and IDE upon SIINFEKL presentation on the cell surface, knockdowns of these proteases were performed using the siRNA technology. The siRNA duplexes were electroporated (Gene Pulser II) under the following conditions: Voltage 240 mV and capacity 600 µF; For the electroporation a single cell suspension of 2*10^6 Flp-In

293K^b transfectants per setting were diluted in 100 µl of medium (DMEM without FCS). In separated RNAse free reaction tubes the siRNA was prepared for the electroporation: 1 µM siRNA per setting in 100 µl DMEM without FCS. Directly before electroporation the siRNA and the cells were added to the 0.4 cm cuvette (Bio-Rad). After electroporation, 1 ml complete medium was added to the siRNA/cells suspension before seedeing them into 6-well-plates for further incubation at 37°C. As a control siRNA the scramble control (SC) randomized siRNA was used.

2.2.5.2 mRNA isolation

The mRNA expression level of the proteases knock-down was analyzed by real time PCR. The first step was isolating the mRNA from the siRNA electroporated cells. The cells were removed from the well, pelleted and 1 ml TRIzol reagent (MBI Fermentas) was added to 1x10^6 cells. This was performed according to the manufacturer's standard protocol.

2.2.5.3 Reverse transcription

A short double stranded nucleic region id formed by the oligo(dT)n-priming method, through the reaction of the oligo(dT)n with the poly(A)-tail of the mRNA molecule. This short dsDNA is needed as a starter for the reverse transcriptase to begin the first-strand sysnthesis.
The rection setting:

4 µl 5x Buffer M-MULV RT (MBI Fermentas)
2 µl 10 mM dNTPs
1 µl OligodT 100 µg/ml
12 µl H_2O DEPC
19 µl add to each mRNA Pellet

This mixture was incubated at 55°C in the thermocycler for 5 min to dissolve the mRNA pellet before adding 1 µl MuLV RT (MBI Fermentas) to each setting. After 1 h incubation at 42°C, 80 µl H_2O without DEPC were added.

2.2.5.4 Real time PCR

The PCR theoretically amplifies DNA exponentially, doubling the number of molecules present with each amplification cycle. The number of amplification cycles and the amount of

PCR end-product should allow one to calculate the initial quantity of genetic material, but numerous factors complicate this calculation. Real-time polymerase chain reaction, also called quantitative real time polymerase chain reaction (QRT-PCR), is a technique used to simultaneously quantify and amplify a specific part of a given DNA molecule. The DNA is quantified after each round of amplification using fluorescent dyes that intercalate with the double-strand DNA and modified DNA oligonucleotide probes that fluoresce when hybridized with a complementary DNA. This is the "real-time" aspect of it.

Therefore triplicates were used to measure the mRNA levels of the potentially knock-downed proteases. The IQ SYBR Green Supermix (Bio-Rad) and the iCycler (Bio-Rad) were used to perform this assay. The housekeeping gene for the elongation factor 1-alpha (EF1a) was used as internal control for the mRNA expression level. The primers used for identification of siRNA knock-down and for real-time PCR are included in section *2.1.8.*

Per triplicate:

28.8 µl	H_2O without DEPC
3.2 µl	primer mix
8 µl	cDNA
40 µl	2x Absolute SYBR Green Fluor (ABgene)
25 µl	per well in a 96-well-plate

2.2.6 Methods for protein analysis

2.2.6.1 Determination of protein concentration

To measure protein concentration the Roti®-Nanoquant (Roth) solution was used. In a 96-well-platte 50 µl of the sample or the BSA standard solution are added into the corresponding wells. The dilution series of the BSA standard: 0, 20, 40, 60, 80 und 100 µg/ml. Then 200 µl Roti®-Nanoquant solution (5x solution, 1:5 diluted with water) are added to each well at the same time with a 12-chanel-pipette. After incubating the plate for 5 min at room temperature the OD can be measured at 590 nm and 450 nm in the spectrometer (SpectraFluor, Tecan GmbH). The protein quantity is calculated out of the slope of the sample, which is determined by the straight line given by the BSA protein amount at the x-axis and the y-axis gives the OD 590/450.

2.2.6.2 Fluorogenic activity assays in vitro

Activity and inhibitor assays *in vitro* were always incubated by 37°C. If the proteasome was used for digesting peptides 1 µg was added to the reaction, otherwise a volume of 10-30 µl of a fraction from the HPLC or lysate was added to the reaction. In both cases the reaction is always diluted in 1x fluo-buffer.

If necessary inhibitors were added before adding the sample or peptides to the proteases and they were incubated for 10 min at 37°C. Afterwards the 100 µM substrate diluted in the 1x fluo-buffer was added and after 5, 30 and 60 min at 37°C the fluorescence of the leaving group was measured in spectrofluorometer (SpectraFluo, Tecan). The substrates used had an AMC (7-amido-4-methylcoumarine) or a ßNA (ß-Naphthylamid) as a fluorochrome. The release was measured by relative fluorescence units (RFU) in a spectrafluorometer at 37°C for 60 minutes.

AMC: λEx = 360 nm and λEm = 450 nm

ßNA: λEx = 340 nm and λEm = 405 nm

10x Fluo buffer:

100 mM Tris pH 7,6; 100 mM NaCl; 100 mM KCl; 20 mM $MgCl_2$; 1 mM EDTA, 5 mM DTT

Substrates*	**Fluorochrome group cleaved by**
Suc-LLVY-AMC	Proteasome: chymotrypsin subunit
Suc-AAF-AMC	Proteasome: chymotrypsin subunit
L-AMC	amino peptidases
Y-AMC	amino peptidases
H-AAF-AMC	TPPII
suc-FGL-ßNA	ThOP1

* All substrates were solved in DMSO as a 10 mM stock, aliquoted and stored at -20°C.

2.2.7 LCL721 cells cytosol purification

2.2.7.1 Cytosol extraction

For the extraction of the cytosol a pellet of 7 ml LCL721 cells was used. After resuspending the pellet in lysis buffer (1:2), the cells were ultrasonicated (Sonoplus RD2070) 5 cycles for

30 sec, tip T73. During sonication the tube with the cells was surrounded by ice water. All steps of the lysis were performed on ice or at 4°C. After controlling the lysis by trypanblue exclusion, the lysate was aliquoted into ultracentrifugation tubes (Eppendorf) and an ultracentrifugation step of 1h at 4°C and 100.000 g followed, using the rotor 70 Ti (CENTRIKON T-1065, Kontron Instruments). After the separation of the lysate from cell debris by the ultracentrifugation step, 11 ml of lysate remained.

Lysis buffer: 30 mM TrisHCl pH 7.6; 2 mM $MgCl_2$; 0.1 mM EDTA; 1.5 mM DTT ; 0,3% TritonX100

2.2.7.2 Lysate purification of LCL721 cells by HPLC

The purification of the complete LCL721 cytosol was carried out using four chromatography columns. All steps were performed in an ÄKTApurifier (GE Healthcare) at 4°C. The buffers used in all purification steps are listed below:

TSGD-Buffer A:

20 mM TrisHCl pH 7.6, 10 mM KCl, 2 mM $MgCl_2$, 0.1 mM EDTA, 0,5 mM DTT,
5% Glycerol

TSGD-Buffer B:

20 mM TrisHCl pH 7.6, 10 mM KCl, 2 mM $MgCl_2$, 0.1 mM EDTA, 0,5 mM DTT,
5% Glycerol, 1 M NaCl

Overview of the purification steps:

Column	CV*	Equilibration	Flow	Gradient	Fraction size
HiTrap Desalting 26/10	50 ml	100% buffer A	3 ml/min	Linear 0% B	4 ml
DEAE-Toyopearl 650 S 16/50	100 ml	100% buffer A	2 ml/min	5 CV 0%-20% B 2 CV to 30% B	4 ml
S200 HR10/300	25 ml	10% buffer B	0.4 ml/min	Linear 10% B	0.5 ml
Mini Q™ (4.6/50 PE)	1 ml	100% buffer B	0.5 ml/min	30 CV 0-20% B	0.5 ml

*CV: column volume

1. Desalting the sample

The desalting of the sample using a "HiTrap Desalting 26/10" column is based on gel filtration chromatography (GC). GC separates proteins, peptides, and oligonucleotides on the basis of size. Molecules move through a bed of porous beads, diffusing into the beads to greater or lesser degrees. Smaller molecules diffuse further into the pores of the beads and therefore move through the bed more slowly, while larger molecules enter less or not at all and thus move through the bed more quickly. Both molecular weight and three dimensional shape contribute to the degree of retention. Gel Filtration Chromatography may be used for analysis of molecular size, for separations of components in a mixture, or for salt removal or buffer exchange from a preparation of macromolecules.

For this first step the buffer used was TSDG-buffer A pH 7.6 (of low ionic strength). Thus the protein fractions collected and pooled from this column were desalted and in an alkali milieu, which is necessary for the next purification step, "Ion Exchange Chromatography" (IEX) column.

2. DEAE column (IEX)

"Ion Exchange Chromatography" (IEX) relies on charge-charge interactions between the proteins in the sample and the charges immobilized on the resin of choice. For this IEX-step a "DEAE Toyopearls 650S HR16/50" column (Tosoh Corporation) was chosen. The immobilized functional group, DEAE (diethylaminoethane), of this column is positive and the binding anions are negative proteins in the lysate. Anion exchange chromatography is often used as a primary chromatography step due to its high capacity and ability to bind up and separate fragmented nucleic acids and lipopolysaccharides from the initial slurry.

After equilibrating and then applying the whole cytosol lysate with a buffer (TSGD-buffer A) of low ionic strength, then the bound molecules were eluted off using a gradient of a second buffer (TSGD-buffer B) which steadily increases the ionic strength of the eluent solution. The salt in the solution competes for binding to the immobilized matrix and releases the protein from its bound state at a given concentration. After testing the fractions for endopeptidase activity using the suc-LLVY-AMC (*2.2.6.4*), the activity fractions were pooled and concentrated using Amicon-devices to 500 µl for the next step.

3. S200 column (GF)

The next purification step was performed using a gel filtration chromatography column, "Superdex S200 HR10/300" (GE Healthcare-Lifesciences). Superdex is a composite medium

based on highly cross-linked porous agarose particles to which, dextran has been covalently bonded. The result is media with high physical and chemical stability, due mainly to the highly cross-linked agarose matrix, and excellent gel filtration properties determined mainly by the dextran chains.

The aim of this gel filtration step is to separate the components in the DEAE pooled fractions and to determine the molecular size of the eluents showing activity. Therefore a linear gradient of 10% TSGD-buffer B was applied. The eluted fractions were tested for endopeptidase activity using the suc-LLVY-AMC (*2.2.6.4*).

4. Mini Q™ column (IEX)

For the last purification step a Mini Q™ (4.6/50 PE) column (GE Healthcare-Lifesciences) was used, which carries a strong quaternary ammonium anion as functional group. The extremely small bead diameter (3 µm) of these mini beads gives exceptional resolution with high reproducibility. Before applying the sample pooled, it was diluted with TSGD-buffer A in a 1:2 ratio to adjust the pH. Like with the DEAE column, the bound proteins were eluted applying a gradient with TSGD-buffer B. The fractions were again tested for endopeptidase activity using the suc-LLVY-AMC (*2.2.6.4*).

Functional groups of the used anion exchange chromatography columns:

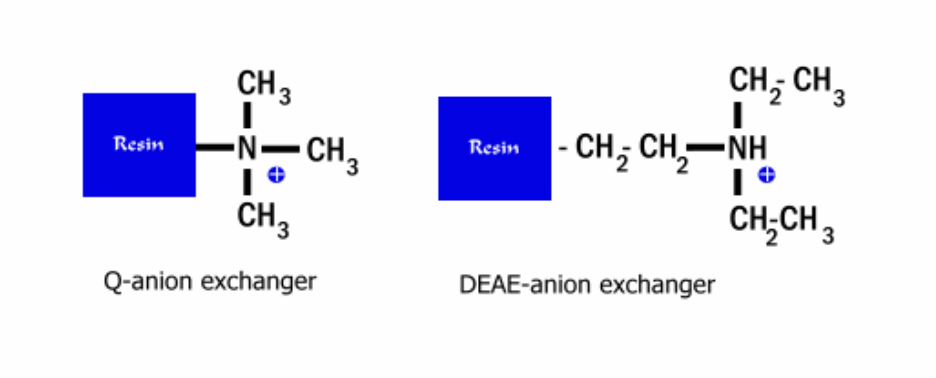

The fractions eluted from the different columns were always tested for activity with the 100 µM suc-LLVY-AMC substrate (see section *2.2.6.4*). This substrate was chosen, because due to the succinyl group that protects the N-terminus, the AMC leaving group can only be cleaved by an endoprotease. For the activity assays 2 µl of the DEAE-fractions and 20 µl of the S200 and Mini Q™ fractions were taken. Test the activity fractions for lactacystin [50 µM] and butabindide [200 µM] dependence incubating the inhibitor first for 10 min with the fraction.

2.2.7.3 Reducing SDS-PAGE

The purpose of the SDS-PAGE (sodium dodecylsulfate polyacrylamide gel electrophoresis) technique is to separate proteins strictly according to their molecular weight. The solution of proteins to be analyzed is first mixed with SDS, an anionic detergent, which denatures secondary and non–disulfide–linked tertiary structures, and applies a negative charge to each protein in proportion to its mass (primary structure, or number (and size) of amino acids). The SDS binds to the protein in a ratio of approximately 1.4 g SDS per 1.0 g protein, giving an approximately uniform mass:charge ratio for most proteins, so that the distance of migration through the gel can be assumed to be directly related to only the size of the protein. Besides the addition of SDS, proteins are briefly heated in the presence of a reducing agent, such as dithiothreitol (DTT) or ß-mercaptoethanol (beta-mercaptoethanol/BME), which further denatures the proteins by reducing disulfide linkages, thus overcoming some forms of tertiary protein folding, and breaking up quaternary protein structure (oligomeric subunits).

In this work a discontinuous buffer system was used. During electrophoresis in a discontinuous gel system, an ion gradient is formed in the early stage of electrophoresis that causes all of the proteins to focus into a single sharp band. To prepare the samples 1x sample buffer and 1 µl 1 M DTT to 10 µl sample was added before incubating them for 5 min at 95 °C. After loading the samples, the gel was run in 1x running buffer at 100-150 V and 20 mA per gel until 1 cm before the tracking band of bromphenol blue is eluted from the gel.

Mol. weight standard:	Prestained protein marker, broad range (6-175) kDa from Fermentas
separating gel:	1.5 M tris-HCl, pH 8.6, 0.1% SDS, 8-15% (w/v) acrylamid/ bisacrylamid (29:1), 0,1% APS, 0.05% TEMED
stacking gel:	0.5 M tris-HCl, pH 6.8, 0.1% SDS, 5% (w/v) acrylamid/bisacrylamid (29:1), 0.1% APS, 0.05% TEMED
5x sample buffer:	50% glycerine, 2% SDS, 5% ß-mercaptoethanol, 0.1% bromphenol blue, 0.5 M tris-HCl pH 6.8
5x running buffer:	1.25 M glycine, 0.125 M tris-HCl, 0.5% SDS

2.2.7.4 Coomassie staining

Following electrophoresis, the gel was stained with Coomassie Brilliant Blue R-250 allowing visualisation of the separated proteins. The anion of Coomassie Brilliant Blue formed in the

acidic staining medium combines with the protonated amino groups of proteins by electrostatic interaction. The resulting complex is reversible under the proper conditions. After electrophoresis the gel is incubated in the coomassie staining solution (0.2 % (w/v) Coomassie Brilliant Blue R-250 in 40 % methanol, 10 % acetic acid, 50% H_2O) for 30 min at room temperature. The destaining takes a few hours in the following solution: 40 % methanol, 50 % ddH_2O, 10 % acetic acid.

2.2.7.5 Analysis by mass spectrometry

Mass spectrometry is an analytical technique used to measure the mass-to-charge ratio of ions. Mass spectrometry is an important method for the characterization of proteins. The two primary methods for ionization of whole proteins are electrospray ionization (ESI) and matrix-assisted laser desorption/ionization (MALDI).

After separation in a SDS-PAGE gel, the activity fractions from the LCL721 cytosol purification were analyzed using an hybrid quadrupole orthogonal acceleration time of flight mass spectrometer (Q-Tof Premier™, Waters) equipped with an electrospray ion source (ESI). First, the bands of interest detected on the SDS-PAGE gel were excised and the proteins in the gel bands enzymatically digested into smaller peptides using trypsin. After Elution of the resulting peptides from the gel, the samples were separated by the reversed phase capillary HPLC. The outlet of the separation column was directly connected to the ESI mass spectrometer, using a nano-electrospray ion source. The resulting mass spectra were automatically processed using PLGS2.3 and searched against the Swissprot database. The identification of the proteins in the gel bands using mass spectrometry was performed by Dr. Tenzer from the mass spectrometry core facility, Institut of Immunology in Mainz.

Aliquots of the tryptic digests (2.5 µl) were separated by HPLC (nanoACQUITY UPLC™, Waters), equipped with a 75 µm x 150 nm BEH C18 1.7 µm column.

Eluent A: 0.1 % formic acid in water (mass spec. grade)

Eluent B: 0.1 % formic acid in acetonitrile (mass spec. grade)

Flow: 300 µl/min

Gradient: start at 3% B; go to 7% in 2 min; go to 25% B in 72 min; go to 35% B in 30 min; go to 90% B in 5 min.

3 Results

3.1 Screening system

Peptides presented by MHC class I molecules for CTL recognition are derived mainly from cytosolic proteins. As already mentioned in the introduction, antigen presentation on the cell surface requires correct proteasomal processing, trimming by cytosolic and ER aminopeptidases, efficient TAP transport and sufficient binding to MHC class I. The efficiency of the epitope generation depends not only on the epitope itself but also on its flanking regions. Furthermore, the prevailing assumption is that proteasomal cleavages are exclusively responsible for the generation of the final C-termini of CTL epitopes (Craiu et al., 1997; Mo et al., 1999).

To investigate the preferences of proteasomal cleavage the following system was developed, based on the CTL epitope SIINFEKL (aa 257-264) as a model antigen. SIINFEKL (also S8L) is a well characterized epitope derived from the chicken ovalbumin and is presented on the murine MHC class I molecule, H-2K^b with high binding affinity. To analyze the influence of the C-terminal flanking region on MHC class I restricted antigen presentation, several constructs were generated containing the S8L sequence, each encoding different C-terminal amino acids at positions P1' and P2' (figure 3.4). After transfecting a specific cell line (Flp-In 293K^b) with the construct coding for S8L, the H-2K^b/SIINFEKL complex can be detected on the cell surface by staining with a specific monoclonal antibody, the 25-D1.16 (Porgador et al., 1997). By comparing the presentation of this epitope on the cell surface of all the different transfectants, it is possible to analyze the influence of different amino acids at the P1' and P2' positions on processing and presentation of SIINFEKL. Furthermore the influence of a functional proteasome was tested to investigate a possible proteasomal dependence on generation of the S8L epitope, employing the generated S8L constructs. According to recent publications (Seifert et al., 2003) it has been shown that the cytosolic peptidase TPPII (tripeptidyl peptidase II) is required for the generation of the correct C-terminus of the HLA-A3-restricted HIV epitope Nef(73-82) and thereby implicating that there might be other endopeptidases involved in antigen processing and presentation than the proteasome in the eukaryotic cytosol. In this work the occurrence of such an endopeptidase was further elucidated.

3.1.1 The Flp-In System

The Flp-In System has been chosen for this project, because it allows a single integration and expression of the gene of interest in mammalian cells at a specific genomic location. Furthermore the resulting transfectants are isogenic stable cell lines. Therefore, the Flp-In 293 cell line, containing a single integrated Flp Recombination Target (FRT) site in the genome and stably expressing the *lacZ*-Zeocin fusion gene under the control of the SV40 early promoter was chosen. The FRT site (figure 3.1) serves as the binding and cleavage site for the Flp recombinase. For our purpose this cell line was transfected with a plasmid for H-2K^b expression on its cell surface (Tenzer, 2004). As mentioned before, the S8L antigen can only be presented on the murine H-2K^b molecule.

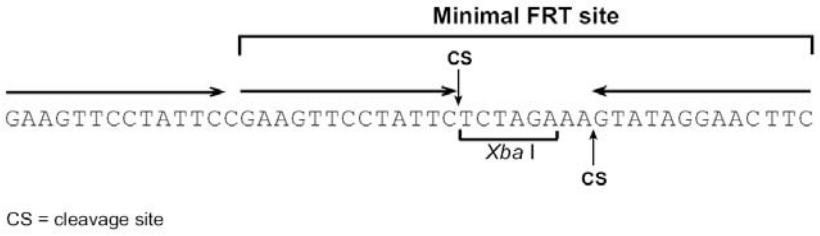

Figure 3.1: The Flp-In Recombination Target (FRT) site. The FRT site, originally isolated from *Saccharomyces cerevisiae*, serves as a binding site for Flp recombinase and has been well-characterized. The minimal FRT site consists of a 34 bp sequence containing two 13 bp imperfect inverted repeats separated by an 8 bp spacer that includes an *Xba* I restriction site. An additional 13 bp repeat is found in most FRT sites, but is not required for cleavage. While Flp recombinase binds to all three of the 13 bp repeats, strand cleavage actually occurs at the boundaries of the 8 bp spacer region.

To transfect the S8L constructs into the Flp-In 293K^b cells, a plasmid is needed called pcDNA5/FRT expression vector, which has a MCS site for the cloning of the gene of interest and a FRT site embedded in the 5′ coding region. The expression of the gene of interest is controlled by the human CMV promoter. The vector also contains the hygromycin resistance gene, which lacks a promoter and the ATG initiation codon. This ensures that only after a correct insertion into the FRT site of the genome the cells are hygromycin B resistant. This antibiotic is used for the selection of stable transfectants. Additionally, the pcDNA5/FRT expression vector has been modified for EGFP monitoring of the SIINFEKL expression (see *2.1.8*). The new resulting vector, which has been used in this project, is called pEntry2. For further information on the cloning steps see the dissertation of Dr. Tenzer, 2004. Furthermore,

for a successful transfection a second plasmid is required, the pOG44, which is responsible for the Flp recombinase expression under the control of the human CMV promoter. Generation of Flp-In expression cell lines requires co-transfection (see Fig. 3.2) of the Flp-In cell line with the pEntry2 and the Flp recombinase expression plasmid, pOG44. Flp recombinase mediates insertion of the Flp-In expression construct into the genome at the integrated FRT site through site-specific DNA recombination.

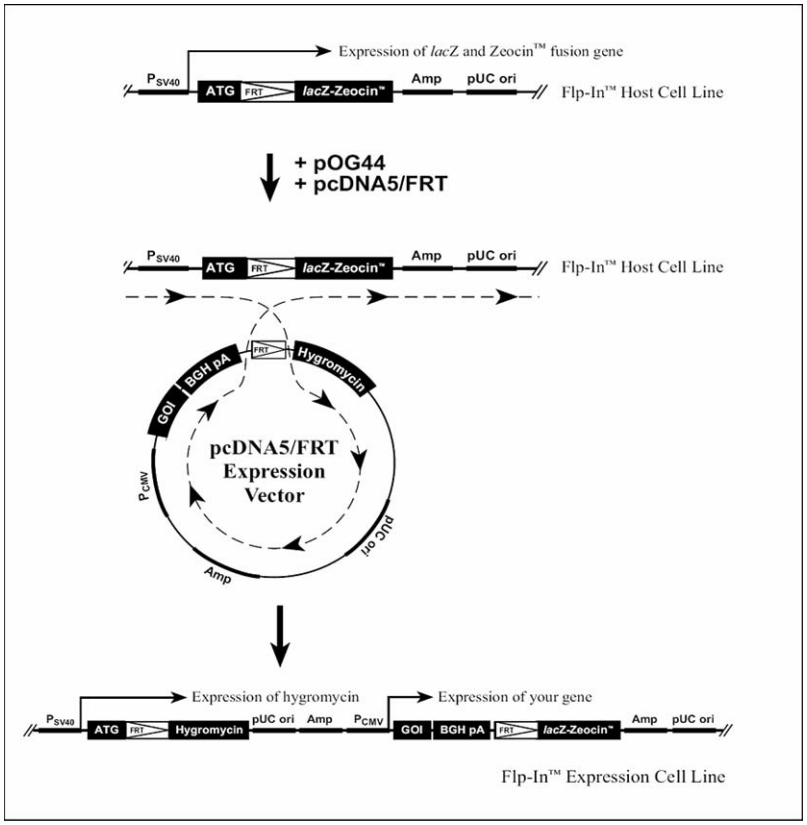

Figure 3.2: Generation of a Flp-In expression cell line. The pOG44 plasmid and the pcDNA5/FRT (pEntry2) are cotransfected into the Flp-In host cell line. Upon cotransfection, the Flp recombinase expressed from pOG44 mediates a homologous recombination event between the FRT sites (one integrated into the genome and the other on pcDNA5/FRT vector) such that the pcDNA5/FRT construct is inserted into the genome at the integrated FRT site. Insertion of pcDNA5/FRT into the genome at the FRT site brings the SV40 promoter and the ATG initiation codon into proximity and frame with the hygromycin resistance gene, and inactivates the *lacZ-Zeocin* fusion gene. Thus, stable Flp-In expression cell lines can be selected for hygromycin resistance, Zeocin sensitivity, lack of β-galactosidase activity, and expression of the recombinant protein of interest.

3.1.2 Generation of the SIINFEKL constructs

To investigate the preferences of proteasomal cleavage the following construct was designed (Fig. 3.3). As mentioned before the CTL epitope SIINFEKL (aa 257-264) has been used as a model antigen. It is a well-characterized epitope derived from the chicken ovalbumin and presented on the murine MHC class I molecule, H-2K^b. The construct starts with an ubiquitin molecule, which targets it for degradation. The last amino acids of the ubiquitin molecule are two glycines that are cleaved by hydrolases. The arginine at the beginning of the SIINFEKL-construct is the strongest known N-terminal degron (Varshavsky, 1997). This assures a rapid

turnover of this peptide construct. For further analysis two regions flank the ovalbumin sequence: on the N-terminal extension the ß-gal epitope (aa 96-103), which is presented on H-2K^b molecules; and on the C-terminal extension the influenza-A viral hemagglutinin (HA) epitope, that can be detected on a western blot with the monoclonal HA.11 antibody from the hybridoma clone 16B12. Both can be used for analysis and standardizing of the SIINFEKL expression level between the different transfected cell lines. The middle of the construct bears the 18 amino acid long sequence from the ovalbumin (252-269), comprising the SIINFEKL epitope (257-264). The two extensions flanking the SIINFEKL epitope, N-terminal (P1-P5) and C-terminal (P1'-P5') region are five amino acids long.

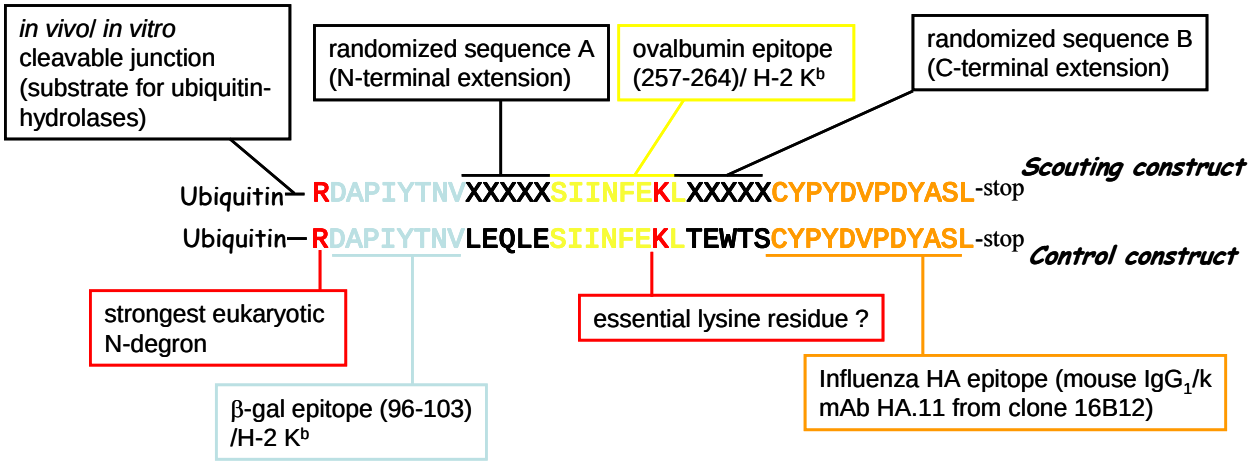

Figure 3.3: The SIINFEKL construct at amino acid level. The control construct contains the original ovalbumin sequence, which has been used for the generation of this construct. The scouting construct shows a randomized region at the c-terminal extension of SIINFEKL, where the amino acid exchanges have been performed to analyze processing and presentation of SIINFEKL. The X stands for the amino acid exchange at its position.

In this project, the focus lies on the influence of amino acids at the C-terminus upon processing and generation of the S8L antigen. Therefore the first three C-terminal positions (P1', P2' and P3') after S8L in the scouting construct are randomized (see Fig. 3.3). To analyze the influence of the C-terminal flanking region on MHC class I restricted antigen presentation, several constructs were generated encoding different C-terminal amino acids at positions P1', P2' and P3'. The positional scanning is shown in figure 3.4. When moving from the first to the second position of the C-terminal flanking region, an alanine was inserted at the first position to minimize the number of constructs. Alanine has been chosen, because it

has the least influence on processing, presumably due to its relative small residue. The amino acid exchanges have been performed in two ways: by oligonucleotide annealing and site-directed mutagenesis quick change PCR.

Oligonucleotide annealing is used to perform random mutagenesis (see *2.2.1.10*). The oligonucleotides were designed using the IUB-Codes (Codes of the International Union of Biochemistry) for mixed wobble bases. The IUB-Code letters V, H, D, B stand for any of three bases possible and N for any of four bases possible (see 2.1.8). Additionally these primers carry at the flanking ends the cleavage sites for *Xho*I and *EcoR*I, which are necessary for further cloning into the expression vector. Upon usage of these primers with the codes for mixed bases at the desired position for amplification by PCR this construct usually carries all four possible nucleotide exchanges. Subsequently, this PCR product was cloned through the *Xho*I/*EcoR*I sites into the pEntry2 expression vector and transformed into *E. coli* DH5α cells. Analyzes of the isolated plasmid DNA of the transformants, revealed that nearly all 20 amino acids were represented at the position of the desired amino acid exchange.

To perform a specific mutagenic insertion in the S8L construct site-directed mutagenesis by quick change PCR (see *2.2.1.9*) was used. This method is more efficient when using plasmids smaller than 4 Kb. In this respect, the pBluescriptKS plasmid was used for the generation of the first step constructs. Then the S8L construct carrying the desired mutation was cleaved (*Xho*I/*EcoR*I) out of the pBluescriptKS plasmid and ligated into the pEntry2 expression vector. All generated cell lines are listed in table 3.1.

Positional scanning:

P1‘X_{ori}: **N- LEQLE SIINFEKL XEWTS -C**

P1‘X&: **N- LEQLE SIINFEKL X -C**

P2‘X_{ori}: **N- LEQLE SIINFEKL AXWTS -C**

P2‘X&: **N- LEQLE SIINFEKL AX -C**

Figure 3.4: Positional scanning of the amino acid exchanges at the c-terminal extension of the S8L construct. At each position two different pools of peptides are generated: one carrying a stop-codon (=”&”) after the amino acid exchange and a second that continues with the original ovalbumin c-terminal sequence (“ori”). The red “X” stands for any amino acid that can be inserted at this position.

Amino acid		P1'Xori	P1'X&	P2'Xori	P2'X&	P'XXXX
&	Stop- Codon		P1'&		P2'C_13	P'RRori
A	Ala	P1'_Ala 1	P1'B_6	P2'D_31	P2'A&	P'RR&
C	Cys	P1'_Cys 11 #2	P1'B_15	P2'D_6	P2'C&	P'RRRori
D	Asp	P1'_Asp 2	P1'B_4	P2'1 Asp	P2'D&	P'RRR&
E	Glu	P1'_Glu #1	P1'A_15	P2'C_1	P2'E&	P'LLori
F	Phe	P1'_Phe 7	P1'B_8	P2'D_14	P2'F&	P'LL&
G	Gly	P1'_Gly 5	P1'A_5	P2'C_7	P2'G&	P'LAori
H	His	P1'_His 6	P1'B_His	P2'D_20	P2'H&	P'LA&
I	Ile	P1'_Ile 17	P1'B_40	P2'D_9	P2'I&	P'IR
K	Lys	P1'_Lys 13	P1'A_2	P2'C_37	P2'K&	
L	Leu	P1'_Leu 16	P1'A_6	P2'C_9	P2'L&	
M	Met	P1'_Met #1	P1'A_10	P2'C_3	P2'M&	
N	Asn	P1'_Asn 36	P1'B_46	P2'D_1	P2'N&	
P	Pro	P1'_Pro 66	P1'B_11	P2'D_29	P2'P&	
Q	Gln	P1'_Gln 55	P1'A_4	P2'C_14	P2'Q&	
R	Arg	P1'_Arg 43	P1'A_11	P2'C_2	P2'R&	
S	Ser	P1'_Ser 48	P1'B_12	P2'D_2	P2'S&	
T	Thr	P1'_Thr 50	P1'B_87	P2'Tori	P2'T&	
V	Val	P1'_Val 34	P1'A_19	P2'C_18	P2'V&	
W	Trp	P1'_Trp 12 #7	P1'A_3	P2'C_27	P2'W&	
Y	Tyr	P1'_Tyr 32	P1'B_Tyr_1.1	P2'D_5	P2'Y&	

Table 3.1: Generated constructs with the amino acid exchanges at P1', P2' and P'XXXX (randomized). The amino acids are listed on the left using the one letter and three letter amino acid codes. &: Stop-codon; ori: original amino acid sequence from the ovalbumin. X: randomized position, where the amino acid exchange takes place.

3.1.3 Detection of the H-2K^b/SIINFEKL complex

Once all SIINFEKL vectors were generated, the pEntry2 expression construct coding for S8L construct and the plasmid pOG44, encoding the recombinase, were co-transfected into the Flp-In 293K^b cells. The presentation of the SIINFEKL epitope on the H-2K^b molecule can be detected on the cell surface with a specific murine monoclonal antibody, the 25-D1.16 that recognizes specifically the H-2K^b/S8L as a complex. After staining with a secondary antibody, an allophycocyanin conjugated goat anti-mouse (gam-APC) antibody, the SIINFEKL presentation was measured by flow cytometry analysis (see figure 3.5). The expression of the SIINFEKL peptide in the transfectants was monitored by the expression level of the EGFP protein by flow cytometry (figure 3.5). Moreover, the EGFP expression level was used to normalize the measured SIINFEKL levels of the transfectants.

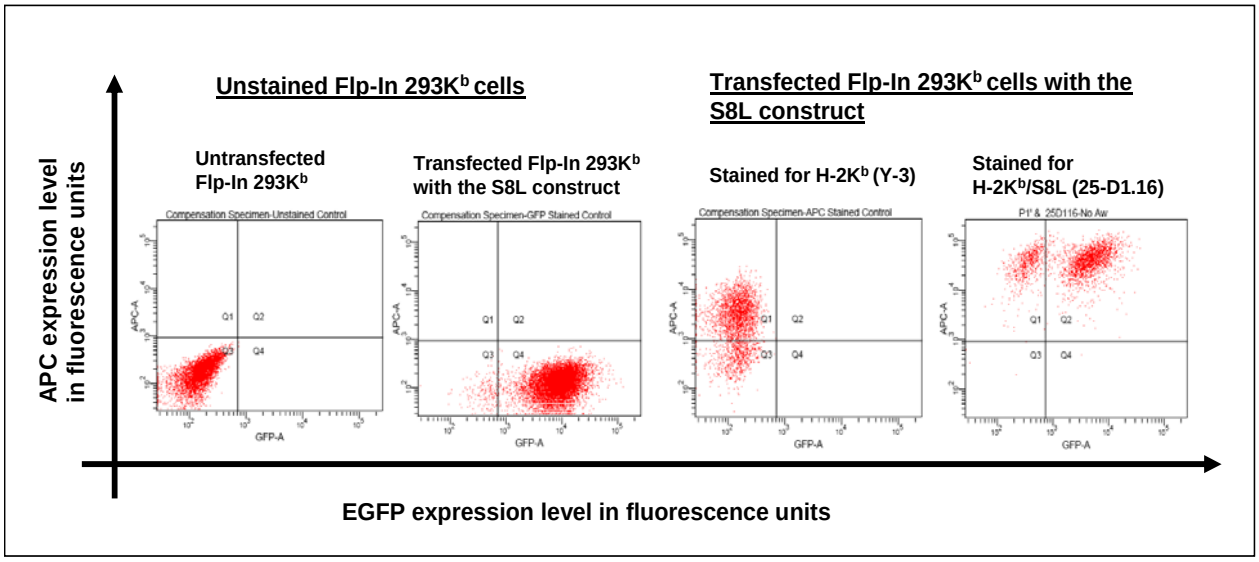

Figure 3.5: FACS analysis of the Flp-In 293K^b cell lines. The first two blots show unstained Flp-In 293K^b cells. The first one represents the host cell line Flp-In 293K^b, which is used for the S8L transfections. In the second blot the host cell line has been transfected with the pEntry2 S8L construct carrying plasmid. Hence, this cells show EGFP expression. The two next blots represent transfectant cells, where H-2K^b expression was detected using the Y-3 antibody (anti-K^b) and detection of the H-2K^b/S8L presentation with the specific monoclonal antibody 25-D1.16 (anti-H-2 K^b/S8L). The APC fluorescence level (Y-axis) of the secondary antibody (gam-APC) used for flow cytometry analysis represents the level of H-2K^b/S8L or the H-2K^b surface expression on these cells.

3.1.4 Steady state SIINFEKL presentation level of the transfectants

The SIINFEKL expression level of the Flp-In expression cell lines carrying the S8L constructs with the varying flanking C-terminal extensions was analyzed and compared with each other. To compare the S8L presentation, it is necessary to have the same turnover rates in these cells. For this purpose, the level of the EGFP expression was used to normalize the detected SIINFEKL presentation. The S8L cassette is directly followed by an IRES-EGFP cassette, which guarantees for uninterrupted, consecutive expression of the S8L and the EGFP. Hence, the SIINFEKL:EGFP expression rates in the cells are equal. Thus, the EGFP levels measured for the corresponding transfectants, can be used to normalize the measured S8L presentation. The SIINFEKL presentation of the cell lines generated with the S8L constructs carrying exchanged amino acids at the C-terminal position P1' and P2' are represented at figures 3.6-3.7. These transfectants show different presentation levels of the SIINFEKL epitope. As controls the following Flp-In 293K^b transfectants have been used: P1'&, P1'A$_{ori}$ and IR. The cell line P1'& carries a stop-codon (&)

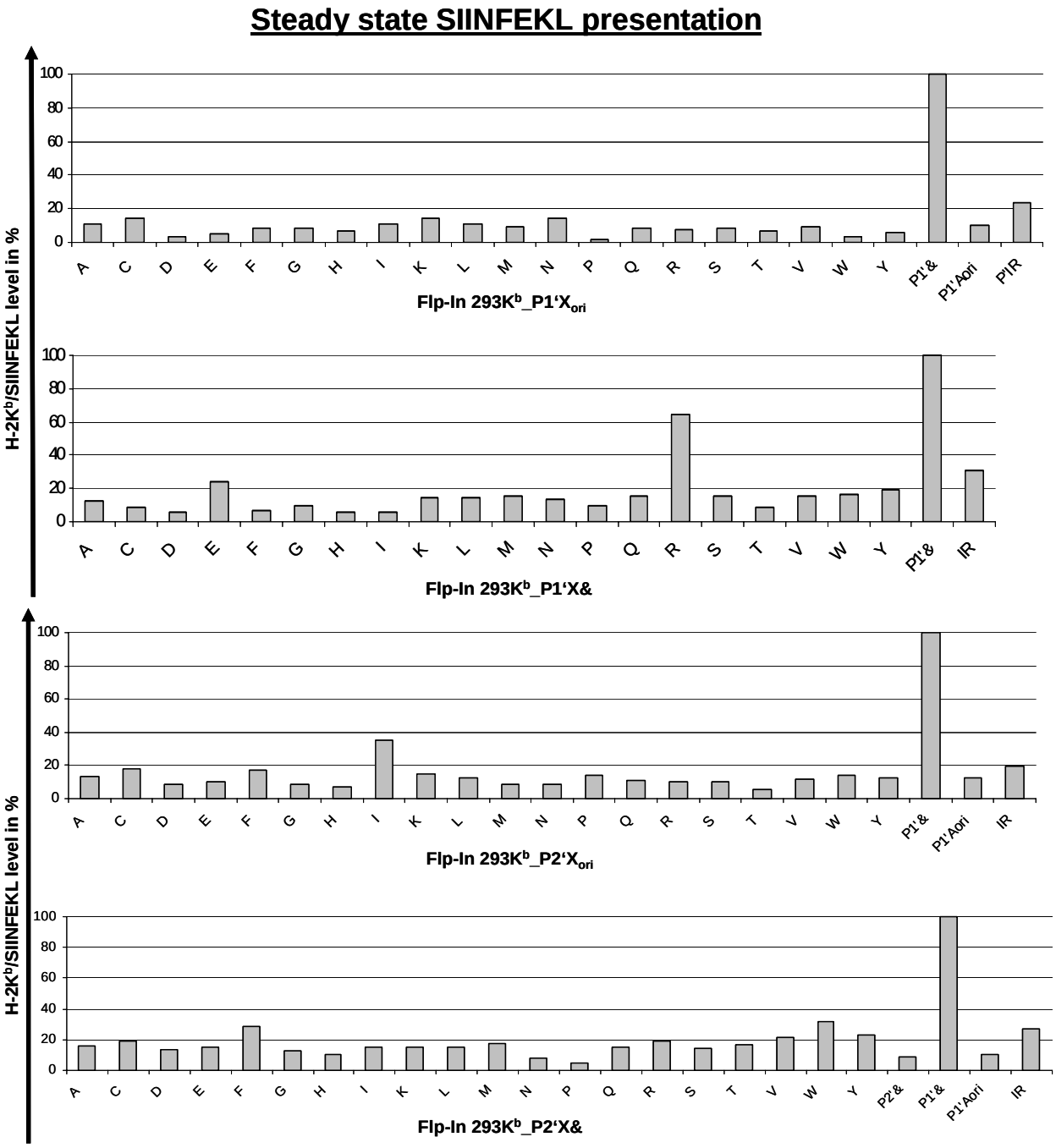

Figure 3.6: Steady state level of SIINFEKL on the cell surface of the Flp-In 293K^b transfectants. The x-axis represents the Flp-In 293K^b transfectants with amino acid exchanges at the P1' and P2' positions. The transfectants are named by the amino acid exchange using the one letter code (e.g. A = Alanine). The y-axis shows the APC mean fluorescence measured by flow cytometry using the gam-APC secondary antibody after having stained with the 25-D1.16 antibody. The APC level of each cell line represents the H-2K^b/S8L on its surface. The cell lines P1'&, P1'Aori and IR, have been used as controls. The symbol "&" is used to indicate a stop-codon at this position and the "ori" means that the precursor peptide carries at its c-terminal extension the original sequence of the ovalbumin up to five amino acids. All APC levels have been normalized with the EGFP expression.

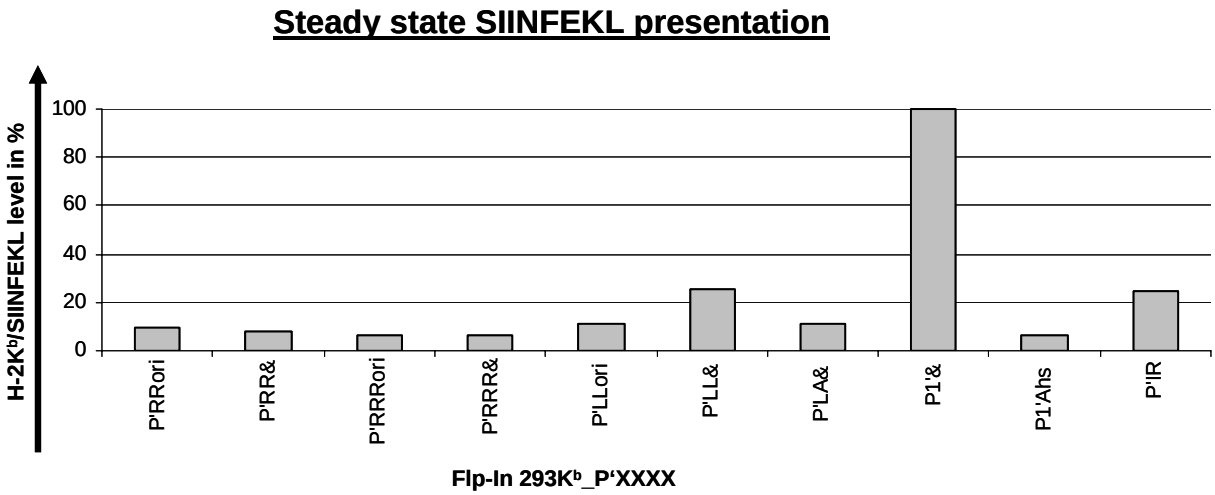

Figure 3.7: Steady state level of SIINFEKL on the cell surface of the Flp-In 293K^b transfectants. The x-axis represents the Flp-In 293K^b transfectants with amino acid exchanges at the P2' position. The transfectants are named by the amino acid exchange using the one letter code (P = proline). The y-axis shows the APC mean fluorescence measured by flow cytometry using the gam-APC secondary antibody after having stained with the 25-D1.16 antibody. The APC level of each cell line represents the H-2K^b/S8L on its surface. The cell lines P1'&, P1'Aori and IR, have been used as controls. The symbol "&" is used to indicate a stop-codon at this position and the "ori" means that the precursor peptide carries at its C-terminal extension the original sequence of the ovalbumin. All APC levels have been normalized with the EGFP expression.

directly after the leucine (L) of the S8L epitope (-SIINFEKL-). The translated N-terminal extended precursor peptide is shorter and ends with the leucine of the SIINFEKL itself. This implies that this precursor peptide does not require C-terminal processing. The cell line P1'A$_{ori}$ contains an alanine (A) after the S8L C-terminal leucine. The "ori" stands for the sequence of the original C-terminal amino acids from the ovalbumin protein. This means that the C-terminal part of this precursor peptide is the following: -SIINFEKL**A**EWTS-. The P'IR transfectant has an isoleucine (I) at P1' position and an arginine (R) at P2' position: -SIINFEKL**IR**WTS-.

3.1.5 Determination of SIINFEKL re-presentation rate on the cell surface

To analyse the re-presentation rate of the SIINFEKL transfectants, the cells were stripped by treating them with a citric acid (pH 2.7-3) for 1.5 minutes. This short "acid wash" makes all peptides dissociate from the MHC class I molecules. Hence, the cell surface is free of any epitope or peptide. Nevertheless, new loaded MHC class I molecules from the ER are transported to the cell surface through the golgi apparatus. The presentation of the new H-2K^b/S8L complexes was determined by staining (25-D1.16) the cell samples after acid wash

treatment and incubation at 37°C for 6 hours. Every two hours, samples were taken for the staining to perform a kinetic of the H-2K^b/S8L presentation. Moreover, by adding inhibitors to the cell media, the influence of proteases on generation of the SIINFEKL epitope can be analysed. In figure 3.8 the kinetic of two transfectants is shown with and without adding 50 µM lactacystin (LC), which is a proteasomal inhibitor. After the acid treatment (time point "0h"), both transfectants show no or very low levels of SIINFEKL on the cell surface. During the incubation at 37°C new loaded MHC class I molecules arrive at the cell surfaces of both transfectants. By adding 50 µM lactacystin the Flp-In 293K^b_P1'A$_{ori}$ cell line is strongly impaired (figure 3.8 A.) on S8L re-presentation, achieving only 27% of the S8L on the surface compared to the level attained by the assay without inhibitor. By treating the P1'& transfectant with lactacystin, a stronger re-presentation of the epitope could be observed. This S8L precursor peptide is only N-terminal extended and ends with the leucine of the SIINFEKL itself. Hence, this peptide does not need

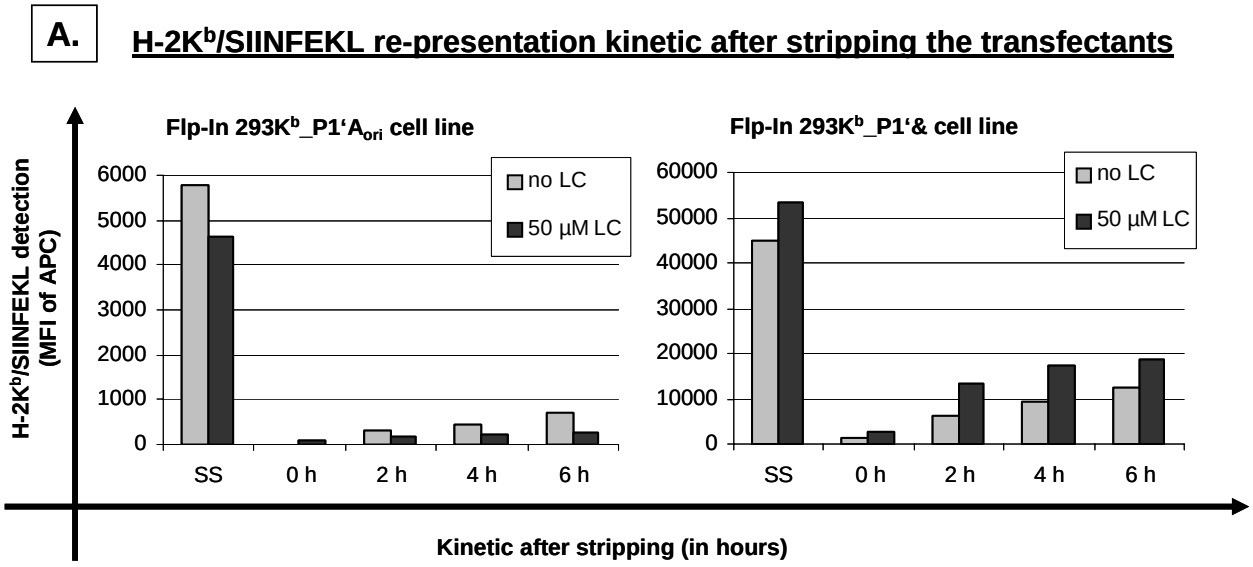

Figure 3.8-A.: H-2K^b/SIINFEKL re-presentation on the cell surface of the Flp-In 293K^b transfectants after stripping. The x-axis represents the different time points taken for the kinetic. The y-axis shows the APC mean fluorescence intensity (MFI) measured by flow cytometry using the gam-APC secondary antibody after having stained with the 25-D1.16 antibody first. The kinetic was also performed adding 50 µM lactacystin (LC) to analyze the proteasomal influence.

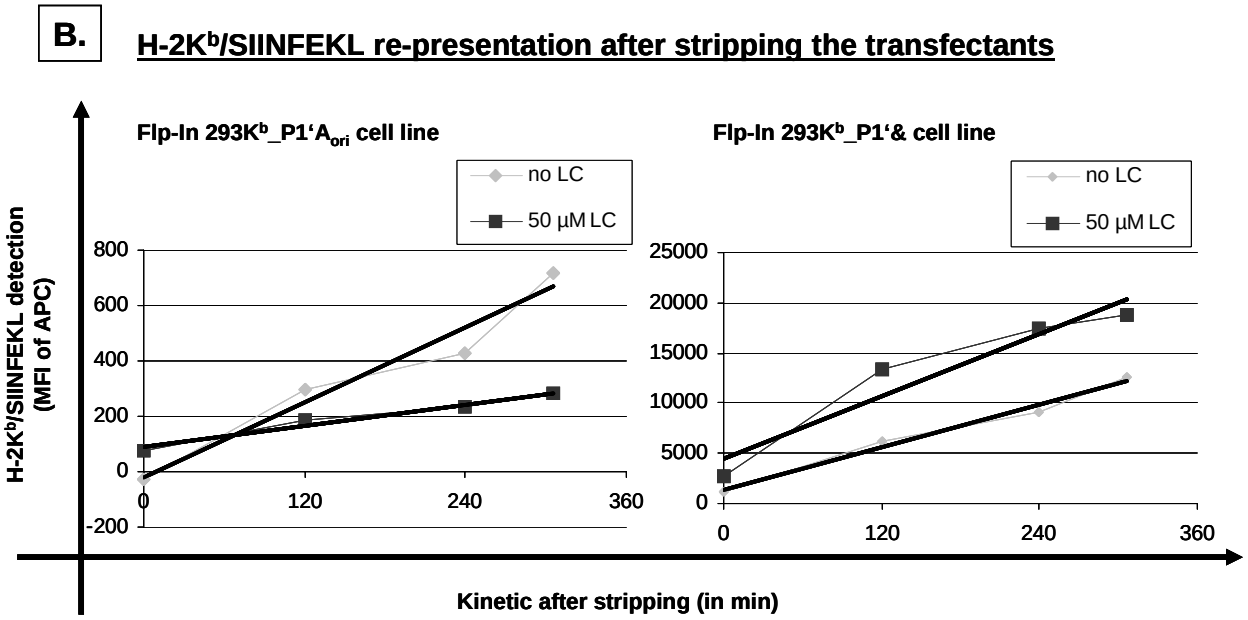

Figure 3.8-B.: Dot chart of the H-2K^b/SIINFEKL re-presentation levels from A. The x-axis represents the kinetic in minutes. The y-axis shows the APC mean fluorescence intensity (MFI) as in A. This diagram is used to calculate the slope of each kinetic.

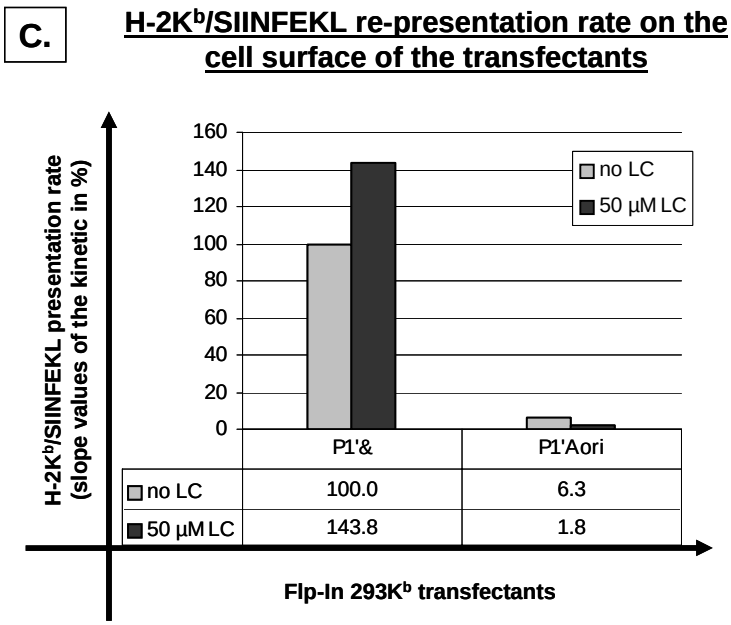

Figure 3.8-C.: H-2K^b/SIINFEKL re-presentation rates. The y-axis shows the S8L re-presentation rates given in %. The transfectant P1'& (no lactacystin) is set to 100% to calculate the rest of the rates, because it has the highest presentation level of S8L.

processing by the proteasome at the C-terminal extension for the generation of the S8L epitope and therefore seems to be independent on proteasomal activity. Furthermore, this S8L precursor peptide has no competition of other H-2K^b-epitopes, because it can be transported directly after N-terminal trimming into the ER, before other peptides still have to undergo proteasomal processing. This cell line (P1'&) has been used in all following stripping assays

as a positive control. After having analyzed the samples of the kinetic of both transfectants by flow cytometry, the APC mean fluorescence intensity (MFI) values are displayed in a dot chart to calculate the slope of each kinetic out of the trend line (figure 3.8 B.). The slope values calculated in % represent the H-2K^b/S8L re-presentation rates (figure 3.8 C.) of each transfectant in the different assays, with or without inhibitors. Because of the high S8L presentation level of the P1'& transfectant, the setting without lactacystin was chosen to be set to 100% to calculate the rates of all other transfectants.

3.1.6 *In vitro* inhibitor assays

Before using inhibitors to analyze the role of proteases in antigen processing and presentation, the inhibitors have been tested in *in vitro* assays. For this purpose, the cytosolic lysates of Flp-In 293K^b cells have been used adding a 100 µM proteasomal substrate (suc-LLVY-AMC) to analyse the chymotryptic activity of the proteasome (figure 3.9). The inhibitor was added to the lysate and incubated at 37°C for 10 minutes before adding the suc-LLVY-AMC. The setting without inhibitor (NI) shows the standard proteasomal cleavage activity in the lysate. In the range of 30 µM to 100 µM lactacystin a strong inhibition of the proteasome has been achieved. In further assays the concentration of lactacystin was of 50 µM. For epoxomicin a concentration of 1 to 3 µM is needed for inhibition. The standard dosage for further assays was 2 µM epoxomicin.

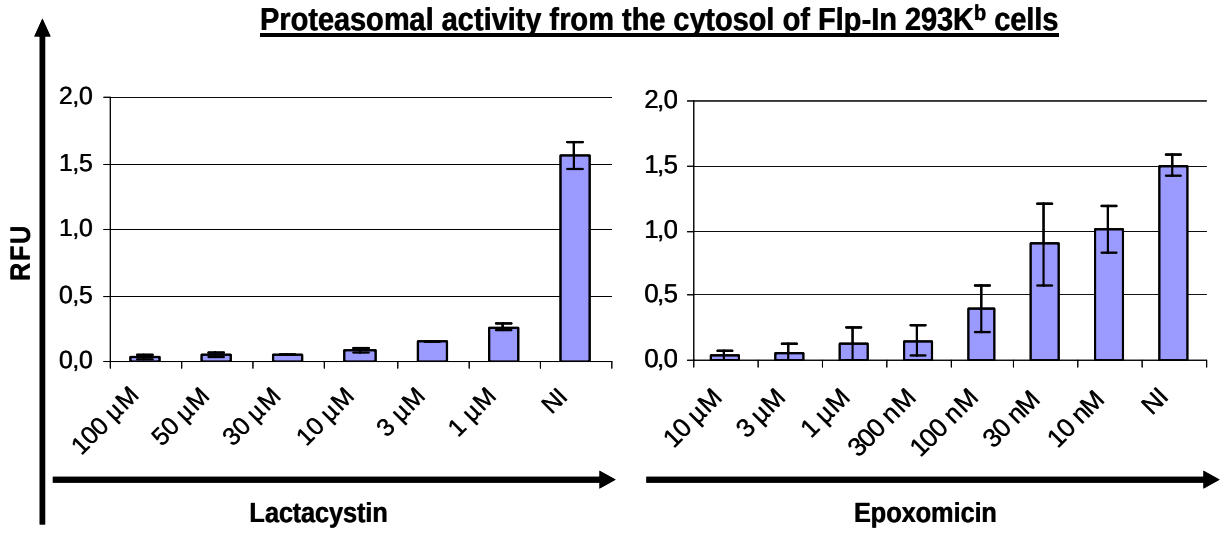

Figure 3.9: Titration of the proteasomal inhibitors lactacystin and epoxomicin. Both inhibitors have been titrated for proteasomal inhibition *in vitro* using the cytosol of Flp-In293K^b cells. In these *in vitro* assays the proteasomal activity has been determined using the substrate suc-LLVY-AMC. The release of AMC was measured by relative fluorescence units (RFU) in a spectrafluorometer (λEx = 360 nm and λEm = 450 nm) at 37°C for 30 minutes. "NI" stands for, No Inhibitor.

Moreover the inhibitors against TPPII (tripeptidyl peptidase II), AAF-CMK (Alanine-alanine-phenylalanine-chloromethylketone) and butabindide were also titrated to find the appropriate concentration for further assays. Lysates of the Flp-In 293K^b cells have been used for this titration to analyze the TPPII activity of these cells. After adding the corresponding inhibitor and incubating it 10 minutes at 37°C the AAF-AMC substrate was added for TPPII activity analysis. By a concentration of approximately 200 µM butabindide and 100 µM AAF-CMK a significant inhibition of the TPPII activity is achieved (figure 3.10).

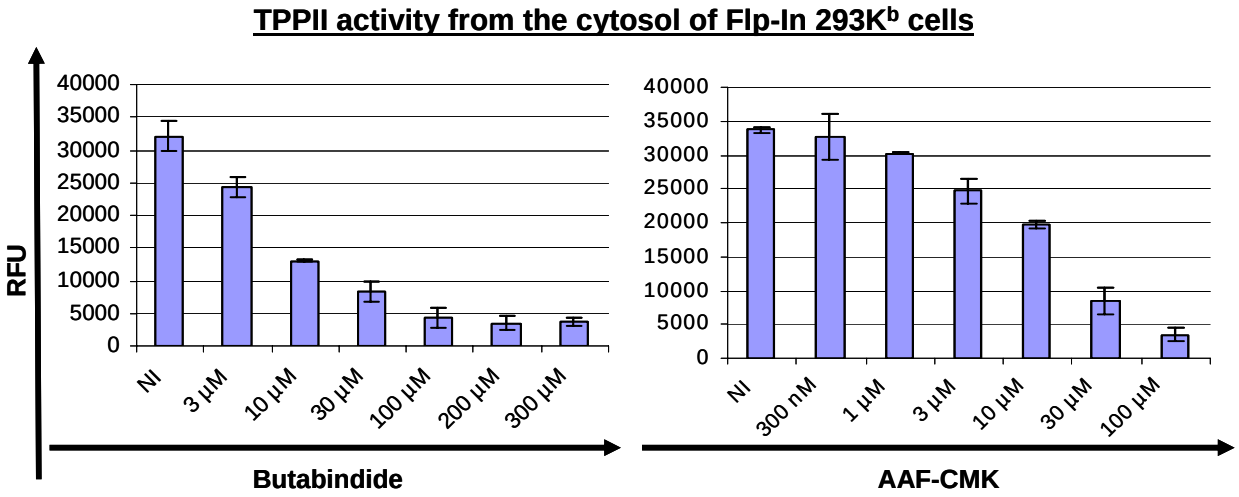

Figure 3.10: Titration of the TPPII inhibitors Butabindide and AAF-CMK. Both inhibitors have been titrated for TPPII inhibition *in vitro* using the cytosol of Flp-In 293K^b cells. The TPPII activity has been determined using the substrate AAF-AMC. The release of AMC was measured by relative fluorescence units (RFU) in a spectrafluorometer (λEx = 360 nm and λEm = 450 nm) at 37°C for 60 minutes. "NI": No Inhibitor.

3.1.7 MHC class I analysis after the acid treatment

In preliminary assays, the expression of the murine H-2K^b has also been analyzed to ensure the transport to the cell surface (figure 3.11). For this purpose, after stripping the cell surface of the cell lines with the constructs P1'A$_{ori}$ and P1'M$_{ori}$, the aliquots taken for the kinetic (every second hour) were stained with the Y-3 antibody (anti H-2K^b). Both kinetics show (figure 3.11) that after acid treatment the MHC class I molecules are still transported to the cell surface, even in the setting with lactacystin. Nevertheless, directly after the acid treatment these molecules are reduced on the cell surface for a short time, presumably because the low pH during the acid wash disrupts the association between the HC molecule and the ß-microglobuline. Nevertheless, they recover ~80% of their original level on the cell surface after four hours.

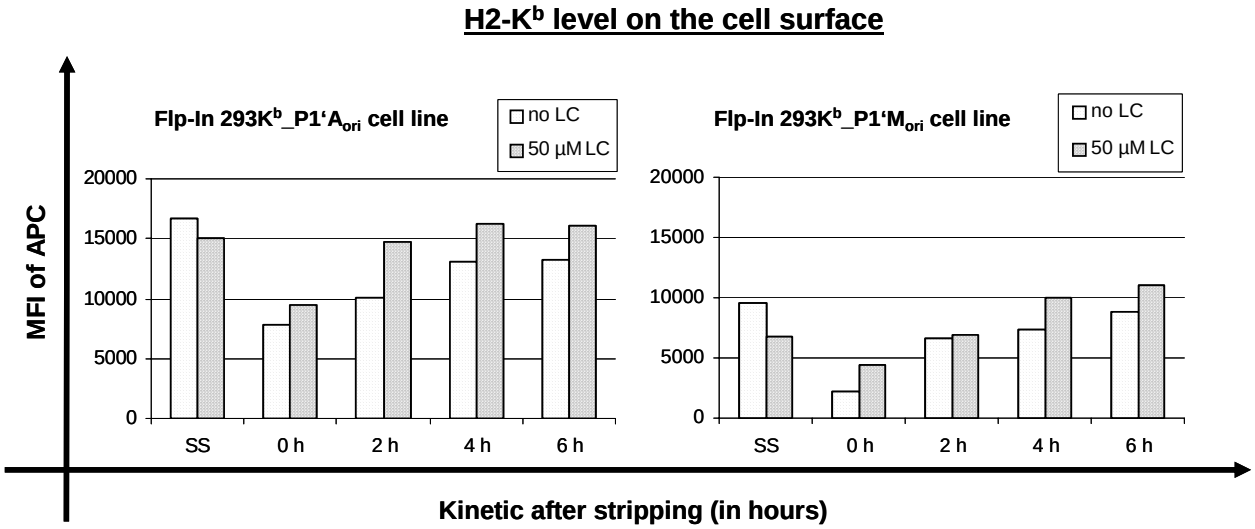

Figure 3.11: H-2K^b molecules on the cell surface of the Flp-In 293K^b transfectants, P1'A$_{ori}$ and P1'M$_{ori}$. The cell lines Flp-In 293K^b with the constructs P1'A$_{ori}$ and P1'M$_{ori}$, were treated with citric acid and then incubated at 37°C for 6 hours. Aliquots were taken each two hours. The aliquots and a reference sample from non treated cells (SS) were stained with the Y-3 antibody (anti H-2K^b) and the secondary gam-APC for FACS analysis. The y-axis shows the APC mean fluorescence intensity (MFI) measured by flow cytometry, which represents the H-2K^b level on the cell surface of the cells.

3.1.8 Determination of SIINFEKL re-presentation rate on the cell surface of all tranfectants and the influence of the proteasome on its presentation

To analyze the role of the different amino acids at the C-terminal flanking region of the SIINFEKL epitope on presentation, the cell surface of all transfectants was stripped as described in (*3.1.5*). Furthermore, the proteasomal dependence on the presentation of this epitope was determined by performing the same stripping assay and adding 50 µM lactacystin to the cells in a preincubation step before the stripping assay and after the stripping during the 6 h incubation. After this acid treatment, the cells were incubated for 6 hours and the re-presentation rate of each cell line was determined by the slope of the S8L re-presentation kinetic. Moreover, these rates were normalized with the EGFP mean fluorescence of each cell line. To be able to compare assays performed at different days, the P1'& cell line was included in each experiment and its S8L re-presentation rate was set to 100%. The following bar charts (figure 3.12 and 3.13) show the average values of the re-presentation rates calculated for at least three to five independent experiments. The steady state levels of the transfectants have already shown that it makes a difference having different amino acids at a specific position of the C-terminal flanking region of the epitope. For example, the construct

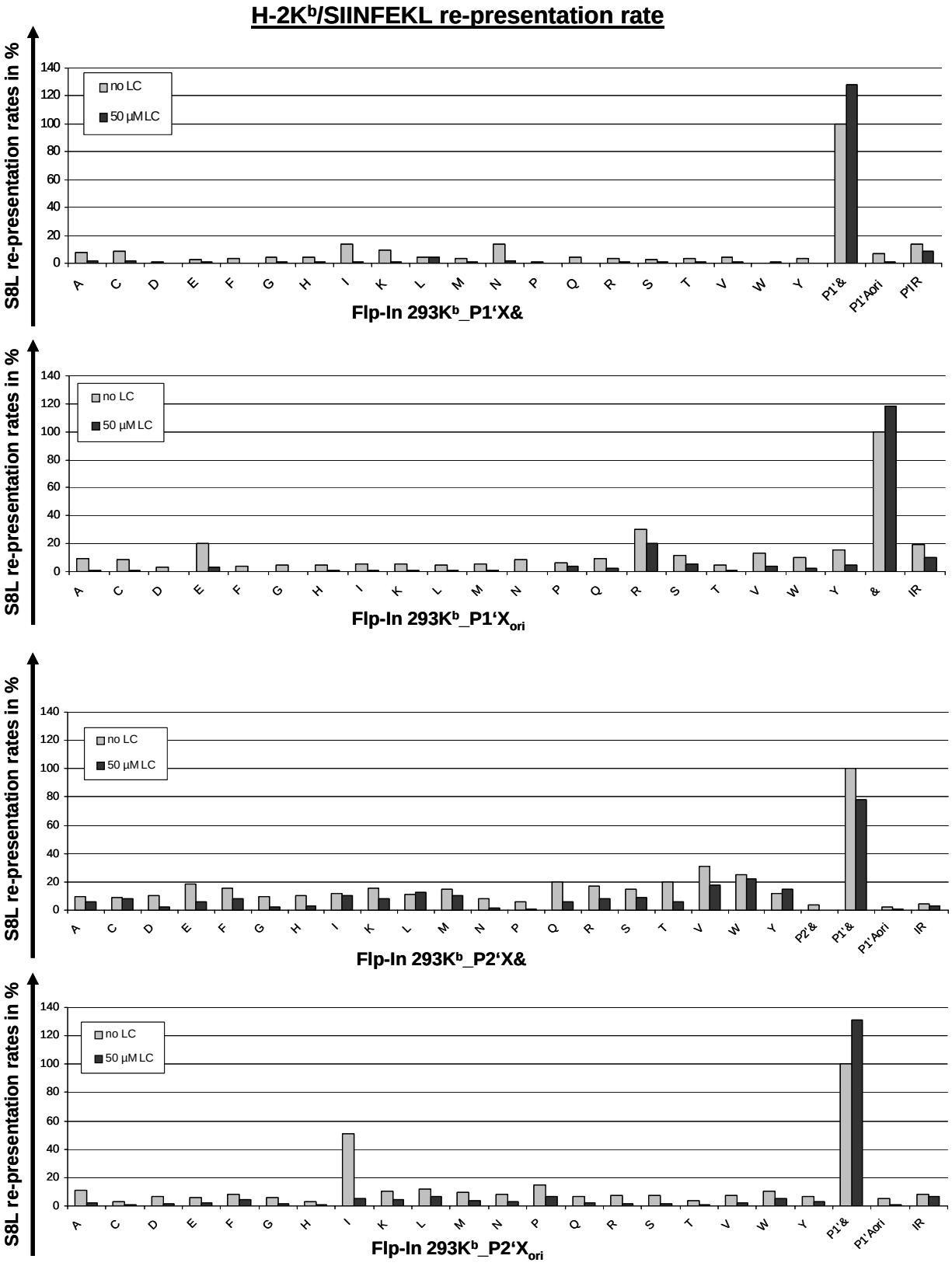

Figure 3.12: H-2K^b/SIINFEKL re-presentation of the Flp-In 293K^b transfectants carrying amino acid exchanges at the positions P1' and P2'.

P1'X_{ori} comprising an arginine exchange has a 4.2 higher S8L presentation rate then the arginine transfectant of the P2'X_{ori}. In addition, the arginine at the P1' followed by a stop-codon has a very low presentation rate. This implies that not only the position of the exchange, also the length of the epitope precursor plays a role in antigen generation. Besides, the re-presentation rates attained by adding lactacystin show in most cases a very low presentation of the S8L epitope. This indicates that if the proteasome is inhibited the S8L cannot be generated from those constructs. Nevertheless, despite proteasomal inhibition some constructs still achieve high rates of S8L presentation indicating a partial independence of the proteasome on generation of the SIINFEKL epitope. The constructs with the most significant rates despite inhibiting the proteasome are: -LEQLE*SIINFEKL***R**EWTS-, -LEQLE*SIINFEKL***IR**WTS-, -LEQLE*SIINFEKL***L**, -LEQLE*SIINFEKL***AW**. The case of the construct P'W& is not going to be analyzed, because the rates of S8L obtained are so low, that the slightest difference (between experiments) can make 100% of the originary rate. It is not a significant result. This is also the case for the transfectants with the constructs: P2'C& and P2'I&.

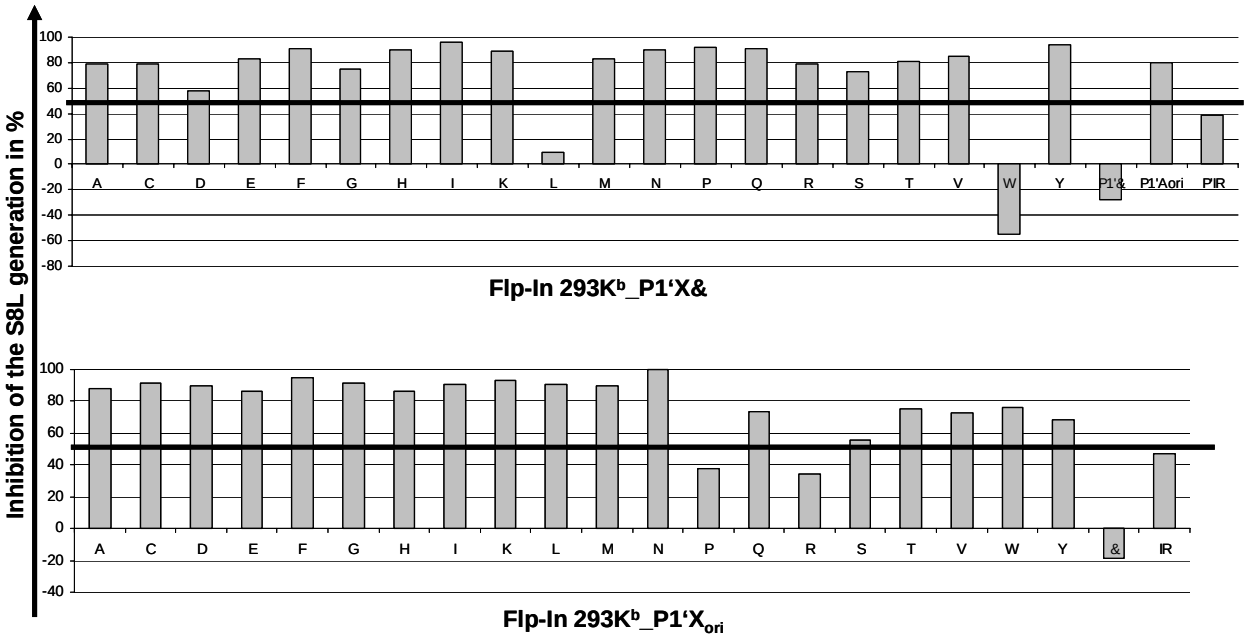

Figure 3.13: The inhibition of the SIINFEKL generation by adding lactacystin to the assay is shown here for the Flp-In 293K^b transfectants carrying amino acid exchanges at the position P1'. The bold line indicates the 50 % inhibition mark.

For a more specific analysis, the inhibition of the S8L epitope by using lactacystin was calculated and represented as a bar chart (figure 3.13, 3.14 and 3.15) for all transfectants. These charts point up that most S8L precursors are dependent on proteasomal cleavage for the generation of the SIINFEKL epitope. Interestingly, despite proteasomal inhibition with lactacystin some constructs still achieve to present more than 50% of S8L when comparing to the control rates without lactacystin (figure 3.13 and 3.14). The precursor peptides from the constructs P1'P_{ori}, P1'R_{ori}, P'L&, P'IR, P'AL&, P'AY& and P'AW& seem to be partially independent from proteasomal cleavage on S8L generation.

For further investigations constructs were cloned containing the amino acids arginine and leucine at specific positions, see figure 3.15. The constructs with one or two leucine amino acids at the C-terminal flanking region of the SIINFEKL epitope show a higher re-presentation rate, meaning that the S8L epitope is generated from this constructs at a higher rate than from the others.

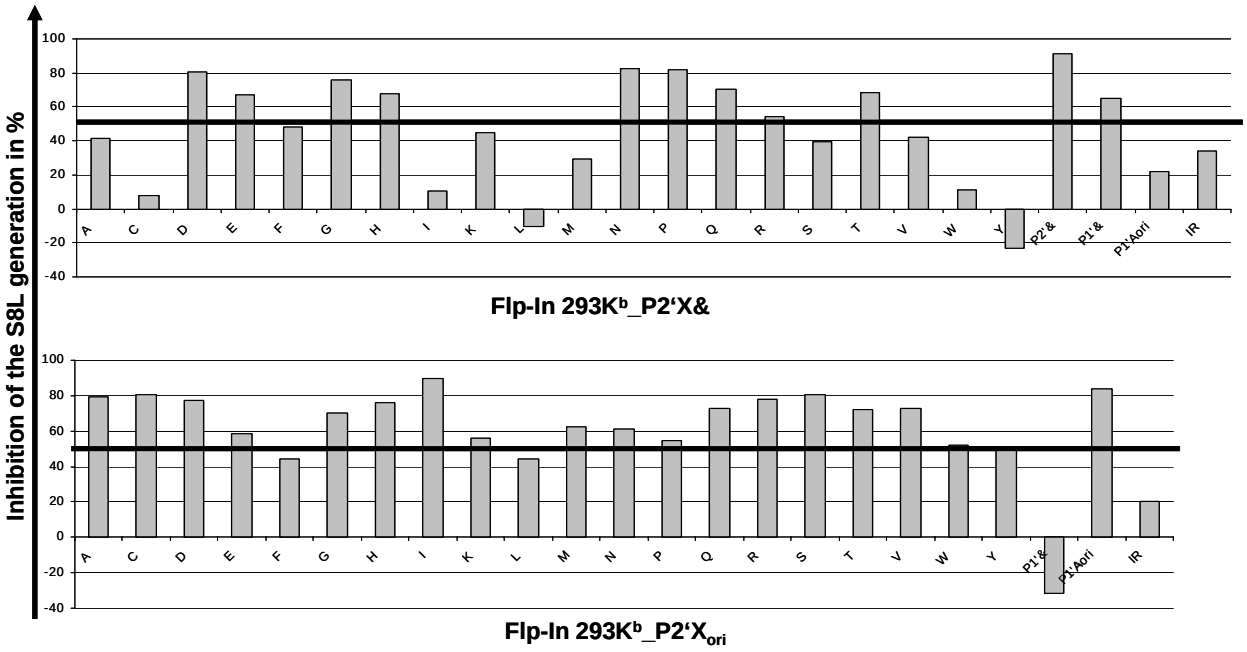

Figure 3.14: The inhibition of the SIINFEKL generation by adding lactacystin to the assay is shown here for the Flp-In 293K^b transfectants carrying amino acid exchanges at the position P2'. The bold line indicates the 50 % inhibition mark.

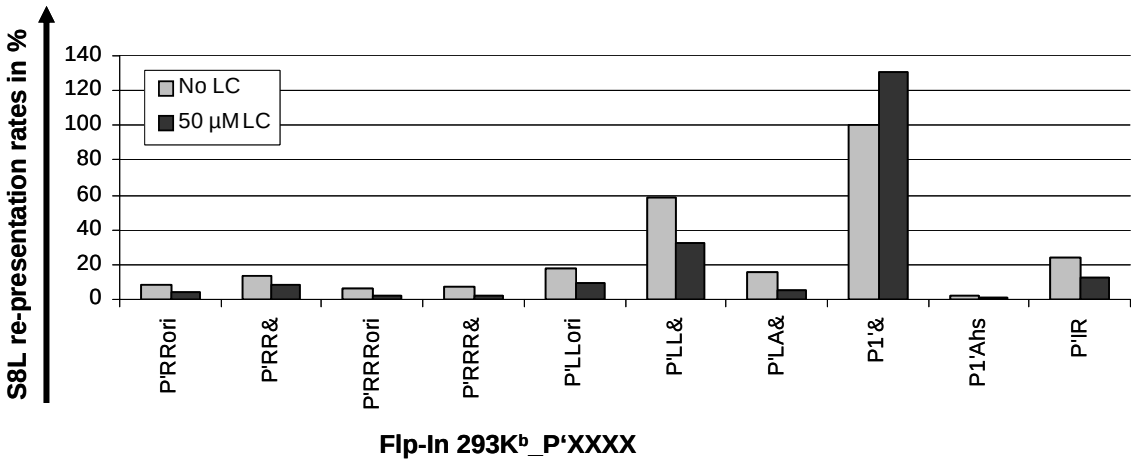

Figure 3.15: H-2K^b/SIINFEKL re-presentation of Flp-In 293K^b transfectants carrying selected amino acid exchanges.

Despite proteasomal inhibition with 50 µM lactacystin in some constructs the generation of the SIINFEKL is only inhibited by ~40 % (figure 3.16). These precursor peptides from the constructs P'RR&, P'LL$_{ori}$ and P'LL& seem to be partially independent from proteasomal cleavage for the S8L generation.

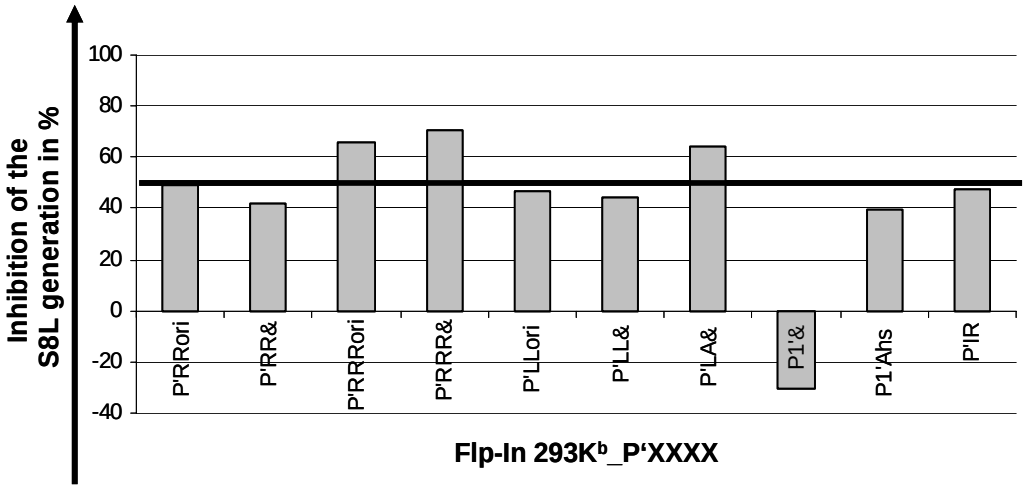

Figure 3.16: The inhibition of the SIINFEKL generation by adding lactacystin to the assay is shown here for the Flp-In 293K^b transfectants carrying specific amino acid exchanges. The bold line indicates the 50 % inhibition mark.

3.1.9 Proteasomal inhibition with epoxomicin

To ensure that the effect on S8L presentation observed by proteasomal inhibition with lactacystin is exclusively due to the missing proteasomal function, a different inhibitor was tested. The chosen inhibitor was epoxomicin, because it has been described to be 100 times

more potent than lactacystin and even more specific (Meng et al., 1999). Therefore, two partially proteasomal independent cell lines with the S8L constructs P1'R_{ori} and P'IR_{ori} were analysed, taking two controls into the assay: P1'& and P1'A_{ori}. The first one, P1'& was used as a positive control, because the S8L presentation is not impaired by adding proteasomal inhibitors. This precursor peptide has no C-terminal flanking region at the S8L epitope and therefore is not dependent on proteasomal cleavage. The second control, the P1'A_{ori} shows proteasomal dependence and thus the S8L presentation is inhibited, when the proteasome is not functional. Even though epoxomicin has been used in this experiment, P1'R_{ori} and P'IR_{ori} still present 69% and 45% of the S8L epitope on their cell surface, indicating its proteasomal independence.

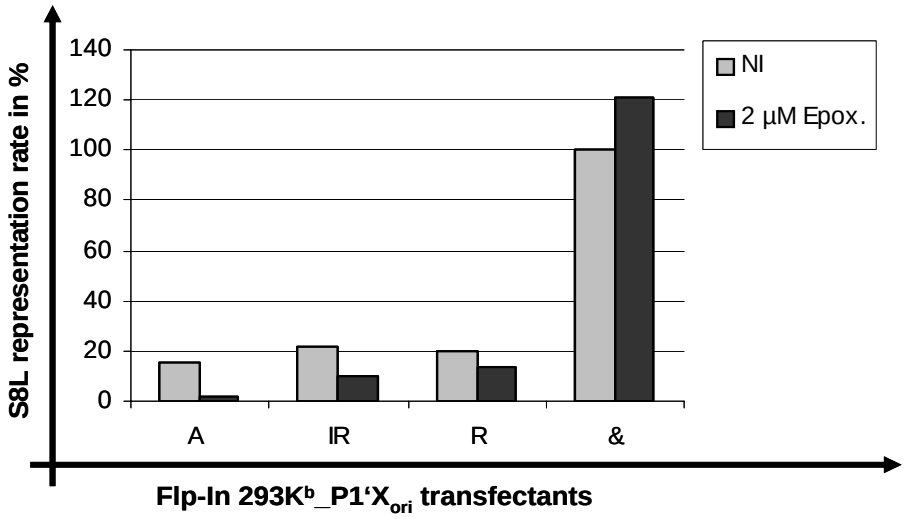

Figure 3.17: H-2K^b/SIINFEKL re-presentation of the Flp-In 293K^b transfectants carrying amino acid exchanges at the positions P1' and P2'. The S8L levels in this bar chart represent the average of three independent assays.

3.1.10 Role of TPPII in antigen processing and presentation of SIINFEKL

After having demonstrated that the proteasome is not alone involved in the generation of the S8L out of specific precursor peptides, TPPII was tested for a possible candidate. TPPII was considered to play a role in the C-terminal cleavage needed for the S8L generation, because in recent studies, it was published to generate both cleavages (N- and C-terminal) for the HLA-A3 HIV Nef(73-82) epitope (Seifert et al., 2003). TPPII is known to have a strong N-terminal exopeptidase activity, cleaving always three amino acids on block and a weaker endopeptidase activity, which has not been investigated intensively so far (Geier et al., 1999).

For this purpose, two TPPII inhibitors, AAF-CMK and butabinde were tested on S8L presentation on the cell surface of these transfectants (figure 3.18). Butabindide is very instable at 37°C and has to be added each 90 minutes to the cell media to ensure TPPII inhibition. Furthermore, it requires media without FCS, which is more stressful for the cells. As butabindide seems to be difficult to handle, the further analysis were performed with AAF-CMK. The next figure 3.19, shows the S8L rates of the different assays performed under inhibition of proteasome, using epoxomicin and the inhibition of TPPII, using AAF-CMK. Furthermore, the combination of both inhibitors has also been tested.

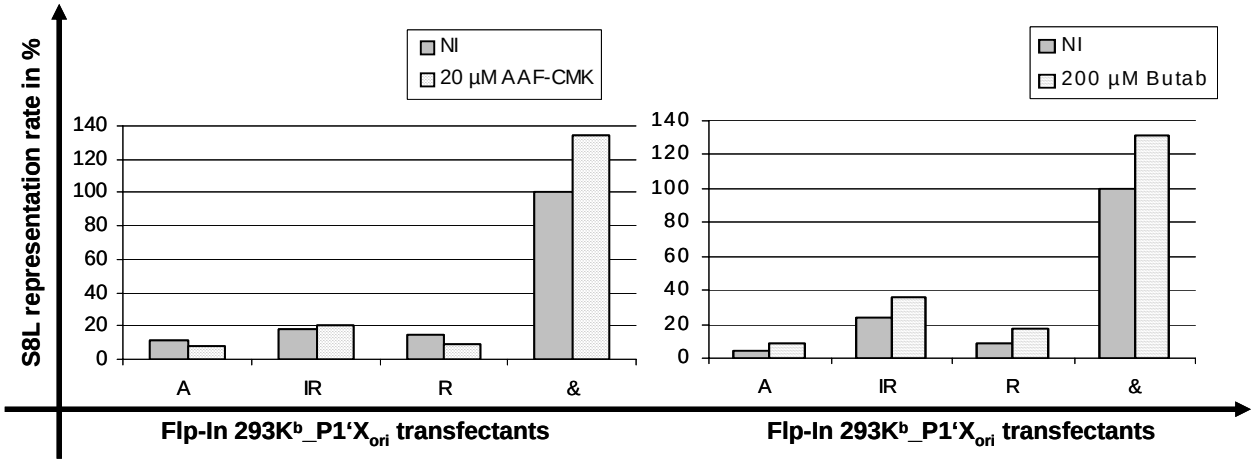

Figure 3.18: H-2K^b/SIINFEKL re-presentation of the Flp-In 293K^b transfectants carrying amino acid exchanges at the positions P1' and P2'. The S8L levels in this bar chart represent the average of two independent assays.

This bar chart represents the average of S8L presentation of five independent assays. Besides the two control cell lines (P1'& and P1'A_{ori}), the three further cell lines, P1'$R_{ori,}$ P1'P_{ori} and P'IR_{ori} have been shown to be partially proteasomal independent in earlier assays. Despite TPPII inhibition the P1'A_{ori}, P1'$R_{ori,}$ P1'P_{ori} and P'IR_{ori} cell lines still show a strong representation of SIINFEKL on the cell surface, indicating that TPPII is not involved in S8L generation. In some cases the re-presentation rate is even higher then the control, meaning that TPPII might destroy the S8L precursor peptides. Adding epoxomicin, the results were similar to the inhibition of the proteasome with lactacystin. Finally, the S8L rates obtained using epoxomicin and AAF-CMK were the lowest. Nevertheless, the cell lines P1'$R_{ori,}$ P1'P_{ori} and P'IR_{ori} still show ~50% generation of the SIINFEKL. The P1'P_{ori} transfectant has not been further analysed, because the re-presentation rate with or without inhibitors is very low. This means that a small intensity change of the APC values, could lead to an important change in

the S8L rate. Therefore it is difficult to achieve significant results with cell lines that have low S8L re-presentation. Further analysis is focused on cell lines with high S8L rates and clear proteasomal independence.

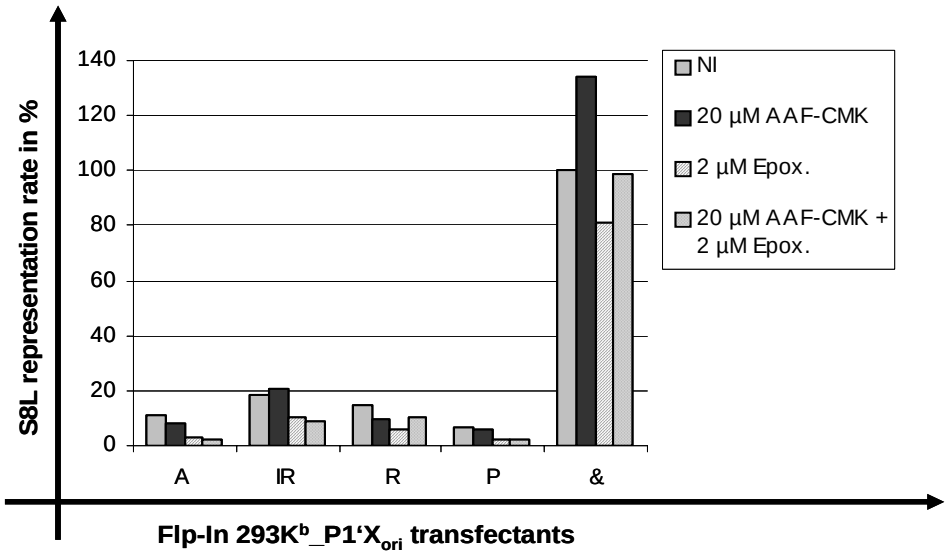

Figure 3.19: H-2K^b/SIINFEKL re-presentation of the Flp-In 293K^b transfectants carrying amino acid exchanges at the positions P1' and P2'. The S8L levels in this bar chart represent the average of two independent assays.

3.2 Silencing of cytosolic aminopeptidases

RNAi (RNA-mediated interference) is a mechanism for RNA-guided regulation of gene expression in which double-stranded ribonucleic acid inhibits the expression of specific genes of interest with complementary nucleotide sequences. This powerful tool for post-transcriptional gene silencing was chosen to analyze the role in antigen processing and presentation of further cytosolic aminopeptidases. TPPII was silenced for a closer analysis and comparison with the inhibitor experiments. Besides TPPII, another interesting candidate is ThOP1 (TOP), which is a cytosolic metallopeptidase involved in antigen processing. It has been shown that THOP1 bears both, the capacity to bind peptides and protect them from degradation (Portaro et al., 1999; Silva et al., 1999), and to cleave peptides for degradation (Saric et al., 2001). Finally, the Insulin-degrading enzyme (IDE) was also silenced to investigate, if it is involved in antigen processing and presentation. It has been suggested that IDE has a multifaceted biological significance with the specificity to cleave small proteins of diverse sequence, many of which share a propensity to form ß-pleated sheet-rich amyloid fibrils under certain conditions (Duckworth et al., 1998; Seta and Roth, 1997; Vekrellis et al., 2000). It has also been demonstrated that it is involved in processing of insulin by antigen-presenting cells (Semple et al., 1989).

3.2.1 Gene silencing of TPPII, THOP1 and IDE in Flp-In 293K^b cells

Ensuring efficient transfection is a hallmark of successful siRNA-mediated “knock-down”. After having found the appropriate settings for the electroporation of siRNA into Flp-In 293K^b cells, the “knock-down” of TPPII, THOP1 and IDE was analysed at mRNA level. The electroporation conditions were 240 volt and 600 µF (Gene Pulser II, BioRad) for $2*10^6$ cells with 1 µM siRNA. The mRNA expression of the electroporated cells was determined on day one and day two after electroporation by Real Time PCR. The relative mRNA expression level in percent (%) is shown in figure 3.20. This data was analyzed by the Real Time PCR software (BioRad iQ5) and the relative mRNA expression levels were calculated using the siRNA scramble controls (SC) as a reference. The “knock-down” of ThOP1 is constant on both days with 58-59% “knock-down”. TPPII achieves the strongest gene silencing on the first day after electroporation with 78% “knock-down”. IDE shows a “knock-down” of 86% on day one and of 68% on day two. The knock-downs attained at the first day were stronger than those at the second day after electroporation. In general, the “knock-downs” attained at the first day were stronger than those at the second day after electroporation.

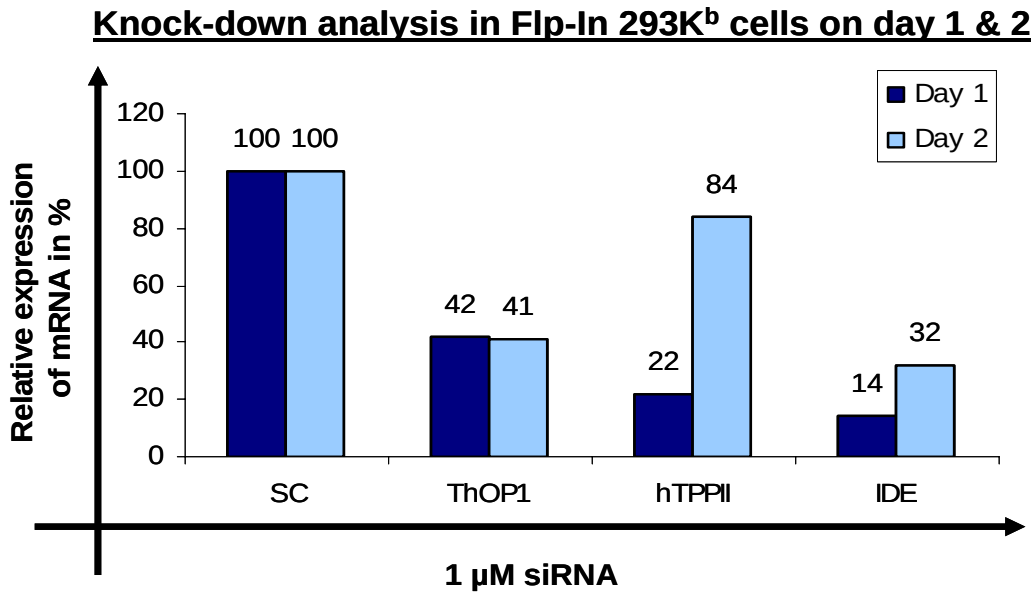

Figure 3.20: Relative mRNA expression in % on day one and two after electroporation of the peptidases ThOP1, hTPPII, IDE. The Flp-In 293K^b cells were electroporated with 1 µM siRNA. In each setting the siRNA silenced a different peptidase. The mRNA expression of the electroporated cells was examined one (day 1) and two days (day 2) after electroporation. The relative expression of mRNA was analyzed by Real Time PCR. This is one experiment of three, which shows a reproducible "knock-down" of the proteases. SC: scramble control. hTPPII: human tripeptidylpeptidase II.

3.2.2 Activity analysis in the electroporated cells for the silenced cytosolic peptidases (ThOP1, TPPII, IDE)

In the next experiments the residual activity of the silenced peptidases (ThOP1 and TPPII) were examined on day 1 and 2 after electroporation of the siRNA against the corresponding peptidases. For this purpose, a sample of the siRNA-transfected Flp-In 293K^b cells was lysed on day one and two after electroporation and the cytosol was further analyzed for the residual activity of the silenced peptidase. Therefore, the substrates AAF-AMC and suc-FGL-ßNA in a 100 µM concentration were used to detect the activity of TPPII and ThOP1 respectively. The activity levels were compared with the fluorescence level reached in the cells electroporated with the scramble control (SC) siRNA. First, the gene silencing of these peptidases was performed as described before in this chapter and the relative expression of the mRNA of the siRNA-transfected Flp-In 293K^b cells was analyzed by Real Time PCR (figure 3.21). The strongest "knock-downs" for both peptidases were achieved on the second day after siRNA electroporation with 100% for ThOP1 and 83% for TPPII.

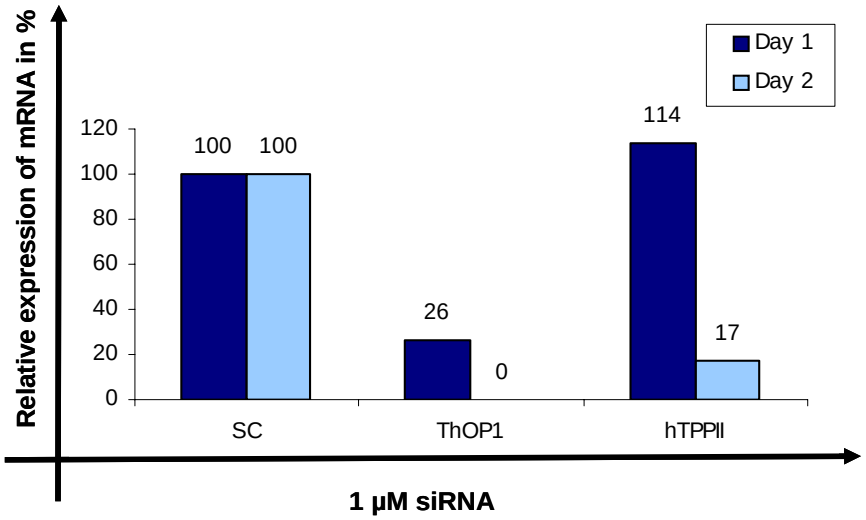

Figure 3.21: Relative mRNA expression in % on day one and two after electroporation of the siRNA against ThOP1 and TPPII. The Flp-In293K^{b} cells were electroporated with 1 µM siRNA. In each setting the siRNA silenced a different peptidase. The mRNA expression of the electroporated cells was examined one (day 1) and two days (day 2) after electroporation. The relative expression of mRNA was analyzed by Real Time PCR. SC was used as a reference value for the calculation in percent. SC: scramble control. hTPPII: human TPPII.

These siRNA-transfected cells were further analyzed for the residual peptidase activity using specific substrates for ThOP1 and TPPII, which were incubated for 60 minutes at 37°C with the cytosol of these siRNA-transfected cells. The AMC fluorescence levels of the cleaved substrates were measured after five and after 60 minutes, to calculate the increase of fluorescence, shown in figure 3.22 and 3.23 in relative fluorescence units (RFU). Moreover, to prove that the measured activity is specific for the corresponding peptidases, the inhibitors against ThOP1 (100 µM Cpp-AAF-pAb) and TPPII (100 µM butabinde) were additionally used. These inhibitors were first incubated with the cytosol samples of the siRNA-transfected cells for 10 minutes at 37°C and subsequently the substrate was added to the reaction. The TPPII siRNA-transfected cells show a 14% decrease in activity on the first day after electroporation and 51% on the second day (figure 3.22). The ThOP1 activity was measured with the substrate suc-FGL-ßNA showing a decrease in activity of 41% one day and of 55% two days after siRNA electroporation (figure 3.23). These results indicate that the first day after siRNA treatment is not adequate for representation analysis, because 86% resp. 59% of the TPPII or ThOP1 activity is still conserved. This implicates that on day one the processing cannot be sufficiently impaired in the cells and therefore no significant effects on the S8L presentation can be concluded. As a consequence, all following RNAi analysis were focused on day two after siRNA electroporation.

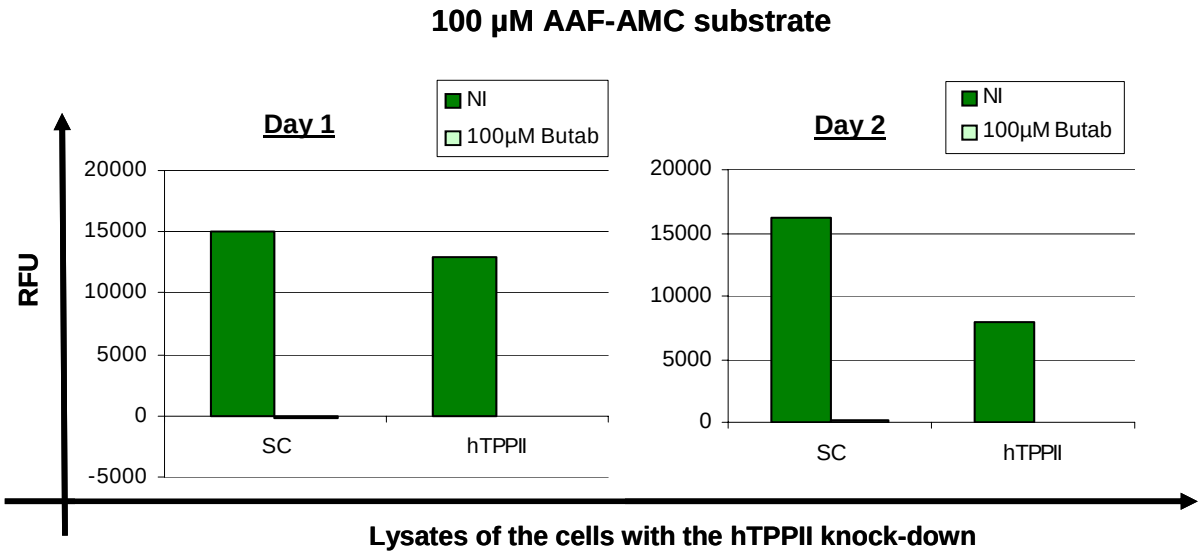

Figure 3.22: Residual activity in the cytosol of Flp-In293K^b cells after gene silencing of TPPII. After lysing the knock-down Flp-In293K^b cells, the remaining TPPII activity was measured *in vitro* with the TPPII specific substrate AAF-AMC. The release of AMC was measured by relative fluorescence units (RFU) in a spectrafluorometer (λEx = 360 nm and λEm = 450 nm) at 37°C for 30 minutes. Additionally, 100 µM butabindide (TPPII inhibitor) was added to demonstrate that the measured activity is specific for TPPII.
NI: No Inhibitor. hTPPII: human tripeptidylpeptidase II.

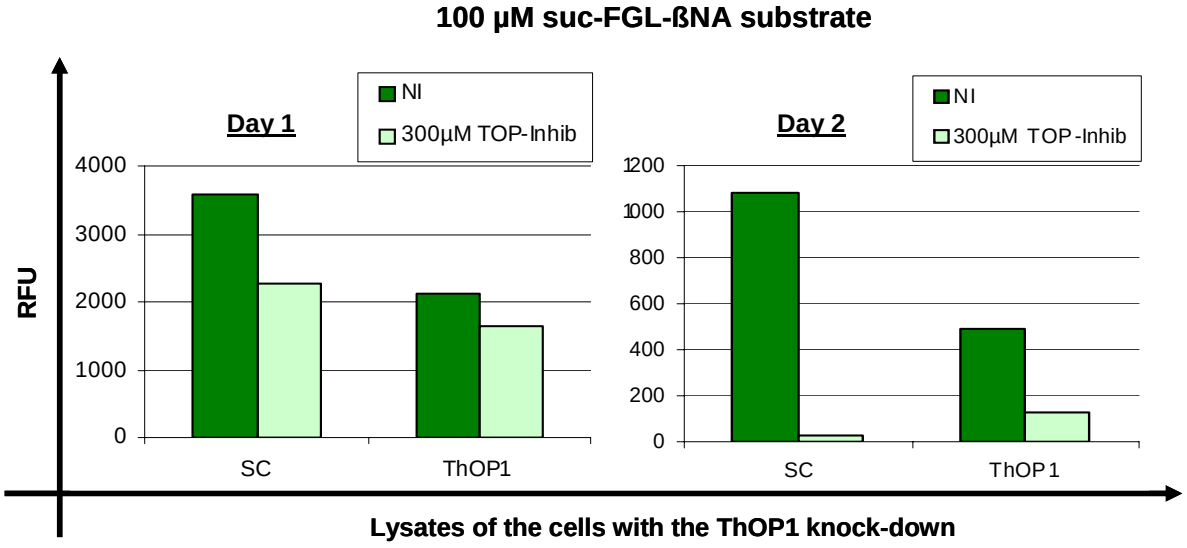

Figure 3.23: Residual activity in the cytosol of Flp-In293K^b cells after gene silencing of ThOP1. After lysing the knock-down Flp-In293K^b cells, the remaining ThOP1 activity was measured *in vitro* with the ThOP1 specific substrate suc-FGL-ßNA. The release of ßNA was measured by relative fluorescence units (RFU) in a spectrafluorometer (λEx = 340 nm and λEm = 405 nm) at 37°C for 60 minutes. Additionally, 300 µM Cpp-AAF-pAb (ThOP1 inhibitor) was added to demonstrate that the measured activity is specific for ThOP1. NI: No Inhibitor; hTPPII: human tripeptidylpeptidase II.

3.2.3 Presentation of H-2K^b/SIINFEKL after gene silencing of the cytosolic peptidases ThOP1, TPPII and IDE in Flp-In 293K^b_P'IR cells

To analyze the role of the cytosolic peptidases ThOP1, TPPII and IDE on H-2K^b/SIINFEKL presentation, these peptidases were silenced by RNAi in the Flp-In 293K^b_P'IR cell line. This cell line was characterized in earlier experiments as partially proteasome independent. The electroporation settings (240 volt and 600 µF for 2*10^6 cells with 1 µM siRNA) remained constant for all following RNAi assays. The relative mRNA expression of the silenced genes for TPPII and ThOP1 in the Flp-In 293K^b_P'IR cells (figure 3.24) and the H-2K^b/SIINFEKL presentation on these cells (figure 3.25) was examined. The relative mRNA expression of the silenced peptidases were analyzed on day two and day four after electroporation by Real Time PCR. The "knock-down" of ThOP1 is stronger on the second day with 74% knockdown. TPPII is silenced on day two with 47% "knock-down" and at day four no gene silencing (114%) was detected any more. IDE shows two strong knock-downs on both days with 71% on day 2 and 88% on day four. The silencing of the peptidases attained at the second day was strong enough to examine the H-2K^b/SIINFEKL presentation on the siRNA-transfected cells (figure 3.25).

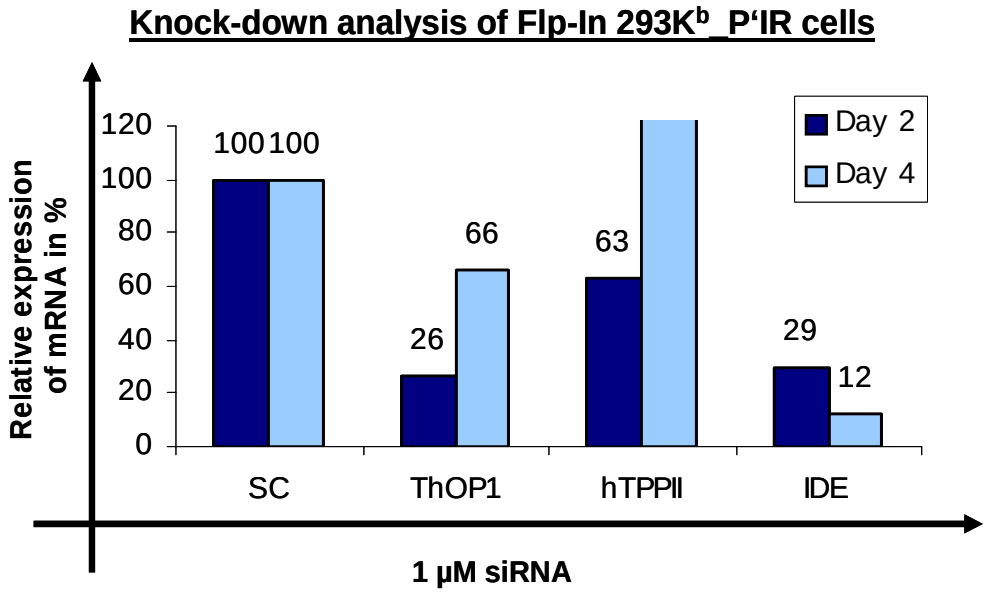

Figure 3.24: Relative mRNA expression in % on day two and four after siRNA electroporation against the peptidases ThOP1, TPPII, IDE. The Flp-In 293K^b_P'IR cells were electroporated with 1 µM siRNA. In each setting the siRNA silenced a different peptidase. The relative mRNA expression of the electroporated cells was examined two (day 2) and four days (day 4) after electroporation of the siRNA. The relative expression of mRNA was analyzed by Real Time PCR. SC: scramble control. hTPPII: human tripeptidylpeptidase II.

According to the SIINFEKL detected on the cells with the knock-downs of the second day after RNAi treatment, ThOP1 "knock-down" cells show an increase of S8L of 25%, compared to the SC control cells. In contrast, TPPII and IDE "knock-downs" do not show a significant change in the amount of SIINFEKL presented. The H-2K^b/SIINFEKL presentation on day four shows a strong reduction for the cells with a TPPII and IDE knock-down, but no significant difference in presentation for the ThOP1 cells. This is one experiment and therefore not representative. Nevertheless, figure 3.25 shows one experiment, which is not representative, because it has to be reproduced and further siRNA experiments should follow to substantiate these results.

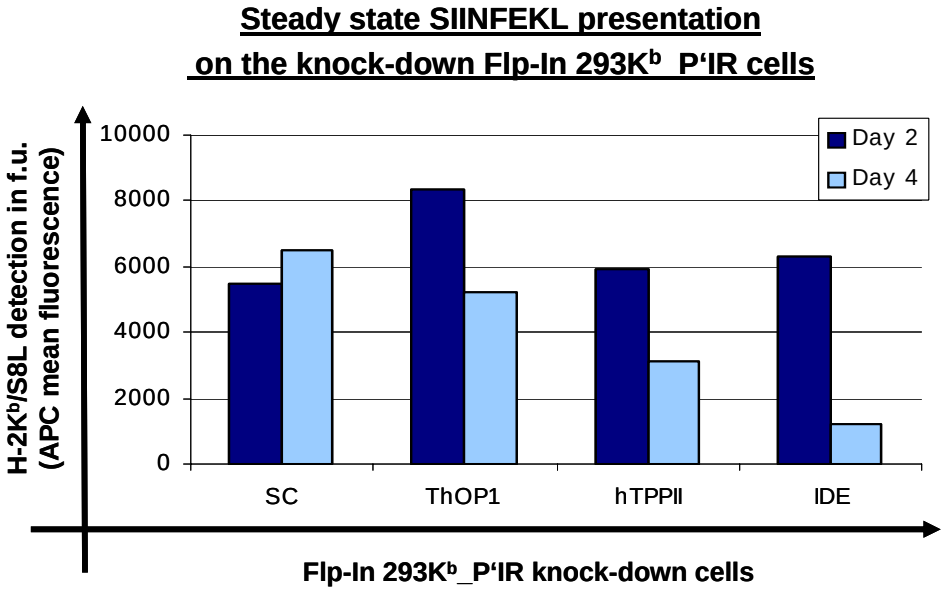

Figure 3.25: Steady state level of SIINFEKL on the cell surface of the different knock-down Flp-In 293K^b_P'IR cells. The x-axis represents the type of peptidase silenced (ThOP1, hTPPII or IDE) in the partially proteasome independent cell line Flp-In 293K^b_P'IR. The H-2K^b/SIINFEKL was detected by FACS using the specific 25-D1.16 antibody and the secondary gam-APC. The APC fluorescence is represented at the y-axis in fluorescence units (f.u.), which correspond to the SIINFEKL amount on the cell surface. This is one experiment and therefore not representative. SC: Scramble control. hTPPII: human tripeptidylpeptidase II.

3.2.4 Presentation of H-2K^b/SIINFEKL after simultaneous gene silencing of two peptidases ThOP1 and TPPII in Flp-In 293K^b_P'IR cells

In this experiment the role of the cytosolic peptidases ThOP1 and TPPII on H-2K^b/SIINFEKL presentation was further examined, performing a double gene silencing in the partially proteasome independent Flp-In 293K^b_P'IR cells. The mRNA expression of the siRNA-

transfected cells was analyzed on day two and day four after siRNA electroporation by Real Time PCR (figure 3.26). The relative mRNA expression level in percent (%) is shown in figure 3.26. The "knock-down" of ThOP1 is stronger on day two with 74% "knock-down" and only 58% on day four. TPPII is silenced on day two with 52% knock-down and on day four only 46% was achieved.

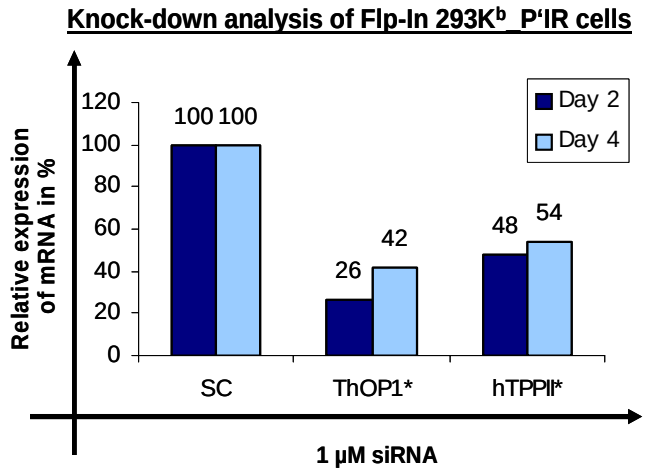

Figure 3.26: Relative mRNA expression in % on day two and four of the double knock-downs for ThOP1 and TPPII. The Flp-In 293K^b_P'IR cells were electroporated with 1 µM of each siRNA (ThOP1 and TPPII) in one setting. The relative mRNA expression of the silenced peptidases was examined two (day 2) and four days (day 4) after electroporation of the siRNA. The relative expression of mRNA was analyzed by Real Time PCR. SC: scramble control. ThOP1* and TPPII*: simultaneous knock-down in the cells. hTPPII: human tripeptidylpeptidase II.

The H-2K^b/SIINFEKL presentation of these double siRNA-transfected cells is represented in figure 3.27. The gene silencing of both peptidases simultaneously shows a significant increase of S8L to 165% (compared to the SC value as a reference) on day two after siRNA electroporation. In contrast, on day four, consistent with the findings obtained in the experiment above (figure 3.25), the SIINFEKL amount detected is diminished.

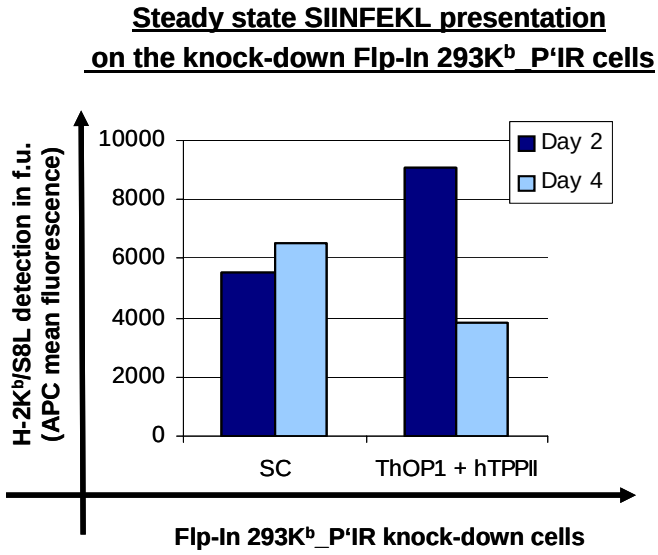

Figure 3.27: Steady state level of SIINFEKL presented on the double knock-down Flp-In 293K^b_P'IR cells. The H-2K^b/SIINFEKL was detected by FACS using the specific 25-D1.16 antibody and the secondary gam-APC. The APC fluorescence is represented at the y-axis in fluorescence units (f. u.), which corresponds to the SIINFEKL amount on the cell surface. SC: Scramble control. hTPPII: human tripeptidylpeptidase II.

3.3 Identification of an endopeptidase activity in the cytosol involved in antigen processing

3.3.1 Purification strategy of the LCL 721 cytosol

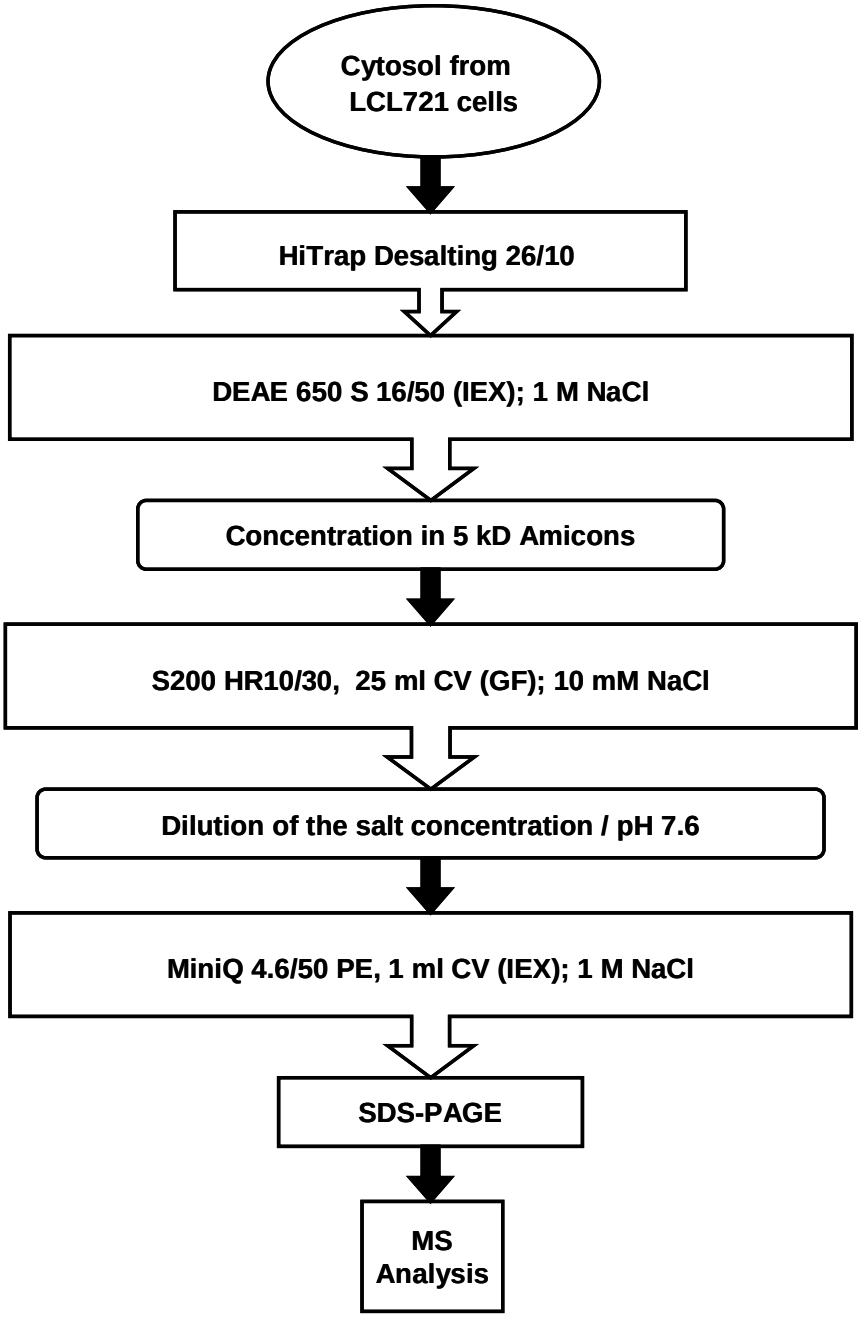

Figure 3.28: Flow-chart of the LCL 721 cytosol purification strategy for the identification of the new cytosolic endopeptidase activity.

3.3.2 Desalting step

After the cytosol extraction of the LCL721 cells as described at *2.2.7.1* (Material and Methods) the lysate separated from cell debris by the ultracentrifugation step was taken for further purification process. From the 7 ml LCL721 cell pellet 11 ml lysate remained after the ultracentrifugation step. This lysate was then desalted by a "HiTrap Desalting 26/10" column (figure 3.29) with TSDG-buffer A pH 7.6. Four ml fractions were collected from this column and the eluted protein fraction (A3-A7) measured by the UV_{280nm} after being pooled comprised 20 ml.

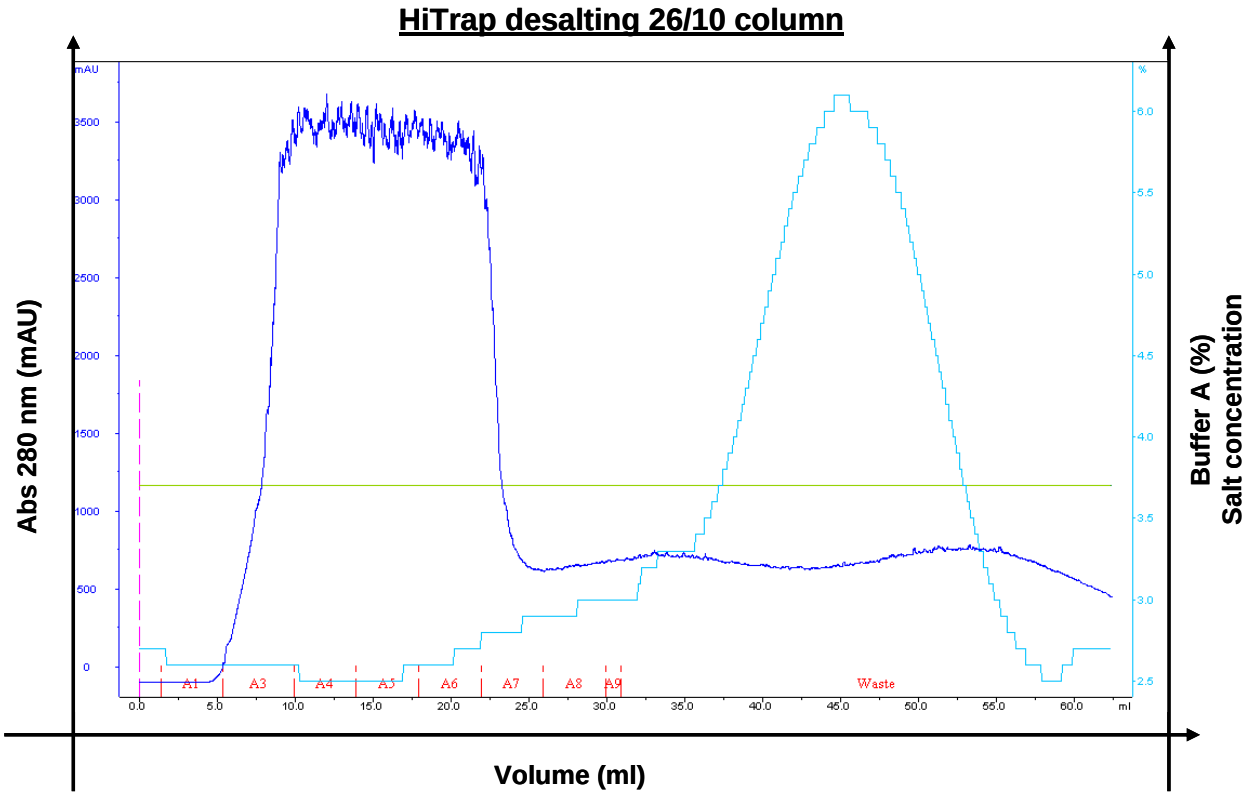

Figure 3.29: Desalting the extracted cytosol from the LCL721 cells through a HiTrap 26/10 desalting column. The dark blue line shows the elution profile measured at 280 nm for the visualization of the proteins. The light blue line corresponds to the salt elution profile. On the x-axis in red the eluted fractions are shown. Fractions A3 to A7 were collected for the further purification steps.

3.3.3 Anion exchange chromatography (DEAE column)

The desalted 20 ml lysate was adjusted with two more ml of TSDG-buffer A to a pH of 7.6, as the next column, DEAE requires a lightly basic pH. The DEAE material carries a positive charged diethylaminoethyl (DEAE) as a functional group. This material serves as a weak anion exchanger, which's protein binding capacity varies with the pH achieving best results in an alkaline medium. After loading the 22 ml LCL721 lysate sample on the DEAE column

(figure 3.29) the following gradient was applied: 0-20% and 20-30% TSDG-buffer B (1 M NaCl). All fractions were collected with a volume of 4 ml. Now the question arose, what kinds of peptidases were in the eluted fractions from the DEAE column? To detect an endopeptidase activity each fraction was tested in a digestion assay adding the 100 µM suc-LLVY-AMC substrate to the samples. The three detected activity peaks, able to perform the cleavage between the tyrosine (Y) and the fluorogenic AMC group are shown in figure 3.30. The fractions E8-E15 were 50% less active then the fractions F8-F1 and G1-G3. Out of these results these fractions were pooled forming two activity pools, pool 1(E8-E15) and pool 2 (F8-F1 and G1-G3), which were purified in the next steps by the same strategy, but separately (figure 3.31: A. and B.).

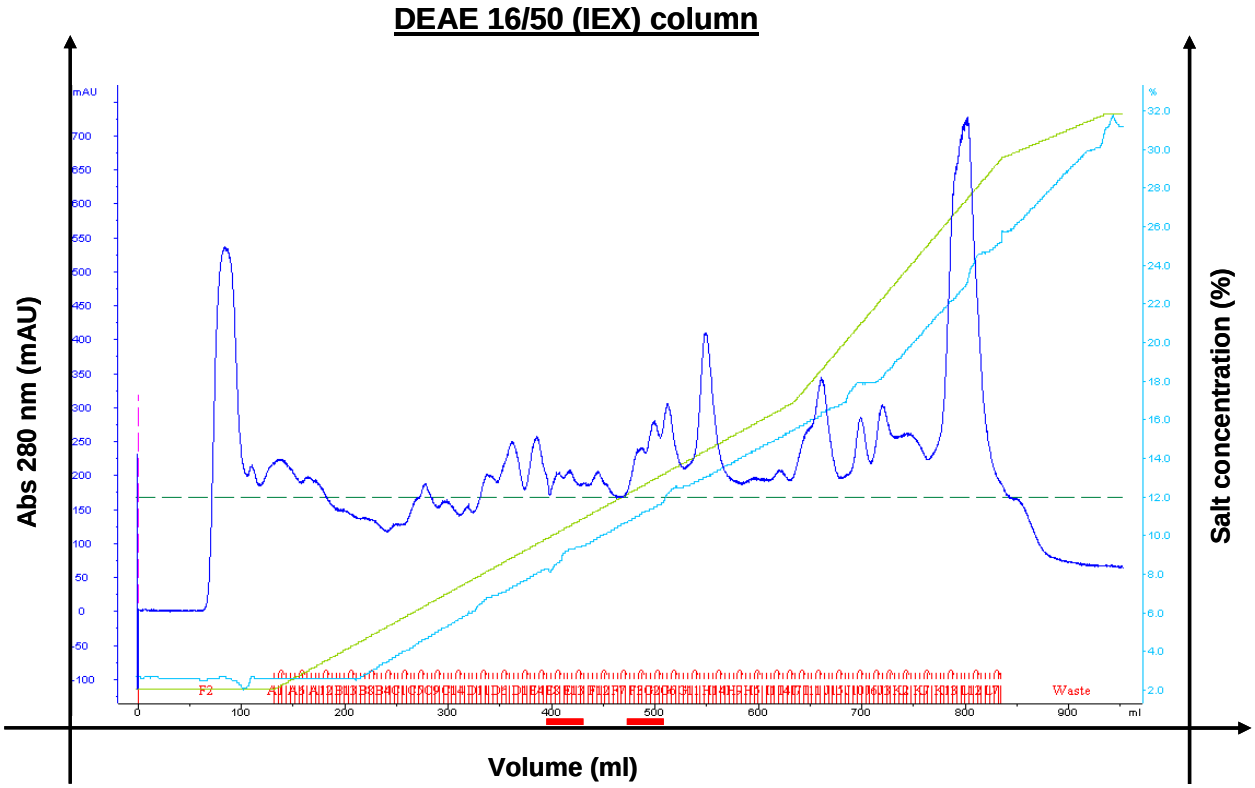

Figure 3.30: Ion exchange chromatography (IEX) of the desalted sample of the LCL721 cytosol. For the IEX a column with a DEAE material acting as an anion exchanger was used. The dark blue line shows the elution profile measured at 280 nm for the visualization of the proteins. The light blue line corresponds to the salt elution profile of the gradient applied with the TSDG-buffer B, which contains 1 M NaCl. Under the x-axis the range of the pooled activity fractions are marked with horizontal bold red bars. The activity fractions E8-E15 (Pool 1) and fractions F8-F1 and G1-G3 (Pool 2) were pooled each for further purification steps.

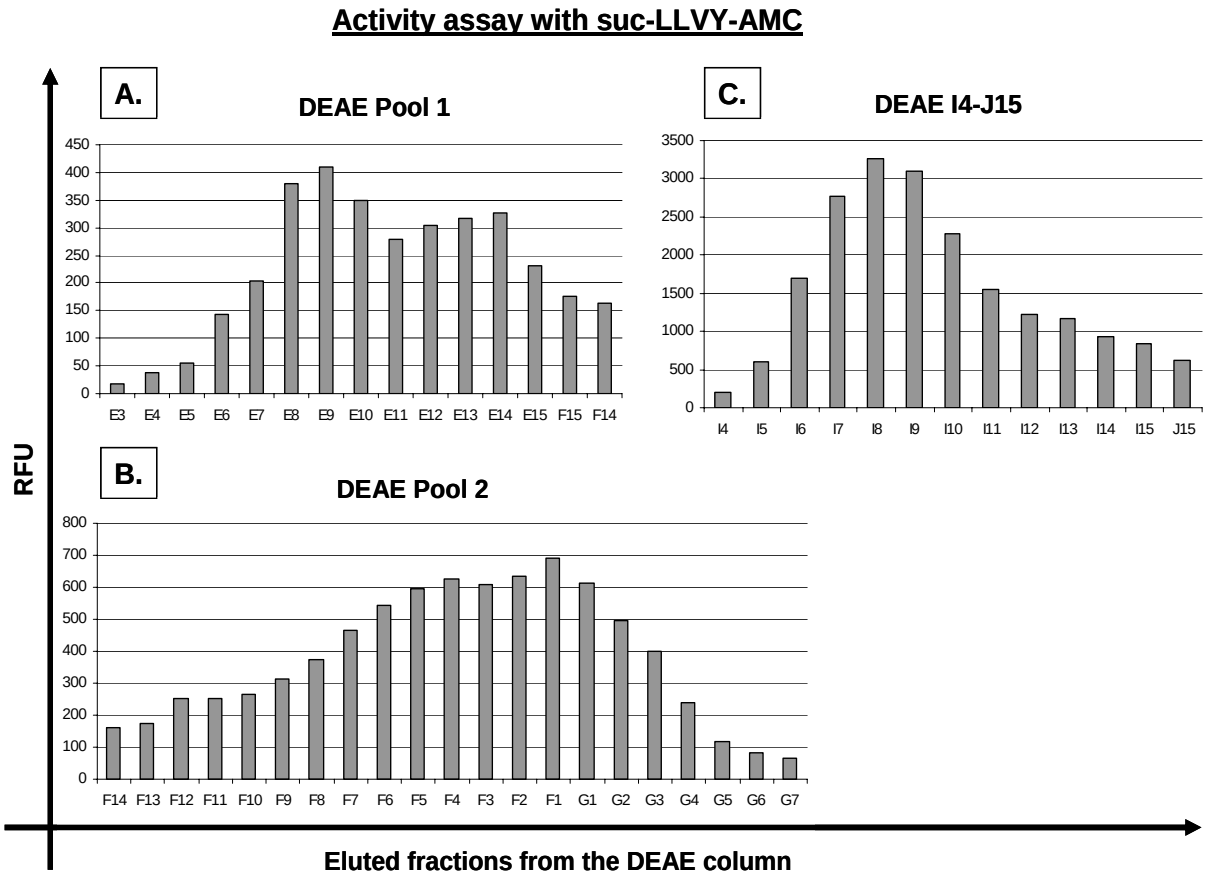

Figure 3.31: Activity assay of the DEAE fractions with the suc-LLVY-AMC substrate. In these *in vitro* fluorogenic assays 100 µM suc-LLVY-AMC substrate was digested with 2 µl of the fractions, to detect the fractions showing endopeptidase activity. The release of AMC was measured by relative fluorescence units (RFU) in a spectrafluorometer (λEx = 360 nm and λEm = 450 nm) at 37°C for 30 minutes. The activity fractions E8-E15 were pooled afterwards to form Pool 1 (A.) and the F8-F1 and G1-G3 to form Pool 2 (B.). These two pools were treated separately in all further purification steps. Figure C. shows proteasomal activity.

The third activity peak detected (I8; figure 3.31: C.) shows a high cleavage affinity to the suc-LLVY-substrate. This substrate is usually used to detect proteasomal activity, as it is cleaved by the chymotrypsin activity of the proteasome. In proteasomal purification assays the proteasome is eluted from a DEAE column at ~16% TSDG-buffer B containing 1 M NaCl. The fraction I8 was eluted at approx. 16% buffer B (figure 3.30), indicating that this peak could correspond to the proteasome. This was substantiated by activity assays adding lactacystin for proteasomal inhibition, see figure 3.32. In this figure, the two pools from the DEAE column and the peak I8 were analysed for proteasomal and TPPII activity. In A. all fractions were able to cleave suc-LLVY-AMC, but only the fraction I8 was susceptible for lactacystin (proteasomal inhibitor). Pool 1 has a 57% higher cleavage activity then pool 2. In B. the cleaving activity of both pools for the AAF-AMC substrate is similar. Nevertheless,

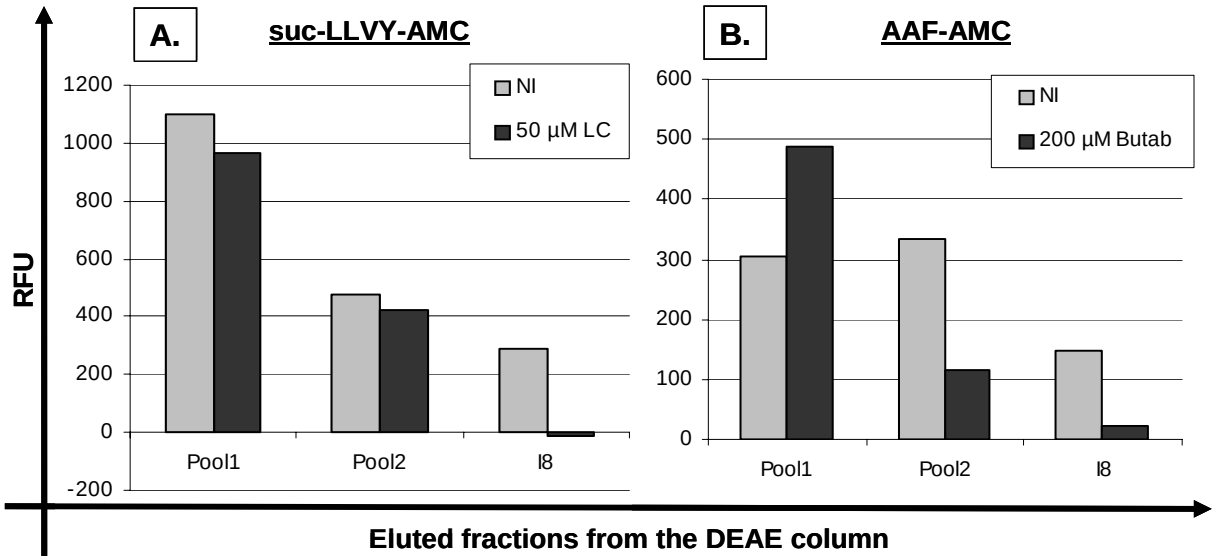

Figure 3.32: Activity assay of the DEAE fractions with inhibitors. The DEAE fractions, which showed endopeptidase activity using the suc-LLVY-AMC substrate (figure 3.30), were examined for proteasomal or TPPII activity adding the corresponding inhibitors to the assay. After incubating the inhibitors for 10 minutes at 37°C with the DEAE fractions the corresponding substrates were added. A.) Lactacystin (50 µM) is a proteasomal inhibitor and was used to detect the proteasomal activity adding the suc-LLVY-AMC (100 µM), which is a substrate cleaved by the chymotrypsin activity of the proteasome. B.) Butabindide (200 µM) is a TPPII inhibitor. Together with the AAF-AMC substrate the activity of TPPII can be detected. Fraction I8 is susceptible for lactacystin and butabindide. The release of AMC was measured by relative fluorescence units (RFU) in a spectrafluorometer (λEx = 360 nm and λEm = 450 nm) at 37°C for 30 minutes.

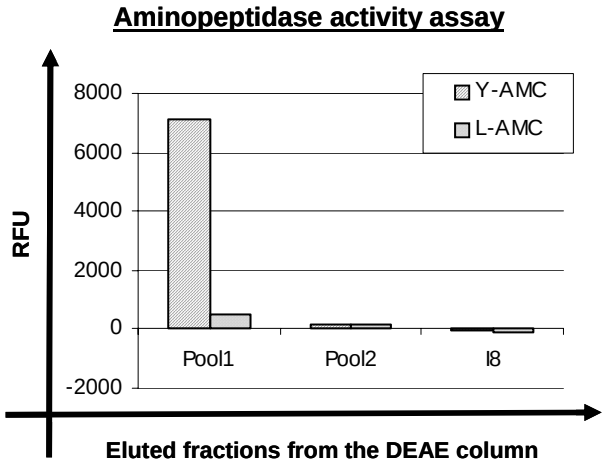

Figure 3.33: Aminopeptidase activity assay of the DEAE fractions. To perform this assay two substrates specific for tyrosine and leucine aminopeptidases were chosen: Y-AMC and L-AMC. Pool 1 shows a high affinity for the Y-AMC substrate. The release of AMC was measured by relative fluorescence units (RFU) in a spectrafluorometer (λEx = 360 nm and λEm = 450 nm) at 37°C for 30 minutes.

pool1 shows only 28% affinity to this substrate comparing it to the suc-LLVY-AMC substrate. In a second setting the TPPII inhibitor butabindide was added to the digestions and the fraction I8 and pool 2 (66% inhibition) were inhibited in its cleaving activity. I8 seems to comprise a mixture of proteasome and TPPII. In further assays (figure 3.33), these DEAE fractions were tested for aminopeptidase activity using the substrates Y-AMC and L-AMC specific for tyrosine and leucine aminopeptidases. Only pool 1 showed a strong cleavage affinity for Y-AMC and a low one for L-AMC.

3.3.4 Gelfiltration (Superdex S200 column)

The two activity pools from the DEAE column (pool 1 and pool 2) were concentrated using 5 kD Amicon filter devices to a volume of 500 µl each. After this concentration step, they were loaded consecutively onto a Superdex S200 gelfiltration column (S200 HR 10/30). Figure 3.34 corresponds to the run of the pool 1 and figure 3.36 to the run of pool 2. The separation by gelfiltration is based on the exclusion of molecules from the intraparticular volume of the matrix, obtaining a separation of the molecules per size exclusion. For this column a linear gradient of 10% TSDG-buffer B was applied. All fractions eluted were collected in a 96-Well-Plate with a volume of 0.75 ml.

To detect the endopeptidase activity the 100 µM suc-LLVY-AMC substrate was added to a sample of each fraction. The activity fractions from pool 1, A11-A12 and B12-B11 show less activity (figure 3.35) after this purification step. The activity peaks achieves 115 rfu, which is only ¼ of the original activity peak, when comparing it with the peak eluted from the DEAE column (figure 3.31, A.). As the activity and the protein level from this eluted fractions were very low, no further analysis were performed for further characterization. In contrast, after the S200 run from pool 2, the activity and the protein level obtained was enough to continue further purification steps. The activity fractions, A11-A12 and B12-B10 (figure 3.37) achieve more than 1200 rfu, when cleaving the suc-LLVY-AMC substrate. These fractions were pooled (forming pool 3) for the next purification step.

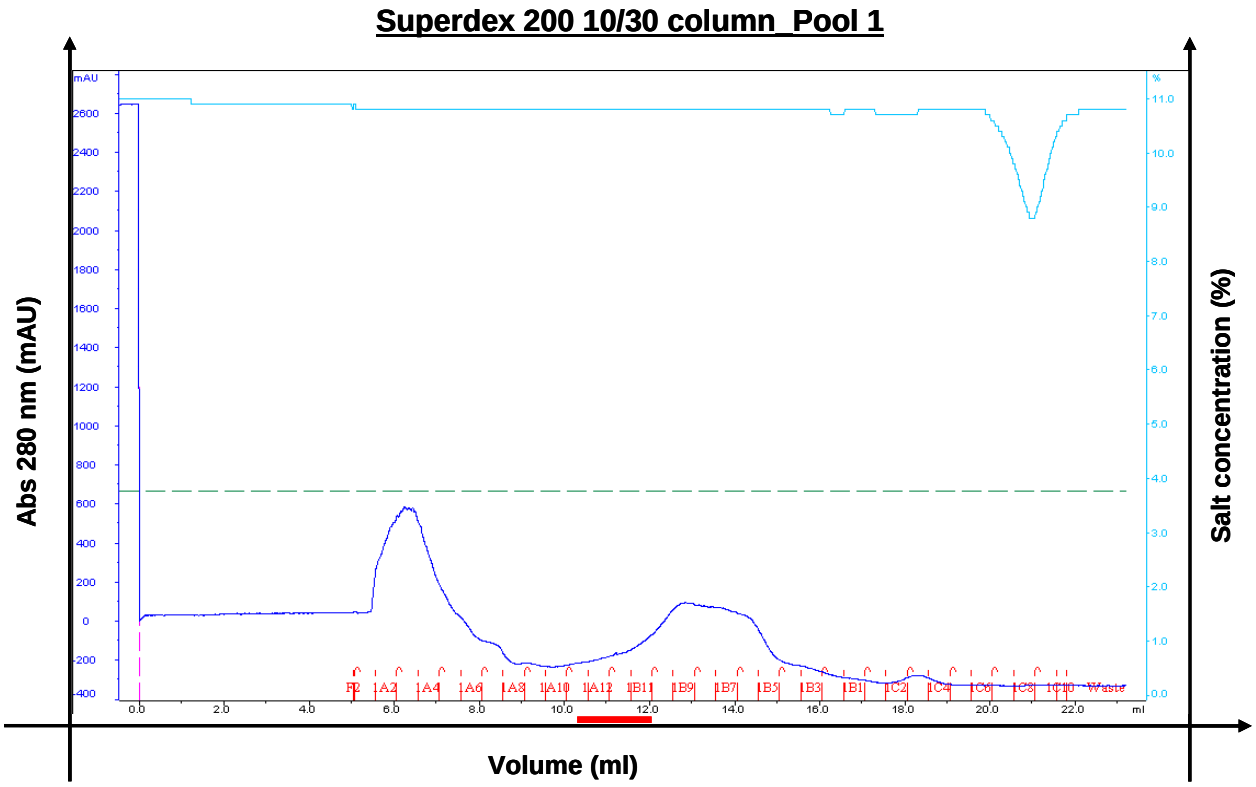

Figure 3.34: Gelfiltration with a Superdex S200 HR 10/30 column of the pool 1 fractions from the DEAE column. The dark blue line shows the elution profile measured at 280 nm for the visualization of the proteins. The light blue line corresponds to the salt elution profile of the buffer B in percent (%), which contains 1 M NaCl. For this run a linear gradient of 10% TSDG-buffer B was applied. The activity fractions (A11-B11) detected in figure 3.32 are marked by a red bar on the x-axis.

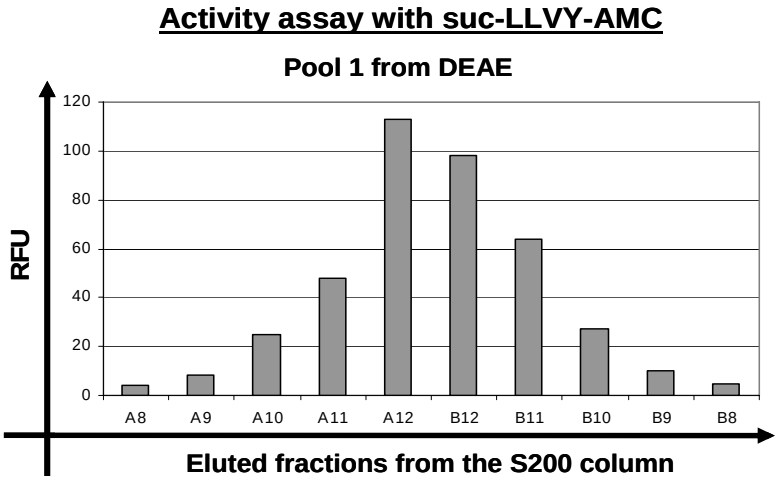

Figure 3.35: Activity assay of the S200 fractions from pool 1 with the suc-LLVY-AMC substrate. In these *in vitro* fluorogenic assays the 100 µM suc-LLVY-AMC substrate was digested with 20 µl from the eluted fractions, to detect endopeptidase activity. The release of AMC was measured by relative fluorescence units (RFU) at λEx = 360 nm and λEm = 450 nm.

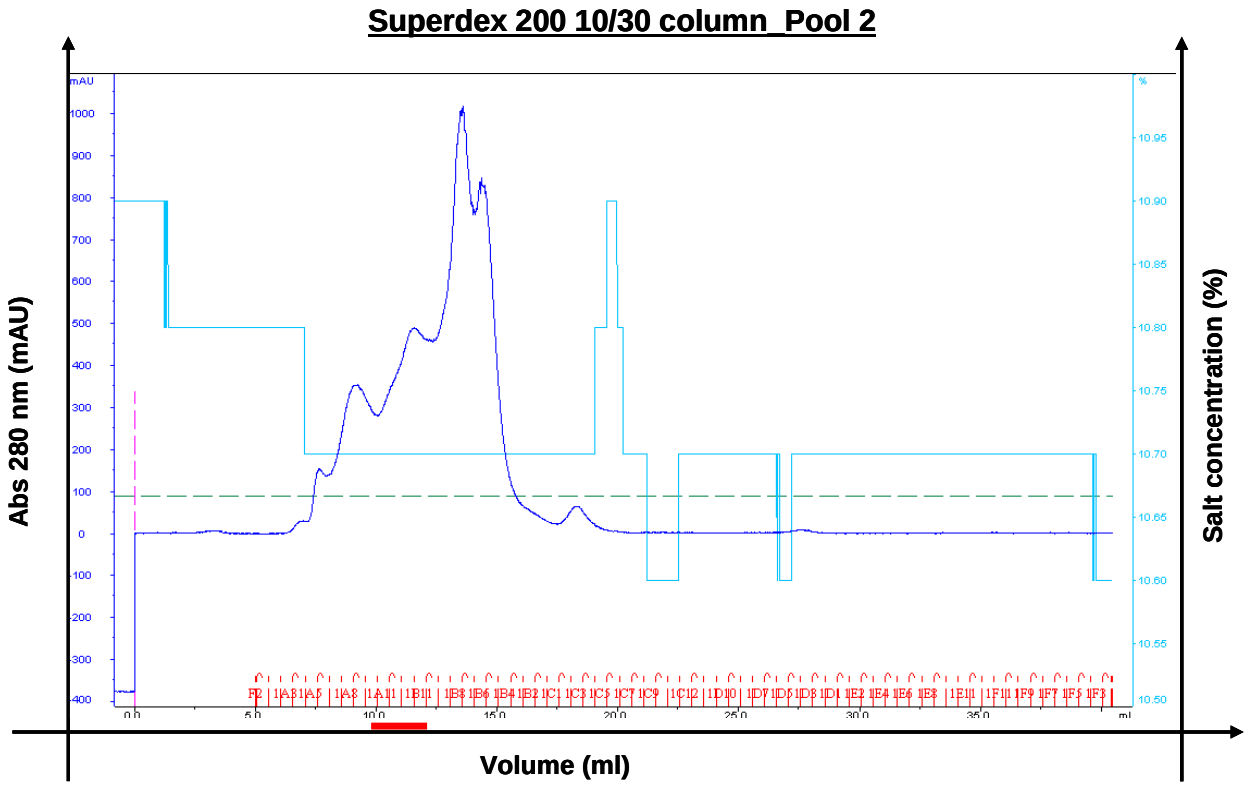

Figure 3.36: Gelfiltration with a Superdex S200 HR 10/30 column of the pool 2 fractions from the DEAE column. The dark blue line shows the elution profile measured at 280 nm for the visualization of the proteins. The light blue line corresponds to the salt elution profile of the TSDG-buffer B in percent (%), which contains 1 M NaCl. For this run a linear gradient of 10% buffer B was applied. The activity fractions (A11-B10) detected in figure 3.32 are marked by a red bar on the x-axis. These were pooled for the next purification step, forming pool 3.

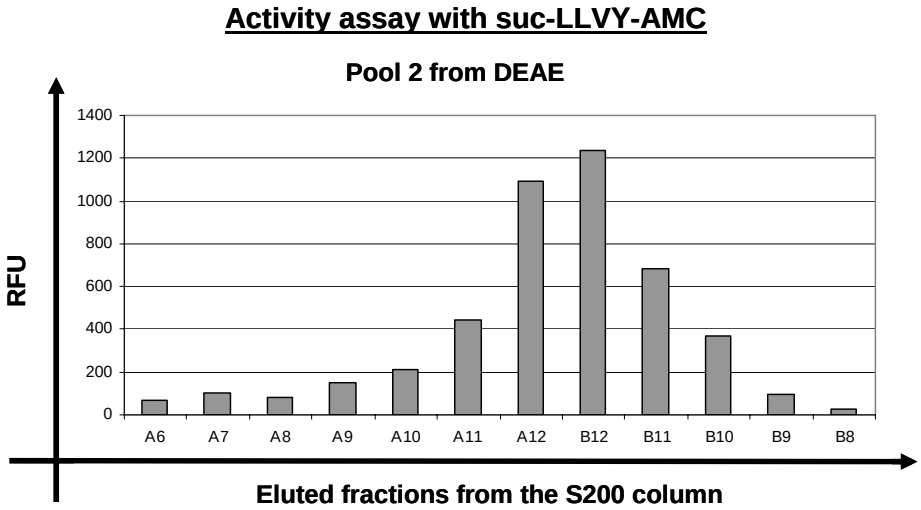

Figure 3.37: Activity assay of the S200 fractions from pool 2 with the suc-LLVY-AMC substrate. In these *in vitro* fluorogenic assays the 100 µM suc-LLVY-AMC substrate was digested with 20 µl from the eluted fractions, to detect endopeptidase activity. The release of AMC was measured by relative fluorescence units (RFU) at λEx = 360 nm and λEm = 450 nm.

Besides its purification properties, a further advantage of the gelfiltration technique is the possibility to determine the approximate molecular weight of the eluent. This is possible using different molecular weight standards (figure 3.38). Using the equation of the standards the molecular weight of the S200 activity peaks from pool 1 (A12) and pool 2 (B12) were calculated. The eluent in fraction A12 from pool 1 has an approximate mass of 83 kDa and the eluent from pool 2 (B12) has about 67 kDa.

S200 Peak	Ve [ml]	K av	log MW	MW [Da]	MW [kDa]
Pool 1 A12	11.1	0.29	4.92	83303	83
Pool 2 B12	12.3	0.38	4.83	66865	67

Standards	MW [Da]	Ve [ml]	K av	log MW
Ribonuclease A	13700	20.6	1.01	4.14
Chymotrypsinogen A	25000	18.1	0.82	4.40
Ovalbumin	43000	14.6	0.56	4.63
Albumin	67000	12.1	0.37	4.83

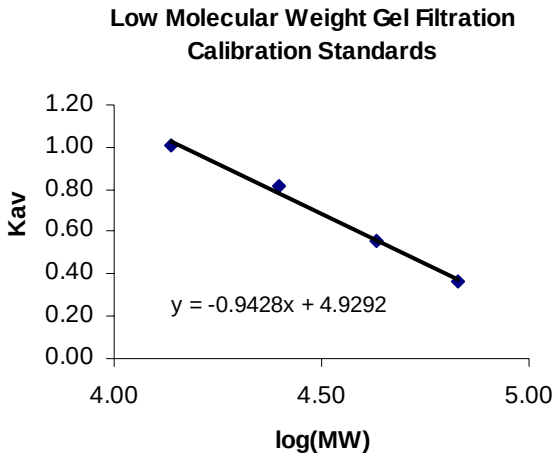

Figure 3.38: Molecular weight determination of the eluents from pool 1 and pool 2 through gelfiltration. The standards used were albumin (67 kDa), ovalbumin (43 kDa), chymotrypsinogen A (25 kDa) and ribonuclease A (13,7 kDa). After the gelfiltration of these standards, the elutionvolume (Ve) was measured. Applying the equation Kav = (Ve-Vo)/(Vt-Vo) and the using the Kav/log(MW)-diagram the molecular mass of the eluents from pool 1and 2 was calculated approximately.

Fix column factors:

Column void volume (Vo) = 7.2; Total bed volume (Vt) = 20.5

3.3.5 Anion exchange chromatography (Mini Q™ column)

The activity fractions, A11-A12 and B12-B10 from the S200 column (figure 3.37) were pooled forming pool 3 comprising a volume of 2 ml. First, the sample was diluted with TSDG-buffer A (pH 7.6) to adjust the pH necessary for the MiniQ column. Then the sample (3 ml) was loaded onto the Mini Q™ column for ion-exchange chromatography, which has been used, because of its greater resolutions potential. The elution profile of the Mini Q™ purification step is shown in figure 3.39. The gradient applied was of 0-20% TSDG-buffer B, which contains 1 M NaCl. The eluted fractions were tested for endopeptidase activity using the suc-LLVY-AMC substrate (figure 3.40). Two main activities were detected: B7-B3 and B1-B3. Recapitulatory it can be stated, that the LCL721 cells bear an endopeptidase activity in the cytosol, which is neither from the proteasome nor from the TPPII peptidase.

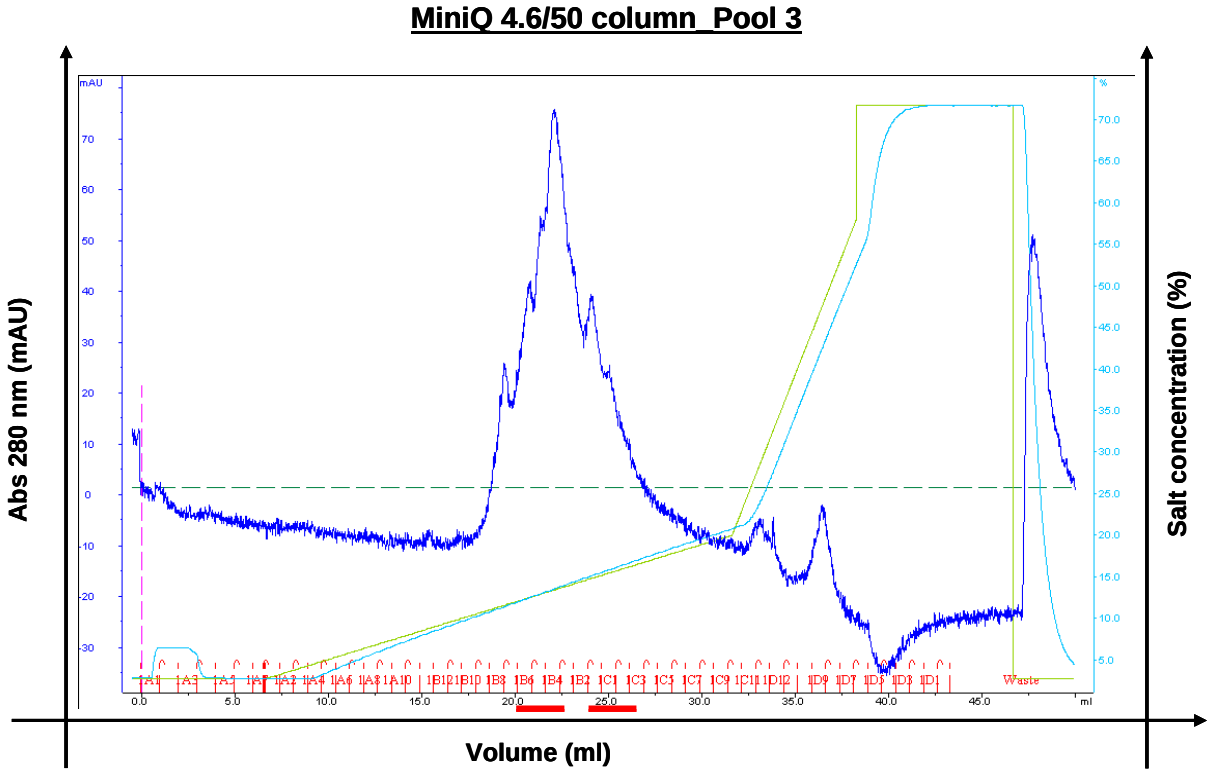

Figure 3.39: Ion exchange chromatography (IEX) of the pool 3 from the S200 purification using a Mini Q™ column. The Mini Q™ material is a strong anion exchanger. The dark blue line shows the elution profile measured at 280 nm for the visualization of the proteins. The light blue line corresponds to the salt elution profile of the gradient applied with the TSDG-buffer B (0-20%), which contains 1 M NaCl. Under the x-axis the range of the pooled activity fractions are marked with horizontal bold red bars. The activity was detected in the fractions B7-B3 and B1-C3.

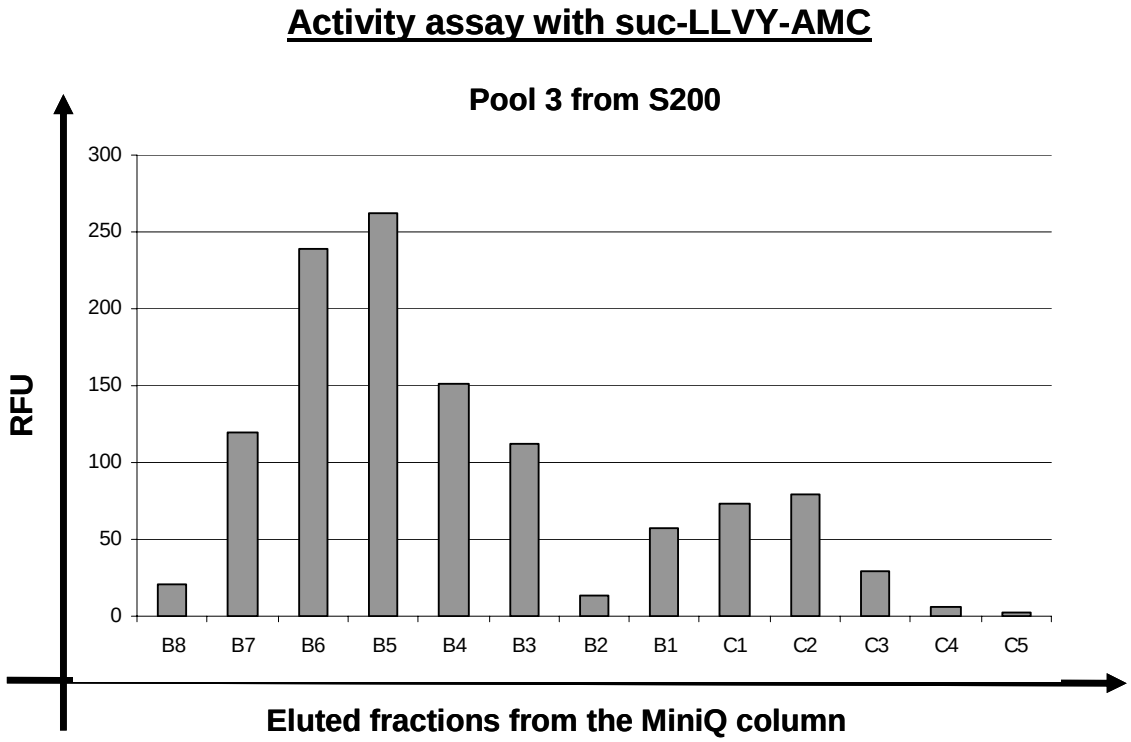

Figure 3.40: Activity assay of the eluted Mini Q™ fractions from pool 3. In these *in vitro* fluorogenic assays the 100 µM suc-LLVY-AMC substrate was digested with 20 µl from the eluted fractions, to detect the fractions showing endopeptidase activity. The release of AMC was measured by relative fluorescence units (RFU) in a spectrafluorometer (λEx = 360 nm and λEm = 450 nm) at 37°C for 30 minutes.

3.3.6 SDS-PAGE and coomassie staining

To characterize these two identified activities (figure 3.40), the corresponding fractions were separated via a reducing SDS-PAGE. Subsequently, the gel was stained with coomassie blue for visualization of the protein bands (figure 3.41). Each second fraction was loaded for separation on a reducing SDS-PAGE gel, to be able to detect band intensity differences between the lanes. The protein bands showing a greater intensity on the lanes were the activity peak fractions were loaded (in comparison with the neighbouring lanes) had been marked with a red rectangle and numbered. These marked bands were cut out afterwards and analyzed via mass spectrometry.

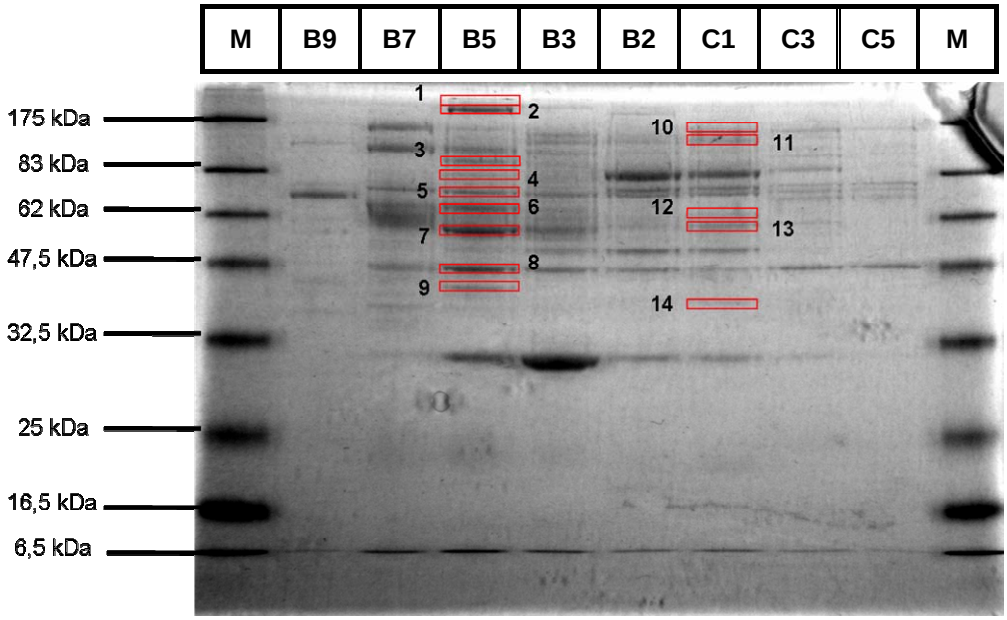

Figure 3.41: SDS-PAGE after coomassie blue staining of the Mini Q™ fractions from pool 3. On top of the gel the corresponding fractions loaded on the gel are labelled. Each second fraction was loaded for separation on a reducing SDS-PAGE gel, to be able to detect band intensity differences between the lanes. Flanking the gel the protein marker was loaded for the identification of the molecular mass of the bands on the gel. The red rectangles symbolize the bands cut for mass spectrometry analysis. These rectangles are serially numbered.

3.3.7 Mass spectrometry analysis of the SDS-PAGE bands

The bands marked with red rectangles of the SDS-PAGE gel, see figure 3.41 were analyzed via mass spectrometry. After cutting them out of the gel a trypsine digestion was performed. The samples were measured in an electrospray ionization (ESI) mass spectrometer and further analyzed using the Swissprot database. The identified proteases in the samples are listed in table 3.2. All hits identified in the samples corresponding to keratin, HSPs or actin, were excluded from the list. The bands 1 to 9 belong to the activity peak B5 and the remaining bands to the C1 peak from the MiniQ purification step. In the fraction B5, three potential endopeptidases were detected, the ubiquitin carboxyl terminal hydrolase 47 (band 2), the dipeptidyl peptidase 9 (band 3 and 4) and the Lon protease (band 4). In fraction C1 no major hit could be found. Taken the results of the LCL721 cytosolic purification, it can be stated, that potential endopeptidases could be found in the cytosol of these cells.

Gelband	Entry	Description	mW (Da)
1	FAS_HUMAN	Fatty acid synthase EC 2 3 1 85	273224
2	UBE1_HUMAN	Ubiquitin activating enzyme E1 A1S9 protein Homo sapiens Human	117774
	ULK1_HUMAN	Serine threonine protein kinase ULK1 EC 2 7 11 1 Unc 51 like kinase 1 Homo	112530
	PPWD1_HUMAN	Peptidylprolyl isomerase domain and WD repeat containing protein 1 EC 5 2 1 8	73527
	TNI3K_HUMAN	Serine threonine protein kinase TNNI3K EC 2 7 11 1 TNNI3 interacting kinase	104112
	UBP47_HUMAN	Ubiquitin carboxyl terminal hydrolase 47 EC 3 1 2 15 Ubiquitin thioesterase	157168
3	DPP9_HUMAN	Dipeptidyl peptidase 9 EC 3 4 14 5 Dipeptidyl peptidase IX DP9	98201
4	DPP9_HUMAN	Dipeptidyl peptidase 9 EC 3 4 14 5 Dipeptidyl peptidase IX DP9	98201
	NEK9_HUMAN	Serine threonine protein kinase Nek9 EC 2 7 11 1 NimA related protein kinase	107100
	LONM_HUMAN	Lon protease homolog mitochondrial precursor EC 3 4 21 Lon protease like p	106422
5	NCF2_HUMAN	Neutrophil cytosol factor 2 NCF 2 Neutrophil NADPH oxidase factor 2 67 kDa	59723
	PLSL_HUMAN	Plastin 2 L plastin Lymphocyte cytosolic protein 1 LCP 1 LC64P Homo sa	70113
6	NCF2_HUMAN	Neutrophil cytosol factor 2 NCF 2 Neutrophil NADPH oxidase factor 2 67 kDa	59723
	2AAA_HUMAN	Serine threonine protein phosphatase 2A 65 kDa regulatory subunit A alpha isofor	65050
	PLSL_HUMAN	Plastin 2 L plastin Lymphocyte cytosolic protein 1 LCP 1 LC64P Human	70113
7	RD23B_HUMAN	UV excision repair protein RAD23 homolog B hHR23B XP C repair complementing	43144
	PLSL_HUMAN	Plastin 2 L plastin Lymphocyte cytosolic protein 1 LCP 1 LC64P Human	70113
	SYHC_HUMAN	Histidyl tRNA synthetase cytoplasmic EC 6 1 1 21 Histidine tRNA ligase	57374
8	NCF4_HUMAN	Neutrophil cytosol factor 4 NCF 4 Neutrophil NADPH oxidase factor 4	39007
	RD23B_HUMAN	UV excision repair protein RAD23 homolog B	43144
	PFTA_HUMAN	Protein farnesyltransferase geranylgeranyltransferase type I alpha subunit	44381
	IF4B_HUMAN	Eukaryotic translation initiation factor 4B eIF 4B Homo sapiens Human	69183
	PGT1_HUMAN	Geranylgeranyl transferase type 1 subunit beta EC 2 5 1 59	42368
9	NCF4_HUMAN	Neutrophil cytosol factor 4 NCF 4 Neutrophil NADPH oxidase factor 4	39007
	PGT1_HUMAN	Geranylgeranyl transferase type 1 subunit beta EC 2 5 1 59	42368
10	CAND1_HUMAN	Cullin associated NEDD8 dissociated protein 1	136288
	OXRP_HUMAN	150 kDa oxygen regulated protein precursor Orp150 Human	111266
	NCF4_HUMAN	Neutrophil cytosol factor 4 NCF 4 Neutrophil NADPH oxidase factor 4	39007
11	CAND1_HUMAN	Cullin associated NEDD8 dissociated protein 1	136288
12	STK4_HUMAN	Serine threonine protein kinase 4 EC 2 7 11 1 Mammalian	55594
13	SYHM_HUMAN	Probable histidyl tRNA synthetase mitochondrial precursor EC 6 1 1 21	56851
14	RASF2_HUMAN	Ras association domain containing protein 2 Homo sapiens Human	37766

Table 3.2: Mass spectrometry analysis of the gelbands from the activity peak fractions B5 and C1. All hits identified in the samples corresponding to keratin, HSPs or actin, were excluded from the list.

4 Discussion

Most peptide ligands presented on the cell surface by MHC class I molecules are the product of the endogenous antigen processing pathway. Some peptides liberated from proteins in the cytosol by proteasomes and other cytosolic peptidases can be transported by the heterodimeric TAP into the ER lumen, where they bind to nascent MHC class I molecules. Once the MHC class I/peptide complex is formed, it is transported in vesicles through the Golgi apparatus to the cell surface for CTL recognition, allowing the immune system to detect infections and malignant mutations in the cells.

The precursors of these MHC class I peptide ligands are created through a multistep pathway starting with the breakdown of proteins by the proteasome alone (Kloetzel, 2004) or in cooperation with TPPII. In some cases the proteasome already generates the final peptide ligand for MHC class I molecules (Lucchiari-Hartz et al., 2000). Furthermore, many identified proteasomal products are peptide precursors with the correct C-terminus (Craiu et al., 1997; Mo et al., 1999; Stoltze et al., 1998) while the N-terminus is extended (Cascio et al., 2001; Komlosh et al., 2001; York et al., 2002). Such precursor peptides are subject to proteolytic attack by endopeptidases and aminopeptidases in the cytosol (Beninga et al., 1998; Reits et al., 2004; Seifert et al., 2003; Stoltze et al., 2000; York et al., 2002). The efficiency of each of these processes depends on the amino acid sequence of the presented ligand and its precursors. Hence, the amino acid sequence of the flanking regions of potential antigens plays a primordial role in the specificity of processing.

4.1 S8L expressing cells with constructs carrying different C-terminal regions

To examine the effect of the amino acids at the C-terminal extension of the SIINFEKL epitope on MHC class I ligand processing and presentation, S8L-constructs with specific amino acid exchanges at the C-terminus were generated. As already mentioned, the S8L is presented on the murine MHC class I molecule H-2K^b and this complex was detected using the monoclonal specific antibody 25-D1.16 (Porgador et al., 1997).

To analyze the generation of S8L from the C-terminal extended S8L precursor peptide carrying the amino acid exchanges, the cell line Flp-In 293K^b was used for transfection of the

S8L-constructs. Due to the Flp-In system, which allows only one insertion at a defined position (FRT) in the genome of this cell line, each transfectant has the same expression level of the S8L epitope. To ensure this and discard that, due to a higher turnover rate, the cells could have an increased production of S8L, this construct bears an IRES-EGFP cassette directly after the S8L. Since the expression of S8L and EGFP is directly proportional, this helps to monitor the S8L expression by detecting the EGFP fluorescence. To compare the presented S8L peptides on the H-2K^b molecule between the transfectants the EGFP level was used to normalize these values. After determining the steady state S8L level of the transfected Flp-In 293K^b cells (figure 3.6), different presentation levels of the SIINFEKL epitope on the cell surface of these cells were detected. These differences in presentation are due to the amino acids exchanged at the corresponding position. The cell line P1'& has been used as a control cell line, because it shows the maximal presentation of S8L. The construct carries a stop-codon (&) directly after the S8L epitope and therefore needs no processing by the proteasome, as the C-terminus is already correctly shaped for presentation. Thus, this precursor peptide does not compete with other K^b-epitopes for proteasomal cleavage. The presentation level of S8L from this construct is defined as 100%. The S8L precursor peptide carrying after the leucine of S8L, an arginine at the first C-terminal position (P1'R_{ori}) followed by the original sequence of the ovalbumin, shows a very high rate of presentation. Therefore, indicating that arginine is approximately 6.5 times preferred for processing & presentation compared to the ovalbumin original amino acid at this place, the threonine (P1'T_{ori}). Also the S8L precursors with an amino acid exchange at the second position after the S8L followed by the original sequence of the ovalbumin (P2'X_{ori}) show some characteristics. At this position aromatic amino acids seem to be preferred for processing, as S8L precursors carrying a phenylalanine, tryptophan or tyrosine present a higher level of S8L than the others. Moreover, the shorter S8L precursors of second pool of exchanges at the second position (P2'X&) the isoleucine amino acid seems to play an important role, showing a high preference for processing. Further interesting amino acid combinations at the C-terminal flanking region of the model epitope are found in the following S8L precursors: -SIINFEKL**LL** and -SIINFEKL**IR**WTS- (figure 3.7). Both show S8L generation/presentation rates of above 20%.

To analyze these preferences on proteasomal processing the proteasomal inhibitor lactacystin was used. Hence, a kinetic to determine the presentation rates of each transfectant with or without adding the inhibitor (lactacystin) was performed by stripping the cell surface of the

transfectants. For the stripping, the cells were treated with an acid solution, which leads to dissociation of the peptides from the MHC class I molecules. The rate of generating new peptides and presenting them on the MHC class I molecules was determined for each transfectant (figure 3.12, 3.15). The results are consistent with the S8L levels detected in the steady state assays. Again the arginine ($P1'R_{ori}$), the P'IR and the aromatic acids ($P2'X_{ori}$) showed not only high S8L presentation levels, but also despite adding lactacystin a strong re-presentation of S8L was obtained: P2'Y& > P2'W& > $P1'R_{ori}$ > P'IR > P'LL& > $P2'L_{ori}$ > $P'LL_{ori}$. Others like P1'L& or P1'W& have very low S8L generation rates and are not going to be further analyzed. This wouldn't be a significant result. The S8L precursor – SIINFEKL**AI**WTS- ($P2'I_{ori}$), which shows a high S8L presentation is generated exclusively by the proteasome, as in the setting with lactacystin shows a very strong reduction of the epitope on the cell surface. The combination of the amino acids A and I at the C-terminus seems to be very favourable for proteasomal processing. Moreover, a general observation can be made when analysing the transfectants of the P1'X& and P2'X& constructs. The short S8L precursor peptides with exchanges at the first position (P1'X&) seem to be unfavoured for processing, presumably because of their lack of a C-terminal extension. Further on, the precursor P2'X& peptides show an overall insensitivity towards the inhibitor lactacystin.

Lactacystin is a natural product of Actinomyces originally isolated by Omura and co-workers (Omura et al., 1991). Its clasto lactacystin ß-lactone is a potent inhibitor of the proteasome. It is also known that lactacystin and related lactones inhibit the chymotrypsin-like and trypsine-like activities of the proteasome irreversibly by the modification of NH_2-terminal threonine residue essential for catalytic activity (Fenteany et al., 1995). Like the peptide aldehydes and vinyl sulfones, lactacystin also inhibits proteases other than the proteasome, like cathepsin A (Ostrowska et al., 1997) and tripeptidyl peptidase II (partially) (Geier et al., 1999). Hence, the efficiency and specificity of the proteasomal inhibition had to be ensured using a different proteasomal inhibitor, epoxomicin. Both, lactacystin and epoxomicin are irreversible proteasomal inhibitors of the chymotrypsin-like subunit, but the action of epoxomicin has been published to be 80-100 times more potent than that from lactacystin (Meng et al., 1999). Meng and co-workers showed in their studies (Meng et al., 1999) that epoxomicin, the natural product from Actinomycetes, covalently binds the LMP7, X, Z, and MECL1 catalytic ß-subunits of the proteasome and selectively inhibits the three major proteasome proteolytic activities at different rates. Epoxomicin inhibits primarily the proteasomal chymotrypsin-like activity; the trypsin-like and PGPH activities were also inhibited at approximately 100- and

1,000-fold weaker rates, respectively. However, unlike several other peptide-based inhibitors, epoxomicin does not inhibit nonproteasomal proteases such as trypsin, chymotrypsin, cathepsin B, papain, and calpain at concentrations of up to 50 mM (Meng et al., 1999).

The cell lines examined for proteasomal cleavage using epoxomicin still achieved a re-presentation rate consistent with the calculated rates using lactacystin. For P1'R_{ori} and P'IR_{ori} the S8L re-presentation rate was about 69% and 45% respectively.

After having demonstrated that the proteasome is not exclusively involved in the generation of the S8L from of specific precursor peptides, TPPII was tested as a possible candidate. TPPII was considered to play a role in the C-terminal cleavage needed for the S8L generation, because in recent studies, it was published to generate both cleavages (N- and C-terminal) for the HLA-A3 HIV Nef(73-82) epitope (Seifert et al., 2003). TPPII is known to have a strong N-terminal exopeptidase activity, which removes tripeptides sequentially from a free N-terminus of larger peptides (Tomkinson, 2000). It has broad substrate specificity, considering that there is little apparent sequence similarity between the tripeptides removed (Tomkinson, 2000). However, the rate of cleavage varies more than 100-fold depending on the sequence of the substrate (Tomkinson and Lindas, 2005). The enzyme seems to have some preference for cleaving after hydrophobic residues, and cannot cleave before or after proline residues. Beside the predominant exopeptidase activity, TPPII also displays a low endopeptidase activity, cleaving preferentially after lysine-residues (Geier et al., 1999; Seifert et al., 2003). For this purpose, two TPPII inhibitors, AAF-CMK and butabinde were tested on S8L presentation on the cell surface of these transfectants (figure 3.18). Because butabindide is very instable at 37°C and it is susceptible for FCS, further analysis was performed with AAF-CMK (figure 3.19). Nevertheless, the inhibition of TPPII did not impair the presentation of the S8L epitope on the cell surface, indicating that TPPII does not play a crucial role in antigen processing of this specific epitope, S8L.

However, several problems emerge when using inhibitors. For instance, AAF-CMK is not specific for any single aminopeptidase since it has been shown to inhibit three cytosolic aminopeptidases, TPPII, PSA, and BH (Seifert et al., 2003; Stoltze et al., 2000; Wherry et al., 2006). Therefore, it is possible that other aminopeptidases responsible for trimming in living cells were inhibited by AAF-CMK. Though butabindide has been suggested to be highly specific for TPPII (Rose et al., 1996), it does inhibit other peptidases, e. g. TPPI (Warburton

and Bernardini, 2002), and further potential effects of butabindide on other aminopeptidases have not been examined yet.

Besides specificity and stability of inhibitors other problems like toxicity, when working with living cells, may dampen the expected effects. For example, prolonged exposure to proteasome inhibitors results in increased cell death in thymocytes even in the absence of other inducers of apoptosis. Epoxomicin is known to inhibit NF-kB activation. Moreover, it induces the accumulation of p53 and ubiquitinated proteins in cell culture (Meng et al., 1999). This shows that inhibition in the cell influences and disturbs the normal cellular metabolism, leading to artefacts during the studies.

4.2 Silencing of cytosolic peptidases

Now, the question arises, who is generating S8L from the partial proteasome independent precursor peptides? This protease or peptidase probably has an endo- or carboxy-peptidase activity, in order to cleave at the C-terminal extention of the S8L precursors. To answer this question three peptidases were selected for examination on S8L processing, TPPII, ThOP1 and IDE. TPPII and ThOP1 have shown to act as endopeptidases and to be involved in antigen processing (Geier et al., 1999; Saric et al., 2001; Seifert et al., 2003; York et al., 2003). Insulin-degrading enzyme (IDE) has been reported to be implicated in regulating growth factor levels, muscle differentiation and to process insulin by antigen-presenting cells. Nevertheless, the role of this enzyme in antigen processing has not been investigated so far and should be further elucidated in this work.

To analyze their role in antigen processing a more specific approach than using inhibitors against these peptidases was developed, gene silencing by RNA interference (RNAi). The selective and robust effect of RNAi on gene expression makes it a valuable research tool. The siRNA transfection was performed in the cell line Flp-In 293K^{b}_IR, which expresses the following precursor peptide: -SIINFEKL**IR**WTS-. The C-terminal cleavage for S8L generation from this precursor peptide lies between the leucine (of the S8L) and the isoleucine.

The analysis of protease activities from the cytosol of the siRNA transfected cells for the silenced peptidases demonstrates that the earliest time point to examine the S8L presentation is two days after electroporation. Nevertheless, residual activity of ThOP1 and TPPII was still detectable in the lysates, probably due to the remaining ThOP1 and TPPII in the siRNA transfected cells, as the "knock-downs" of the peptidases did not achieve 100%. Presumably, it is also possible that other peptidases in the cytosol have some affinity to the substrates used. Additionally, to ensure that the activity obtained by the fluorescent substrate digestion assays is specific for the peptidase considered, specific inhibitors were used. The inhibitor for ThOP1 did not show a strong inhibition, thus the specificity of the activity obtained in this assay cannot be completely assigned to the protease ThOP1.

A strong reduction of the protease ThOP1 showed consistently a clear increase in S8L presentation, indicating a role in antigen destruction. These results are concordant with the reported antigen destruction in cells over-expressing ThOP1 (Saric et al., 2001) and the improvement of the presentation of antigenic peptides by down-regulation of ThOP1 using RNAi techniques (York et al., 2003).

After siRNA electroporation for TPPII silencing, a maximal reduction of approximately 50% of the peptidase expression at mRNA level was detected. This is not a strong gene silencing and therefore not sufficient to make a statement about its role in processing of the S8L. Some improvements regarding TPPII gene silencing should follow. Maybe, the siRNA used for silencing TPPII did not impair the formation of new TPPII peptidases efficiently. Therefore, one possibility would be designing a new siRNA duplex that targets a different region of the TPPII gene or even using several siRNA duplexes targeting different regions at a time, to impede the generation of TPPII completely.

The "knock-down" of IDE was carried out using four siRNA duplexes targeting different regions at a time. The best gene silencing levels were obtained using these mixed duplexes. By an IDE reduction of 71% (detected at mRNA level) the S8L amount presented did not differ from the levels achieved with the control cells. Though by a reduction of 88% on day four after siRNA electroporation the S8L presented decreased dramatically, indicating a strong influence of IDE on processing and generating S8L. This single experiment will be repeated to ensure reproducibility.

Additionally, western blots could be performed to quantify the remaining amount of protease remaining after siRNA transfection. Consequently, a better time point for the presentation analysis can be determined.

4.3 Identification of endopeptidases from the LCL721 cytosol

There is considerable evidence that, other peptidases than the proteasome (mostly aminopeptidases) are important in trimming antigenic precursors for presentation. Proteasomes have been shown *in vitro* (Cascio et al., 2001; Gileadi et al., 1999) and in living cells (York et al., 2002) to generate many N-extended precursors. Other experiments have shown that if N-extended peptide precursors are expressed or injected into cells they are trimmed and presented by MHC class I on the cell surface (Craiu et al., 1997; Reits et al., 2003). Processing of such peptides can occur in the presence of proteasome inhibitors (Craiu et al., 1997; Golovina et al., 2002; Stoltze et al., 1998), indicating that other peptidases in the cell can cleave N-terminal residues. Aminopeptidases can trim N-extended precursors that have a free amino terminus, but not if the N-terminus is blocked (Mo et al., 1999; Reits et al., 2003). Eliminating or inhibiting aminopeptidases in cells reduces antigen presentation (Levy et al., 2002; Reits et al., 2004; York et al., 2002). Moreover, in studies performed by Reits et al. (2004) and Seifert et al. (2003) it was demonstrated that not only the proteasome performs the correct C-terminal cut, but also TPPII plays a role in precursor generation, with or without the proteasome.

Considering this and the results obtained in the S8L presentation assays, the purification of the cytosol from LCL721 cells was the next step to identify an endopeptidase activity. This endopeptidase is supposed to be responsible for the generation of S8L out of the partial proteasome independent precursors. For this purpose, the suc-LLVY-AMC substrate was used in the digestions of the eluting peaks from every column. The succinyl-group protects the substrate from aminopeptidase cleavage and the AMC can only be released if the activity comes from an endopeptidase. After desalting the cytosol and separating activity peaks after certain characteristics, the activity peaks eluted from the third and last column (MiniQ) were run on a SDS-PAGE to obtain clear bands upon molecular weight. After mass spectrometry analysis of the bands that came into question, three peptidases were identified, which

potentially could act as endopeptidases. These peptidases are UBP47_Human, DPP9_Human, LONM_Human.

UBP47_Human

Ubiquitin carboxy-terminal hydrolases (UCHs) are thought to hydrolyse bonds between small adducts and ubiquitin to generate free monomeric ubiquitin (Dang et al., 1998). Thus, UCHs are essential in continuing the function of the ubiquitin system, which has a role in the breakdown of abnormal proteins (Hershko and Ciechanover, 1998). In mammals, at least three isoforms of UCH have been biochemically identified (Wilkinson et al., 1992) and two (UCHL1 and UCHL3) have been characterized at the molecular level (Kajimoto et al., 1992). UCHL1 is a ubiquitous protein making up 2% of all proteins in the brain and alterations of this enzyme have been involved in Parkinson disease. Mutations in the UCHL1 gene result in 50% decrease of catalytic activity, implying that loss of UCHL1 activity in Parkinson disease might lead to reduced ubiquitination and therefore impaired clearance of abnormal proteins. Accumulation of certain proteins may be toxic too (Betarbet et al., 2004). While the monomeric form of UCHL1 catalyzes deubiquitination, the dimers display a ubiquitin ligase activity that generates ubiquitin-K63 bonds (Betarbet et al., 2004; Liu et al., 2002).

DPP9_Human

The heterogenous S9b family of DPPs (dipeptidyl peptidases) is a growing family of serine peptidases, which is characterized by the first identified member DPP-IV (also called CD26; EC 3.4.14.5) (Rawlings and Barrett, 1999). DPP-IV was first identified by Hopsu-Havu and Glenner (Hopsu-Havu and Glenner, 1966) and has a general ability to cleave prolyl and alanyl peptide bonds at the penultimate position from the N-terminus (Kenny et al., 1976; Rawlings and Barrett, 1993). More recently, two members of the S9b family DPP-8 and DPP-9 have been discovered (Abbott et al., 2000; Olsen and Wagtmann, 2002). DPP-9 was identified in silico by Abbott et al. (2000). An 863-amino-acid cDNA variant was expressed, giving a mass of approx. 98 kDa as determined from SDS/PAGE analysis (Olsen and Wagtmann, 2002). No *in vivo* functions have been described for DPP-9. In studies performed by (Bjelke et al., 2006) they found that only the full-length variants of both DPP-8 and DPP-9 were enzymatically active, and both were able to cleave the naturally occurring peptides of the incretin and pancreatic hormone families: GLP-1 (glucagonlike peptide 1), GLP-2, NPY (neuropeptide Y) and PYY (peptide YY).

LONM_Human

The Lon protease has been studied intensively in prokaryotes (Tsilibaris et al., 2006). It is a member of the AAA+ protein family (ATPases associated with various cellular activities) (Neuwald et al., 1999). After recognition and binding of the substrate to the protease, hydrolysis of ATP permits substrate unfolding; the unfolded substrate is then translocated into the proteolytic chamber of the protease where processive peptide bond cleavage takes place (Wickner et al., 1999). Lon is an oligomer of identical subunits (87 kDa). Although no crystal structure of the full-length protein has yet been reported, crystallization of the carboxy-terminal domain of the *E. coli* Lon led to the demonstration that Lon forms a ring-shaped hexamer (Botos et al., 2004). Each subunit contains three domains: the amino-terminal domain, possibly involved in substrate recognition and binding (Ebel et al., 1999), the central ATPase domain (A domain) containing the ATP binding (Walker) motif (Fischer and Glockshuber, 1994) and responsible for polyphosphate and DNA binding (Nomura et al., 2004), and the carboxy-terminal domain (P domain) containing the proteolytic active site formed by a serine–lysine catalytic dyad (Amerik et al., 1991). An additional region located between the A and the P domains, the SSD domain (sensor and substrate discrimination domain), has been shown to be involved in substrate recognition (Smith et al., 1999). Lon degrades naturally unstable proteins that are involved in a great variety of biological processes. Lon also plays an important role in protein quality control by degrading misfolded proteins that would otherwise aggregate. Aggregation is prevented by the synergic action of chaperones (DnaK system) and proteases, mainly Lon (Tomoyasu et al., 2001). The mechanism by which Lon recognizes these two types of substrates is not fully understood. Although Lon has been found to preferentially recognize certain key amino acids or key domains of some substrates (e.g., the carboxy-terminal histidine of SulA) (Ishii and Amano, 2001), no consensus motif—or combination of motifs—specifically recognized by Lon has yet been identified. Instead, substrate discrimination appears to be mediated through protein structure. The common feature of unfolded proteins and naturally unstable proteins degraded by Lon is likely to be their nonglobular conformation (Van et al., 1996). Recognition of a protein and its subsequent degradation by Lon might thus result from exposure, at the protein surface, of hydrophobic patches or structural motifs that are normally hidden in the protein core.

In mammalian cells, Lon is located in the mitochondrium and removes oxidatively damaged proteins, chaperones the assembly of inner membrane complexes and is implicated in age-related mitochondrial dysfunction (Bota and Davies, 2002). Mitochondrial Lon is essential for

viability: reduction of Lon activity impairs cell division and leads to necrosis (Bota et al., 2005). A total loss of Lon activity leads to apoptosis (Bota et al., 2005).

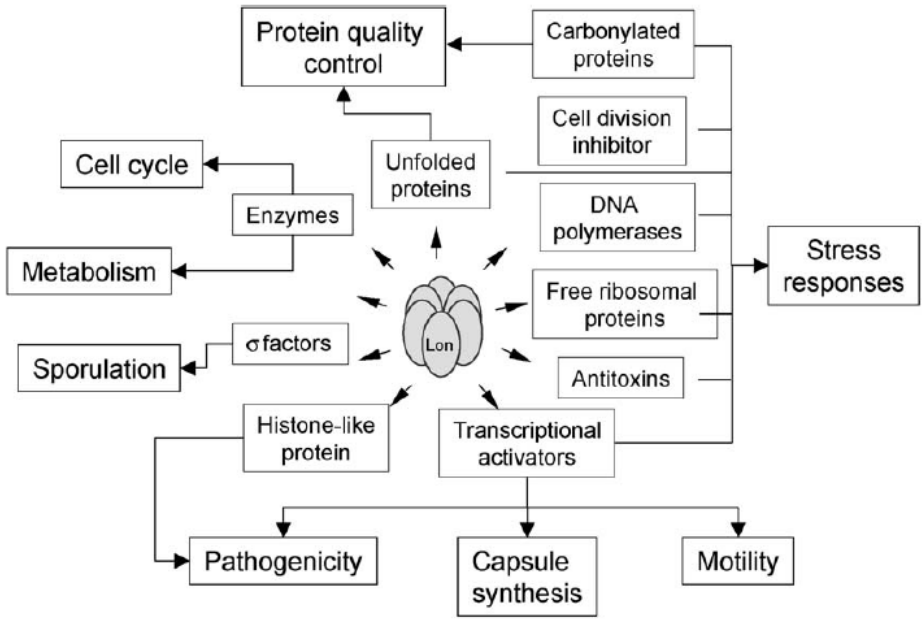

Fig. 1. Substrate diversity and biological functions of the Lon protease. General diagram showing the diversity of the Lon substrates and the large number of biological processes regulated through their proteolysis (boxed). It is interesting to note that Lon is often involved in the regulation of specific cellular processes by degrading different classes of proteins involved in different pathways (Tsilibaris et al., 2006).

Of these three identified hits via mass spectrometry, the most promising peptidase might be the Lon protease, which has been investigated intensively in prokaryotes. The authors of this field have shown that Lon plays an important role in different pathways of the cells metabolism. Because of the broad variability of Lon substrates, one could imagine to perform the cleavage of the suc-LLVY-AMC substrate and therefore to posses the endopeptidase activity for the generation of the S8L from the partially proteasome independent precursor peptides for presentation. However, Lon has not been well investigated in mammals and is supposed to be localized in the mitochondrion. Though, in this project the purification was performed from cytosolic samples of the human LCL721 cells, it could be possible that some impurities from the mitochondrial organelles have been mixed or have not been separated well enough by centrifugation.

4.4 Further analysis of the S8L generation

Regarding the results obtained, it has been verified that there is a preference on processing of an antigen depending on the amino acids flanking at C-terminus of the epitope and several partially proteasome independent S8L precursor peptides could be identified. However, evidence is still missing about what exactly is the sequence presented on the MHC class I molecule and the endopeptidases identified still need further analysis to demonstrate their role in antigen processing.

To ensure that the precursor peptides are cleaved after the last leucine of the -SIINFEKLXXXXX- peptide, it should also be analyzed, if it is always just S8L presented. The antibody 25-D1.16 recognizes the H-2K^b/S8L complex, but it doesn't discriminate between a SIINFEKL or a SIINFEKL**L** presented on the MHC class I molecule, when pooling synthetic generated peptides on the cells for recognition by the 25.D1-16 (data not shown). Therefore, immunoprecipitation (IP) assays of the H-2K^b/peptide complexes from the cells of interest should be examined for the exact sequence of the presented peptide. After the IP assay using the Y-3 antibody (anti-H-2K^b), the peptides can be eluted from the MHC class I binding groove and further analyzed by mass spectrometry.

To improve the detection assays during purification of the cytosol of the LCL721 cells a modified activity assay should be used. The activity detected using the suc-LLVY-AMC substrate is just showing an endopeptidase activity with a preference for tyrosine (Y) cleavage. Due to the succinyl group at the N-terminus the substrate is protected from N-terminal processing. Therefore, the following substrates should be tested on processing, to identify if the purified activity fractions are also able to generate the S8L from the S8L precursor peptides that were partially proteasome independent: suc-SIINFEKL**IR**WTS, suc-SIINFEKL**R**EWTS; suc-SIINFEKL**AW**; suc-SIINFEKL**AY**.

4.5 The link between vaccine design and antigen processing/presentation

Vaccination is one of the most successful public health initiatives ever achieved, with the global eradication of diseases such as smallpox and the virtual eradication of poliomyelitis. Despite such successes, vaccines for many diseases remain elusive and as such several strategies have been devised to deliver specific and immunogenic vaccine components to the

immune system in the hope of eliciting a therapeutic or prophylactic immune response (Purcell et al., 2007).

Understanding the science of antigen processing and presentation has provided crucial investigative leads for the generation of immune responses against cancer and viral infections. Here, the peptide vaccines play an important main role. These peptide epitopes represent the minimal immunogenic region of a protein antigen and allow for precise direction of immune responses. Synthetic peptides offer several advantages over other forms of vaccines, particularly with regards to safety and ease of production (Sundaram et al., 2002). However, drawbacks include poor immunogenicity of the simple peptides and the need to potently stimulate T cells and elicit immunological memory (Purcell et al., 2003). Adjuvant science, lipopeptide conjugation and direct delivery to dendritic cells are some of the approaches currently being used to overcome these problems (Purcell et al., 2007).

Several strategies have been adopted to enhance the effectiveness of peptide therapeutics, including glycosylation, amino-acid-sequence modification, pegylation (process of attaching one or more chains of polyethylene glycol to a peptide molecule, resulting in increased bioavailability and stability) and cyclization (Purcell et al., 2007). Of these modalities only the replacement of amino acids within the sequence of a peptide epitope is directly relevant to vaccination studies. Simple epitope modifications have typically consisted of MHC-anchor substitutions in which suboptimal anchor residues are substituted to improve MHC binding and immunogenicity (Sette et al., 1994). The analogues through other modifications (e. g. cyclization) are of interest in the development of vaccines as they can achieve more potent immune responses. This observation might be explained by the increased stability of the MHC/peptide complex, and the increased avidity and residence time of the TCR–peptide/MHC complex (Slansky et al., 2000). To improve class I binding and TCR avidity, and to introduce favourable biophysical properties to the epitope such as protease resistance and oral stability, it is often desirable to introduce non-natural amino-acid analogues into the peptide epitope. Several studies have explored further modifications that not only provide subtle conformational changes to the peptide/MHC structure, but also incorporate resistance against proteases. For instance, the incorporation of β-amino-acids into epitopes can increase the binding affinity of the mimetic peptide for the MHC molecule relative to the wild-type peptide (Reinelt et al., 2001; Tangri et al., 2001; Webb et al., 2005). Additionally, modification of the N and C termini of a peptide can also prevent its degradation by

exopeptidases (Marschutz et al., 2002), like N-acetylation and C-amidation. The ability to stabilize short peptide epitopes and to control the proteolysis of longer precursor peptides by protecting scissile-peptide bonds or by directing antigen processing allows for the precise delivery of peptide-based therapeutics to the immune system (Purcell et al., 2007).

To overcome several drawbacks of peptide vaccines, like poor immunogenicity (already discussed above), polyepitope (or polytope) vaccines have been developed, which contain different epitopes derived from several antigens. These $CD8^+$ cytotoxic T-lymphocyte eptitopes (usually 8–10 amino acids long) are conjoined into single artificial constructs (Suhrbier, A., 2002) to create the vaccine. Due to the different epitopes presented on different MHC class I alleles an enhancement of the overall CTL response can be achieved. Furthermore, with this polyepitope vaccine approach, it is also possible to induce both $CD8^+$ and $CD4^+$ immune responses. For the construction of these polyepitope vaccines it is crucial to consider the amino acid sequence of the linkers between the epitopes. These play an important role by ensuring correct processing of the epitopes and assure TAP transport of each of them. Once in the ER, these epitopes should have the correct MHC class I binding sequence or at least have the N-terminal extension that can be trimmed in the ER by resident aminopeptidases.

Fig. 2. Polyepitope construct with linkers between the single epitopes. The N-terminal amino acids of an epitope are defined as N3, N2, N1 and the C-terminal amino acids are P1', P2', P3'. The linkers between to epitopes carry amino acids corresponding to the C-terminal extension of the epitope "upstream" (P1', P2', P3', on top), which also correspond to the N-terminal amino acids of the epitope "downstream" (N3, N2, N1, at the bottom).

The studies have also highlighted the role of the more variable amino acids at other positions within the peptide that project out of the antigen-binding cleft and form crucial specificity determining contacts with receptors on the surface of T cells. This approach has allowed the identification of specific binding motifs, which have been used to successfully predict T-cell epitopes. Listings of motifs are conveniently web based (for example, SYFPEITHI, a database

of MHC ligands and peptide motifs). However, the success rate for *de novo* prediction of T-cell epitopes, even for well-studied and abundant MHC alleles, is only about 60% for many alleles (for new alleles or MHC I molecules from poorly studied ethnic populations no binding motifs are available). However, recent studies have substantially improved the predictive capacity of algorithms for some well-studied alleles (Moutaftsi et al., 2006; Rammensee et al., 1999; Zhang et al., 2007). Reasons for poor predictability include the occurrence of non-motif-based ligands, peptides of unusual length, post-translationally modified ligands or the failure of antigen processing to liberate the predicted peptides (Andersen et al., 2000; Kuckelkorn et al., 2002; Slingluff, Jr. et al., 2006; Tynan et al., 2007). Furthermore, many T-cell responses are focused on one or two immunodominant peptides that are selected from the numerous potential MHC ligands of a given pathogen (Yewdell and Bennink, 1999). The participation of so few epitopes limits the number of distinct epitopes that are required in a peptide-based vaccine to elicit a protective immune response. Thus, predictive markers of immunogenicity must take into account not only peptide binding but also the abundance and density of the antigen that is present on the cell surface; the time of expression of the antigen during the infection or pathological process; the correct processing and luminal transport of the epitope; and the available T-cell repertoire in the host organism (Purcell et al., 2007). Nonetheless, epitope prediction remains a popular first-screening method to identify candidate T-cell determinants for subsequent biological validation, and predictive algorithms are frequently combined with in vitro MHC-binding assays to confirm that the predicted ligands bind to the targeted MHC molecule (Buus, 1999; Chang et al., 2003). Given the long development time experienced with therapeutic peptides, and their recent emergence into the pharmaceutical field, it is likely that peptide-based vaccines will enter the human therapeutics marketplace in the near future.

4.6 Further possible model involved in antigen processing/presentation: Heat Shock Proteins

A number of studies, particularly in tumour immunology models, have indicated that heat shock proteins (HSPs) can chaperone antigenic peptides and promote their delivery to antigen-presenting cells for presentation to T cells (Srivastava, 2002a). This indicates that not only the knowledge of cleaving characteristics of the proteases/peptidases, TAP transport

preferences and MHC class I binding specificities are primordial for understanding antigen presentation, but also HSPs are involved in this pathway.

Heat shock proteins are molecular chaperones expressed in eukaryotic and prokaryotic cells that associate with non-native protein substrates through recognition of hydrophobic patches buried in the native structure (Caplan, 1999; Frydman and Hohfeld, 1997). Besides inhibiting protein aggregation and folding them to the native state (Bukau and Horwich, 1998; Hartl, 1996), they play a crucial role in protein regulation. With the help of so called cofactors or co-chaperones, they can be involved in protein folding or protein degradation (Hohfeld et al., 2001). The main cytosolic HSP70/90 have been shown to cooperate with the degradation machinery (Dul et al., 2001). In addition, certain groups have suggested that HSPs may bind peptides that could serve as MHC class I peptides, thereby protecting them from trimming and/or degradation by cytosolic aminopeptidases (Srivastava, 2002b).

In *in vitro* assays, Chen and Androlewicz (Androlewicz and Cresswell, 1994) reported a physical association between HSP70 and TAP, and showed that purified HSP70 enhances TAP function to a modest degree. In experiments with injection of exogenous peptides into the cytosol of a cell line, free peptides or albumin-bound peptides were introduced into the cytosol and became ligands of MHC class I molecules at a far lower efficiency than peptides chaperoned by the HSPs (Binder et al., 2001). In addition, treatment of cells with deoxyspergualin — a specific inhibitor of HSP70 and HSP90 — abrogated the ability of cells to present endogenously generated antigenic peptides on MHC class I; introduction of additional HSP70, but not albumin, into the cytosol overcame this abrogation.

However, HSPs are not the only proteins suggested to bind peptides *in vivo*. A recent report using a modified SIINFEKL substrate (KOVAK) suggests that instead of binding HSPs, proteolytic peptide intermediates can bind a cytosolic chaperonin TRiC which protects them from degradation by cytosolic proteases (Kunisawa and Shastri, 2003). By tracking proteolytic intermediates in living cells, the authors show that intracellular proteolysis yields a mixture of antigenic peptides containing N-terminal flanking residues for ER transport. Some of these peptides were bound to the group II chaperonin TRiC and were protected from degradation. Destabilization of TRiC by RNA interference inhibited the expression of peptide-loaded MHC I molecules on the surface. Thus, the TRiC chaperonin serves a function in protecting proteolytic intermediates in the MHC I antigen processing pathway. Other

chaperones that reside in the ER including gp96, calreticulin, and protein disulfide isomerase have also been suggested to protect peptides from degradation and increase presentation of specific epitopes (Spee and Neefjes, 1997).

These data support the idea of HSPs protectively "shuttling" peptides from the proteasome to the TAP complex for presentation and rescuing them from further trimming. If there are preferences in peptides being bound to HSPs, this could also explain why the same antigen with different flanking C-terminal amino acids could be generated with a higher preference. Hence, the characteristics of this pathway should be further elucidated to improve vaccine design.

5 Summary

Peptides presented by MHC class I molecules for CTL recognition are derived mainly from cytosolic proteins. For antigen presentation on the cell surface, epitopes require correct processing by cytosolic and ER proteases, efficient TAP transport and MHC class I binding affinity. The efficiency of epitope generation depends not only on the epitope itself, but also on its flanking regions.

In this project, the influence of the C-terminal region of the model epitope SIINFEKL (S8L) from chicken ovalbumin (aa 257-264) on antigen processing has been investigated. S8L is a well characterized epitope presented on the murine MHC class I molecule, H-2K^b. The Flp-In 293K^b cell line was transfected with different constructs each enabling the expression of the S8L sequence with different defined C-terminal flanking regions. The constructs differed at the two first C-terminal positions after the S8L epitope, so called P1' and P2'. At these sites, all 20 amino acids were exchanged consecutively and tested for their influence on H-2K^b/S8L presentation on the cell surface of the Flp-In 293K^b cells. The detection of this complex was performed by immunostaining and flow cytometry.

The prevailing assumption is that proteasomal cleavages are exclusively responsible for the generation of the final C-termini of CTL epitopes. Nevertheless, recent publications showed that TPPII (tripeptidyl peptidase II) is required for the generation of the correct C-terminus of the HLA-A3-restricted HIV epitope Nef(73-82). With this background, the dependence of the S8L generation on proteasomal cleavage of the designed constructs was characterized using proteasomal inhibitors. The results obtained indicate that it is crucial for proteasomal cleavage, which amino acid is flanking the C-terminus of an epitope. Furthermore, partially proteasome independent S8L generation from specific S8L-precursor peptides was observed. Hence, the possibility of other existing endo- or carboxy-peptidases in the cytosol that could be involved in the correct trimming of the C-terminus of antigenic peptides for MHC class I presentation was investigated, performing specific knockdowns and using inhibitors against the target peptidases. In parallel, a purification strategy to identify the novel peptidase was established. The purified peaks showing an endopeptidase activity were further analyzed by mass spectrometry and some potential peptidases (like e.g. Lon) were identified, which have to be further characterized.

6 References

Abbott,C.A., Yu,D., McCaughan,G.W., and Gorrell,M.D. (2000). Post-proline-cleaving peptidases having DP IV like enzyme activity. Post-proline peptidases. Adv. Exp. Med. Biol. *477*, 103-109.

Abul K.Abbas and Andrew H.Lichtman (2003). Cellular and Molecular Immunology. Elsevier Science (USA).

Amerik,A.Y., Antonov,V.K., Gorbalenya,A.E., Kotova,S.A., Rotanova,T.V., and Shimbarevich,E.V. (1991). Site-directed mutagenesis of La protease. A catalytically active serine residue. FEBS Lett. *287*, 211-214.

Andersen,M.H., Tan,L., Sondergaard,I., Zeuthen,J., Elliott,T., and Haurum,J.S. (2000). Poor correspondence between predicted and experimental binding of peptides to class I MHC molecules. Tissue Antigens *55*, 519-531.

Anderson,K., Cresswell,P., Gammon,M., Hermes,J., Williamson,A., and Zweerink,H. (1991). Endogenously synthesized peptide with an endoplasmic reticulum signal sequence sensitizes antigen processing mutant cells to class I-restricted cell-mediated lysis. J. Exp. Med. *174*, 489-492.

Androlewicz,M.J. and Cresswell,P. (1994). Human transporters associated with antigen processing possess a promiscuous peptide-binding site. Immunity. *1*, 7-14.

Antoniou,A.N., Ford,S., Alphey,M., Osborne,A., Elliott,T., and Powis,S.J. (2002a). The oxidoreductase ERp57 efficiently reduces partially folded in preference to fully folded MHC class I molecules. EMBO J. *21*, 2655-2663.

Antoniou,A.N., Ford,S., Pilley,E.S., Blake,N., and Powis,S.J. (2002b). Interactions formed by individually expressed TAP1 and TAP2 polypeptide subunits. Immunology *106*, 182-189.

Arendt,C.S. and Hochstrasser,M. (1997). Identification of the yeast 20S proteasome catalytic centers and subunit interactions required for active-site formation. Proc. Natl. Acad. Sci. U. S. A *94*, 7156-7161.

Authier,F., Cameron,P.H., and Taupin,V. (1996a). Association of insulin-degrading enzyme with a 70 kDa cytosolic protein in hepatoma cells. Biochem. J. *319 (Pt 1)*, 149-158.

Authier,F., Posner,B.I., and Bergeron,J.J. (1996b). Insulin-degrading enzyme. Clin. Invest Med. *19*, 149-160.

Bangia,N. and Cresswell,P. (2005). Stoichiometric tapasin interactions in the catalysis of major histocompatibility complex class I molecule assembly. Immunology *114*, 346-353.

Bangia,N., Lehner,P.J., Hughes,E.A., Surman,M., and Cresswell,P. (1999). The N-terminal region of tapasin is required to stabilize the MHC class I loading complex. Eur. J. Immunol. *29*, 1858-1870.

Beninga,J., Rock,K.L., and Goldberg,A.L. (1998). Interferon-gamma can stimulate post-proteasomal trimming of the N terminus of an antigenic peptide by inducing leucine aminopeptidase. J. Biol. Chem. *273*, 18734-18742.

Bennett,R.G., Hamel,F.G., and Duckworth,W.C. (2000). Insulin inhibits the ubiquitin-dependent degrading activity of the 26S proteasome. Endocrinology *141*, 2508-2517.

Betarbet,R., Poisik,O., Sherer,T.B., and Greenamyre,J.T. (2004). Differential expression and ser897 phosphorylation of striatal N-methyl-d-aspartate receptor subunit NR1 in animal models of Parkinson's disease. Exp. Neurol. *187*, 76-85.

Binder,R.J., Blachere,N.E., and Srivastava,P.K. (2001). Heat shock protein-chaperoned peptides but not free peptides introduced into the cytosol are presented efficiently by major histocompatibility complex I molecules. J. Biol. Chem. *276*, 17163-17171.

Bjelke,J.R., Christensen,J., Nielsen,P.F., Branner,S., Kanstrup,A.B., Wagtmann,N., and Rasmussen,H.B. (2006). Dipeptidyl peptidases 8 and 9: specificity and molecular characterization compared with dipeptidyl peptidase IV. Biochem. J. *396*, 391-399.

Bjorkman,P.J., Saper,M.A., Samraoui,B., Bennett,W.S., Strominger,J.L., and Wiley,D.C. (1987). Structure of the human class I histocompatibility antigen, HLA-A2. Nature *329*, 506-512.

Boes,B., Hengel,H., Ruppert,T., Multhaup,G., Koszinowski,U.H., and Kloetzel,P.M. (1994). Interferon gamma stimulation modulates the proteolytic activity and cleavage site preference of 20S mouse proteasomes. J. Exp. Med. *179*, 901-909.

Bota,D.A. and Davies,K.J. (2002). Lon protease preferentially degrades oxidized mitochondrial aconitase by an ATP-stimulated mechanism. Nat. Cell Biol. *4*, 674-680.

Bota,D.A., Ngo,J.K., and Davies,K.J. (2005). Downregulation of the human Lon protease impairs mitochondrial structure and function and causes cell death. Free Radic. Biol. Med. *38*, 665-677.

Botos,I., Melnikov,E.E., Cherry,S., Khalatova,A.G., Rasulova,F.S., Tropea,J.E., Maurizi,M.R., Rotanova,T.V., Gustchina,A., and Wlodawer,A. (2004). Crystal structure of the AAA+ alpha domain of E. coli Lon protease at 1.9A resolution. J. Struct. Biol. *146*, 113-122.

Brown,J.H., Jardetzky,T.S., Gorga,J.C., Stern,L.J., Urban,R.G., Strominger,J.L., and Wiley,D.C. (1993). Three-dimensional structure of the human class II histocompatibility antigen HLA-DR1. Nature *364*, 33-39.

Brown,M.G., Driscoll,J., and Monaco,J.J. (1991). Structural and serological similarity of MHC-linked LMP and proteasome (multicatalytic proteinase) complexes. Nature *353*, 355-357.

Bukau,B. and Horwich,A.L. (1998). The Hsp70 and Hsp60 chaperone machines. Cell *92*, 351-366.

Buus,S. (1999). Description and prediction of peptide-MHC binding: the 'human MHC project'. Curr. Opin. Immunol. *11*, 209-213.

Caplan,A.J. (1999). Hsp90's secrets unfold: new insights from structural and functional studies. Trends Cell Biol. *9*, 262-268.

Cardozo,C., Chen,W.E., and Wilk,S. (1996). Cleavage of Pro-X and Glu-X bonds catalyzed by the branched chain amino acid preferring activity of the bovine pituitary multicatalytic proteinase complex (20S proteasome). Arch. Biochem. Biophys. *334*, 113-120.

Cascio,P., Hilton,C., Kisselev,A.F., Rock,K.L., and Goldberg,A.L. (2001). 26S proteasomes and immunoproteasomes produce mainly N-extended versions of an antigenic peptide. EMBO J. *20*, 2357-2366.

Chang,L., Kjer-Nielsen,L., Flynn,S., Brooks,A.G., Mannering,S.I., Honeyman,M.C., Harrison,L.C., McCluskey,J., and Purcell,A.W. (2003). Novel strategy for identification of candidate cytotoxic T-cell epitopes from human preproinsulin. Tissue Antigens *62*, 408-417.

Chen,D. and Androlewicz,M.J. (2001). Heat shock protein 70 moderately enhances peptide binding and transport by the transporter associated with antigen processing. Immunol. Lett. *75*, 143-148.

Ciechanover,A., Orian,A., and Schwartz,A.L. (2000). The ubiquitin-mediated proteolytic pathway: Mode of action and clinical implications. J. Cell Biochem. *77*, 40-51.

Constam,D.B., Tobler,A.R., Rensing-Ehl,A., Kemler,I., Hersh,L.B., and Fontana,A. (1995). Puromycin-sensitive aminopeptidase. Sequence analysis, expression, and functional characterization. J. Biol. Chem. *270*, 26931-26939.

Craiu,A., Akopian,T., Goldberg,A., and Rock,K.L. (1997). Two distinct proteolytic processes in the generation of a major histocompatibility complex class I-presented peptide. Proc. Natl. Acad. Sci. U. S. A *94*, 10850-10855.

Dang,L.C., Melandri,F.D., and Stein,R.L. (1998). Kinetic and mechanistic studies on the hydrolysis of ubiquitin C-terminal 7-amido-4-methylcoumarin by deubiquitinating enzymes. Biochemistry *37*, 1868-1879.

Davidson,H.W., Reid,P.A., Lanzavecchia,A., and Watts,C. (1991). Processed antigen binds to newly synthesized MHC class II molecules in antigen-specific B lymphocytes. Cell *67*, 105-116.

Delamarre,L., Pack,M., Chang,H., Mellman,I., and Trombetta,E.S. (2005). Differential lysosomal proteolysis in antigen-presenting cells determines antigen fate. Science *307*, 1630-1634.

Deng,H., Apple,R., Clare-Salzler,M., Trembleau,S., Mathis,D., Adorini,L., and Sercarz,E. (1993). Determinant capture as a possible mechanism of protection afforded by major histocompatibility complex class II molecules in autoimmune disease. J. Exp. Med. *178*, 1675-1680.

Deveraux,Q., Ustrell,V., Pickart,C., and Rechsteiner,M. (1994). A 26 S protease subunit that binds ubiquitin conjugates. J. Biol. Chem. *269*, 7059-7061.

Dick,T.P., Bangia,N., Peaper,D.R., and Cresswell,P. (2002). Disulfide bond isomerization and the assembly of MHC class I-peptide complexes. Immunity. *16*, 87-98.

Dick,T.P., Nussbaum,A.K., Deeg,M., Heinemeyer,W., Groll,M., Schirle,M., Keilholz,W., Stevanovic,S., Wolf,D.H., Huber,R., Rammensee,H.G., and Schild,H. (1998). Contribution of proteasomal beta-subunits to the cleavage of peptide substrates analyzed with yeast mutants. J. Biol. Chem. *273*, 25637-25646.

Donermeyer,D.L. and Allen,P.M. (1989). Binding to Ia protects an immunogenic peptide from proteolytic degradation. J. Immunol. *142*, 1063-1068.

Dongre,A.R., Kovats,S., deRoos,P., McCormack,A.L., Nakagawa,T., Paharkova-Vatchkova,V., Eng,J., Caldwell,H., Yates,J.R., III, and Rudensky,A.Y. (2001). In vivo MHC class II presentation of cytosolic proteins revealed by rapid automated tandem mass spectrometry and functional analyses. Eur. J. Immunol. *31*, 1485-1494.

Duckworth,W.C., Bennett,R.G., and Hamel,F.G. (1998a). Insulin acts intracellularly on proteasomes through insulin-degrading enzyme. Biochem. Biophys. Res. Commun. *244*, 390-394.

Duckworth,W.C., Bennett,R.G., and Hamel,F.G. (1998b). Insulin degradation: progress and potential. Endocr. Rev. *19*, 608-624.

Dul,J.L., Davis,D.P., Williamson,E.K., Stevens,F.J., and Argon,Y. (2001). Hsp70 and antifibrillogenic peptides promote degradation and inhibit intracellular aggregation of amyloidogenic light chains. J. Cell Biol. *152*, 705-716.

Ebel,W., Skinner,M.M., Dierksen,K.P., Scott,J.M., and Trempy,J.E. (1999). A conserved domain in Escherichia coli Lon protease is involved in substrate discriminator activity. J. Bacteriol. *181*, 2236-2243.

Engelhard,V.H. (1994). Structure of peptides associated with class I and class II MHC molecules. Annu. Rev. Immunol. *12*, 181-207.

Falk,K., Rotzschke,O., Stevanovic,S., Jung,G., and Rammensee,H.G. (1991). Allele-specific motifs revealed by sequencing of self-peptides eluted from MHC molecules. Nature *351*, 290-296.

Fehling,H.J., Swat,W., Laplace,C., Kuhn,R., Rajewsky,K., Muller,U., and von,B.H. (1994). MHC class I expression in mice lacking the proteasome subunit LMP-7. Science *265*, 1234-1237.

Fenteany,G., Standaert,R.F., Lane,W.S., Choi,S., Corey,E.J., and Schreiber,S.L. (1995). Inhibition of proteasome activities and subunit-specific amino-terminal threonine modification by lactacystin. Science *268*, 726-731.

Ferrando,A.A., Pendas,A.M., Llano,E., Velasco,G., Lidereau,R., and Lopez-Otin,C. (1997). Gene characterization, promoter analysis, and chromosomal localization of human bleomycin hydrolase. J. Biol. Chem. *272*, 33298-33304.

Fischer,H. and Glockshuber,R. (1994). A point mutation within the ATP-binding site inactivates both catalytic functions of the ATP-dependent protease La (Lon) from Escherichia coli. FEBS Lett. *356*, 101-103.

Frydman,J. and Hohfeld,J. (1997). Chaperones get in touch: the Hip-Hop connection. Trends Biochem. Sci. *22*, 87-92.

Garbi,N., Tiwari,N., Momburg,F., and Hammerling,G.J. (2003). A major role for tapasin as a stabilizer of the TAP peptide transporter and consequences for MHC class I expression. Eur. J. Immunol. *33*, 264-273.

Geier,E., Pfeifer,G., Wilm,M., Lucchiari-Hartz,M., Baumeister,W., Eichmann,K., and Niedermann,G. (1999). A giant protease with potential to substitute for some functions of the proteasome. Science *283*, 978-981.

Gileadi,U., Gallimore,A., Van der,B.P., and Cerundolo,V. (1999). Effect of epitope flanking residues on the presentation of N-terminal cytotoxic T lymphocyte epitopes. Eur. J. Immunol. *29*, 2213-2222.

Goldberg,A.L. (2003). Protein degradation and protection against misfolded or damaged proteins. Nature *426*, 895-899.

Goldberg,A.L., Cascio,P., Saric,T., and Rock,K.L. (2002). The importance of the proteasome and subsequent proteolytic steps in the generation of antigenic peptides. Mol. Immunol. *39*, 147-164.

Golovina,T.N., Wherry,E.J., Bullock,T.N., and Eisenlohr,L.C. (2002). Efficient and qualitatively distinct MHC class I-restricted presentation of antigen targeted to the endoplasmic reticulum. J. Immunol. *168*, 2667-2675.

Gorbulev,S., Abele,R., and Tampe,R. (2001). Allosteric crosstalk between peptide-binding, transport, and ATP hydrolysis of the ABC transporter TAP. Proc. Natl. Acad. Sci. U. S. A *98*, 3732-3737.

Groll,M., Ditzel,L., Lowe,J., Stock,D., Bochtler,M., Bartunik,H.D., and Huber,R. (1997). Structure of 20S proteasome from yeast at 2.4 A resolution. Nature *386*, 463-471.

Groll,M., Heinemeyer,W., Jager,S., Ullrich,T., Bochtler,M., Wolf,D.H., and Huber,R. (1999). The catalytic sites of 20S proteasomes and their role in subunit maturation: a mutational and crystallographic study. Proc. Natl. Acad. Sci. U. S. A *96*, 10976-10983.

Groll,M. and Huber,R. (2004). Inhibitors of the eukaryotic 20S proteasome core particle: a structural approach. Biochim. Biophys. Acta *1695*, 33-44.

Groll,M., Koguchi,Y., Huber,R., and Kohno,J. (2001). Crystal structure of the 20 S proteasome:TMC-95A complex: a non-covalent proteasome inhibitor. J. Mol. Biol. *311*, 543-548.

Gromme,M. and Neefjes,J. (2002). Antigen degradation or presentation by MHC class I molecules via classical and non-classical pathways. Mol. Immunol. *39*, 181-202.

Hartl,F.U. (1996). Molecular chaperones in cellular protein folding. Nature *381*, 571-579.

Hattori,A., Kitatani,K., Matsumoto,H., Miyazawa,S., Rogi,T., Tsuruoka,N., Mizutani,S., Natori,Y., and Tsujimoto,M. (2000). Characterization of recombinant human adipocyte-derived leucine aminopeptidase expressed in Chinese hamster ovary cells. J. Biochem. (Tokyo) *128*, 755-762.

Hattori,A., Matsumoto,H., Mizutani,S., and Tsujimoto,M. (1999). Molecular cloning of adipocyte-derived leucine aminopeptidase highly related to placental leucine aminopeptidase/oxytocinase. J. Biochem. (Tokyo) *125*, 931-938.

Hegerl,R., Pfeifer,G., Puhler,G., Dahlmann,B., and Baumeister,W. (1991). The three-dimensional structure of proteasomes from Thermoplasma acidophilum as determined by electron microscopy using random conical tilting. FEBS Lett. *283*, 117-121.

Heinemeyer,W., Fischer,M., Krimmer,T., Stachon,U., and Wolf,D.H. (1997). The active sites of the eukaryotic 20 S proteasome and their involvement in subunit precursor processing. J. Biol. Chem. *272*, 25200-25209.

Hershko,A. and Ciechanover,A. (1998). The ubiquitin system. Annu. Rev. Biochem. *67*, 425-479.

Hilt,W. and Wolf,D.H. (1996). Proteasomes: destruction as a programme. Trends Biochem. Sci. *21*, 96-102.

Hisamatsu,H., Shimbara,N., Saito,Y., Kristensen,P., Hendil,K.B., Fujiwara,T., Takahashi,E., Tanahashi,N., Tamura,T., Ichihara,A., and Tanaka,K. (1996). Newly identified pair of proteasomal subunits regulated reciprocally by interferon gamma. J. Exp. Med. *183*, 1807-1816.

Hoffman,L., Pratt,G., and Rechsteiner,M. (1992). Multiple forms of the 20 S multicatalytic and the 26 S ubiquitin/ATP-dependent proteases from rabbit reticulocyte lysate. J. Biol. Chem. *267*, 22362-22368.

Hohfeld,J., Cyr,D.M., and Patterson,C. (2001). From the cradle to the grave: molecular chaperones that may choose between folding and degradation. EMBO Rep. *2*, 885-890.

Hopsu-Havu,V.K. and Glenner,G.G. (1966). A new dipeptide naphthylamidase hydrolyzing glycyl-prolyl-beta-naphthylamide. Histochemie. *7*, 197-201.

Hough,R., Pratt,G., and Rechsteiner,M. (1986). Ubiquitin-lysozyme conjugates. Identification and characterization of an ATP-dependent protease from rabbit reticulocyte lysates. J. Biol. Chem. *261*, 2400-2408.

Hough,R. and Rechsteiner,M. (1986). Ubiquitin-lysozyme conjugates. Purification and susceptibility to proteolysis. J. Biol. Chem. *261*, 2391-2399.

Ishii,T., Udono,H., Yamano,T., Ohta,H., Uenaka,A., Ono,T., Hizuta,A., Tanaka,N., Srivastava,P.K., and Nakayama,E. (1999). Isolation of MHC class I-restricted tumor antigen peptide and its precursors associated with heat shock proteins hsp70, hsp90, and gp96. J. Immunol. *162*, 1303-1309.

Ishii,Y. and Amano,F. (2001). Regulation of SulA cleavage by Lon protease by the C-terminal amino acid of SulA, histidine. Biochem. J. *358*.

Janeway,C.A., Travers,P., Walport,M., and Shlomchik,M. (2001). Immunobiology. Garland Publishing).

Kajimoto,Y., Hashimoto,T., Shirai,Y., Nishino,N., Kuno,T., and Tanaka,C. (1992). cDNA cloning and tissue distribution of a rat ubiquitin carboxyl-terminal hydrolase PGP9.5. J. Biochem. (Tokyo) *112*, 28-32.

Kayalar,C. and Wong,W.T. (1989). Metalloendoprotease inhibitors which block the differentiation of L6 myoblasts inhibit insulin degradation by the endogenous insulin-degrading enzyme. J. Biol. Chem. *264*, 8928-8934.

Kenny,A.J., Booth,A.G., George,S.G., Ingram,J., Kershaw,D., Wood,E.J., and Young,A.R. (1976). Dipeptidyl peptidase IV, a kidney brush-border serine peptidase. Biochem. J. *157*, 169-182.

Kisselev,A.F., Akopian,T.N., Woo,K.M., and Goldberg,A.L. (1999). The sizes of peptides generated from protein by mammalian 26 and 20 S proteasomes. Implications for understanding the degradative mechanism and antigen presentation. J. Biol. Chem. *274*, 3363-3371.

Kleijmeer,M.J., Morkowski,S., Griffith,J.M., Rudensky,A.Y., and Geuze,H.J. (1997). Major histocompatibility complex class II compartments in human and mouse B lymphoblasts represent conventional endocytic compartments. J. Cell Biol. *139*, 639-649.

Kloetzel,P.M. (2004). The proteasome and MHC class I antigen processing. Biochim. Biophys. Acta *1695*, 225-233.

Koch,J., Guntrum,R., Heintke,S., Kyritsis,C., and Tampe,R. (2004). Functional dissection of the transmembrane domains of the transporter associated with antigen processing (TAP). J. Biol. Chem. *279*, 10142-10147.

Koch,J., Guntrum,R., and Tampe,R. (2005). Exploring the minimal functional unit of the transporter associated with antigen processing. FEBS Lett. *579*, 4413-4416.

Komlosh,A., Momburg,F., Weinschenk,T., Emmerich,N., Schild,H., Nadav,E., Shaked,I., and Reiss,Y. (2001). A role for a novel luminal endoplasmic reticulum aminopeptidase in final trimming of 26 S proteasome-generated major histocompatability complex class I antigenic peptides. J. Biol. Chem. *276*, 30050-30056.

Koopmann,J.O., Post,M., Neefjes,J.J., Hammerling,G.J., and Momburg,F. (1996). Translocation of long peptides by transporters associated with antigen processing (TAP). Eur. J. Immunol. *26*, 1720-1728.

Kopito,R.R. (1997). ER quality control: the cytoplasmic connection. Cell *88*, 427-430.

Kuckelkorn,U., Ruppert,T., Strehl,B., Jungblut,P.R., Zimny-Arndt,U., Lamer,S., Prinz,I., Drung,I., Kloetzel,P.M., Kaufmann,S.H., and Steinhoff,U. (2002). Link between organ-specific antigen processing by 20S proteasomes and CD8(+) T cell-mediated autoimmunity. J. Exp. Med. *195*, 983-990.

Kunisawa,J. and Shastri,N. (2003). The group II chaperonin TRiC protects proteolytic intermediates from degradation in the MHC class I antigen processing pathway. Mol. Cell *12*, 565-576.

Kurochkin,I.V. (2001). Insulin-degrading enzyme: embarking on amyloid destruction. Trends Biochem. Sci. *26*, 421-425.

Lam,Y.A., Xu,W., DeMartino,G.N., and Cohen,R.E. (1997). Editing of ubiquitin conjugates by an isopeptidase in the 26S proteasome. Nature *385*, 737-740.

Levy,F., Burri,L., Morel,S., Peitrequin,A.L., Levy,N., Bachi,A., Hellman,U., Van den Eynde,B.J., and Servis,C. (2002). The final N-terminal trimming of a subaminoterminal proline-containing HLA class I-restricted antigenic peptide in the cytosol is mediated by two peptidases. J. Immunol. *169*, 4161-4171.

Liu,Y., Fallon,L., Lashuel,H.A., Liu,Z., and Lansbury,P.T., Jr. (2002). The UCH-L1 gene encodes two opposing enzymatic activities that affect alpha-synuclein degradation and Parkinson's disease susceptibility. Cell *111*, 209-218.

Lucchiari-Hartz,M., van Endert,P.M., Lauvau,G., Maier,R., Meyerhans,A., Mann,D., Eichmann,K., and Niedermann,G. (2000). Cytotoxic T lymphocyte epitopes of HIV-1 Nef: Generation of multiple definitive major histocompatibility complex class I ligands by proteasomes. J. Exp. Med. *191*, 239-252.

Madden,D.R. (1995). The three-dimensional structure of peptide-MHC complexes. Annu. Rev. Immunol. *13*, 587-622.

Marschutz,M.K., Zauner,W., Mattner,F., Otava,A., Buschle,M., and Bernkop-Schnurch,A. (2002). Improvement of the enzymatic stability of a cytotoxic T-lymphocyte-epitope model peptide for its oral administration. Peptides *23*, 1727-1733.

Meng,L., Mohan,R., Kwok,B.H., Elofsson,M., Sin,N., and Crews,C.M. (1999). Epoxomicin, a potent and selective proteasome inhibitor, exhibits in vivo antiinflammatory activity. Proc. Natl. Acad. Sci. U. S. A *96*, 10403-10408.

Mo,X.Y., Cascio,P., Lemerise,K., Goldberg,A.L., and Rock,K. (1999). Distinct proteolytic processes generate the C and N termini of MHC class I-binding peptides. J. Immunol. *163*, 5851-5859.

Momburg,F., Roelse,J., Hammerling,G.J., and Neefjes,J.J. (1994). Peptide size selection by the major histocompatibility complex-encoded peptide transporter. J. Exp. Med. *179*, 1613-1623.

Mouritsen,S., Hansen,A.S., Petersen,B.L., and Buus,S. (1992). pH dependence of the interaction between immunogenic peptides and MHC class II molecules. Evidence for an acidic intracellular compartment being the organelle of interaction. J. Immunol. *148*, 1438-1444.

Moutaftsi,M., Peters,B., Pasquetto,V., Tscharke,D.C., Sidney,J., Bui,H.H., Grey,H., and Sette,A. (2006). A consensus epitope prediction approach identifies the breadth of murine T(CD8+)-cell responses to vaccinia virus. Nat. Biotechnol. *24*, 817-819.

Mukherjee,A., Song,E., Kihiko-Ehmann,M., Goodman,J.P., Jr., Pyrek,J.S., Estus,S., and Hersh,L.B. (2000). Insulysin hydrolyzes amyloid beta peptides to products that are neither neurotoxic nor deposit on amyloid plaques. J. Neurosci. *20*, 8745-8749.

Mullins,D.W. and Engelhard,V.H. (2006). Limited infiltration of exogenous dendritic cells and naive T cells restricts immune responses in peripheral lymph nodes. J. Immunol. *176*, 4535-4542.

Musson,J.A., Walker,N., Flick-Smith,H., Williamson,E.D., and Robinson,J.H. (2003). Differential processing of CD4 T-cell epitopes from the protective antigen of Bacillus anthracis. J. Biol. Chem. *278*, 52425-52431.

Neumann,L. and Tampe,R. (1999). Kinetic analysis of peptide binding to the TAP transport complex: evidence for structural rearrangements induced by substrate binding. J. Mol. Biol. *294*, 1203-1213.

Neuwald,A.F., Aravind,L., Spouge,J.L., and Koonin,E.V. (1999). AAA+: A class of chaperone-like ATPases associated with the assembly, operation, and disassembly of protein complexes. Genome Res. *9*, 27-43.

Nijenhuis,M. and Hammerling,G.J. (1996). Multiple regions of the transporter associated with antigen processing (TAP) contribute to its peptide binding site. J. Immunol. *157*, 5467-5477.

Nijenhuis,M., Schmitt,S., Armandola,E.A., Obst,R., Brunner,J., and Hammerling,G.J. (1996). Identification of a contact region for peptide on the TAP1 chain of the transporter associated with antigen processing. J. Immunol. *156*, 2186-2195.

Nimmerjahn,F., Milosevic,S., Behrends,U., Jaffee,E.M., Pardoll,D.M., Bornkamm,G.W., and Mautner,J. (2003). Major histocompatibility complex class II-restricted presentation of a cytosolic antigen by autophagy. Eur. J. Immunol. *33*, 1250-1259.

Nomura,K., Kato,J., Takiguchi,N., Ohtake,H., and Kuroda,A. (2004). Effects of inorganic polyphosphate on the proteolytic and DNA-binding activities of Lon in Escherichia coli. J. Biol. Chem. *279*, 34406-34410.

Olsen,C. and Wagtmann,N. (2002). Identification and characterization of human DPP9, a novel homologue of dipeptidyl peptidase IV. Gene *299*, 185-193.

Omura,S., Fujimoto,T., Otoguro,K., Matsuzaki,K., Moriguchi,R., Tanaka,H., and Sasaki,Y. (1991). Lactacystin, a novel microbial metabolite, induces neuritogenesis of neuroblastoma cells. J. Antibiot. (Tokyo) *44*, 113-116.

Orlowski,M. (1993). The multicatalytic proteinase complex (proteasome) and intracellular protein degradation: diverse functions of an intracellular particle. J. Lab Clin. Med. *121*, 187-189.

Ortiz-Navarrete,V., Seelig,A., Gernold,M., Frentzel,S., Kloetzel,P.M., and Hammerling,G.J. (1991). Subunit of the '20S' proteasome (multicatalytic proteinase) encoded by the major histocompatibility complex. Nature *353*, 662-664.

Ortmann,B., Copeman,J., Lehner,P.J., Sadasivan,B., Herberg,J.A., Grandea,A.G., Riddell,S.R., Tampe,R., Spies,T., Trowsdale,J., and Cresswell,P. (1997). A critical role for tapasin in the assembly and function of multimeric MHC class I-TAP complexes. Science *277*, 1306-1309.

Osada,T., Ikegami,S., Takiguchi-Hayashi,K., Yamazaki,Y., Katoh-Fukui,Y., Higashinakagawa,T., Sakaki,Y., and Takeuchi,T. (1999). Increased anxiety and impaired pain response in puromycin-sensitive aminopeptidase gene-deficient mice obtained by a mouse gene-trap method. J. Neurosci. *19*, 6068-6078.

Ostrowska,H., Wojcik,C., Omura,S., and Worowski,K. (1997). Lactacystin, a specific inhibitor of the proteasome, inhibits human platelet lysosomal cathepsin A-like enzyme. Biochem. Biophys. Res. Commun. *234*, 729-732.

Pamer,E. and Cresswell,P. (1998). Mechanisms of MHC class I--restricted antigen processing. Annu. Rev. Immunol. *16*, 323-358.

Park,B., Lee,S., Kim,E., Cho,K., Riddell,S.R., Cho,S., and Ahn,K. (2006). Redox regulation facilitates optimal peptide selection by MHC class I during antigen processing. Cell *127*, 369-382.

Pierre,P., Denzin,L.K., Hammond,C., Drake,J.R., Amigorena,S., Cresswell,P., and Mellman,I. (1996). HLA-DM is localized to conventional and unconventional MHC class II-containing endocytic compartments. Immunity. *4*, 229-239.

Pieters,J. (1997). MHC class II compartments: specialized organelles of the endocytic pathway in antigen presenting cells. Biol. Chem. *378*, 751-758.

Porgador,A., Yewdell,J.W., Deng,Y., Bennink,J.R., and Germain,R.N. (1997). Localization, quantitation, and in situ detection of specific peptide-MHC class I complexes using a monoclonal antibody. Immunity. *6*, 715-726.

Portaro,F.C., Gomes,M.D., Cabrera,A., Fernandes,B.L., Silva,C.L., Ferro,E.S., Juliano,L., and de Camargo,A.C. (1999). Thimet oligopeptidase and the stability of MHC class I epitopes in macrophage cytosol. Biochem. Biophys. Res. Commun. *255*, 596-601.

Princiotta,M.F., Finzi,D., Qian,S.B., Gibbs,J., Schuchmann,S., Buttgereit,F., Bennink,J.R., and Yewdell,J.W. (2003). Quantitating protein synthesis, degradation, and endogenous antigen processing. Immunity. *18*, 343-354.

Purcell,A.W., McCluskey,J., and Rossjohn,J. (2007). More than one reason to rethink the use of peptides in vaccine design. Nat. Rev. Drug Discov. *6*, 404-414.

Purcell,A.W., Todd,A., Kinoshita,G., Lynch,T.A., Keech,C.L., Gething,M.J., and Gordon,T.P. (2003a). Association of stress proteins with autoantigens: a possible mechanism for triggering autoimmunity? Clin. Exp. Immunol. *132*, 193-200.

Purcell,A.W., Zeng,W., Mifsud,N.A., Ely,L.K., Macdonald,W.A., and Jackson,D.C. (2003b). Dissecting the role of peptides in the immune response: theory, practice and the application to vaccine design. J. Pept. Sci. *9*, 255-281.

Qiu,W.Q., Walsh,D.M., Ye,Z., Vekrellis,K., Zhang,J., Podlisny,M.B., Rosner,M.R., Safavi,A., Hersh,L.B., and Selkoe,D.J. (1998). Insulin-degrading enzyme regulates extracellular levels of amyloid beta-protein by degradation. J. Biol. Chem. *273*, 32730-32738.

Qiu,W.Q., Ye,Z., Kholodenko,D., Seubert,P., and Selkoe,D.J. (1997). Degradation of amyloid beta-protein by a metalloprotease secreted by microglia and other neural and non-neural cells. J. Biol. Chem. *272*, 6641-6646.

Rammensee,H., Bachmann,J., Emmerich,N.P., Bachor,O.A., and Stevanovic,S. (1999). SYFPEITHI: database for MHC ligands and peptide motifs. Immunogenetics *50*, 213-219.

Rawlings,N.D. and Barrett,A.J. (1993). Evolutionary families of peptidases. Biochem. J. *290 (Pt 1)*, 205-218.

Rawlings,N.D. and Barrett,A.J. (1999). Tripeptidyl-peptidase I is apparently the CLN2 protein absent in classical late-infantile neuronal ceroid lipofuscinosis. Biochim. Biophys. Acta *1429*, 496-500.

Rechsteiner,M. and Hill,C.P. (2005). Mobilizing the proteolytic machine: cell biological roles of proteasome activators and inhibitors. Trends Cell Biol. *15*, 27-33.

Rechsteiner,M., Realini,C., and Ustrell,V. (2000). The proteasome activator 11 S REG (PA28) and class I antigen presentation. Biochem. J. *345 Pt 1*, 1-15.

Reidlinger,J., Pike,A.M., Savory,P.J., Murray,R.Z., and Rivett,A.J. (1997). Catalytic properties of 26 S and 20 S proteasomes and radiolabeling of MB1, LMP7, and C7 subunits associated with trypsin-like and chymotrypsin-like activities. J. Biol. Chem. *272*, 24899-24905.

Reinelt,S., Marti,M., Dedier,S., Reitinger,T., Folkers,G., de Castro,J.A., and Rognan,D. (2001). Beta-amino acid scan of a class I major histocompatibility complex-restricted alloreactive T-cell epitope. J. Biol. Chem. *276*, 24525-24530.

Reits,E., Griekspoor,A., Neijssen,J., Groothuis,T., Jalink,K., van,V.P., Janssen,H., Calafat,J., Drijfhout,J.W., and Neefjes,J. (2003). Peptide diffusion, protection, and degradation in nuclear and cytoplasmic compartments before antigen presentation by MHC class I. Immunity. *18*, 97-108.

Reits,E., Neijssen,J., Herberts,C., Benckhuijsen,W., Janssen,L., Drijfhout,J.W., and Neefjes,J. (2004). A major role for TPPII in trimming proteasomal degradation products for MHC class I antigen presentation. Immunity. *20*, 495-506.

Rock,K.L. and Goldberg,A.L. (1999). Degradation of cell proteins and the generation of MHC class I-presented peptides. Annu. Rev. Immunol. *17*, 739-779.

Rock,K.L., York,I.A., Saric,T., and Goldberg,A.L. (2002). Protein degradation and the generation of MHC class I-presented peptides. Adv. Immunol. *80*, 1-70.

Rose,C., Vargas,F., Facchinetti,P., Bourgeat,P., Bambal,R.B., Bishop,P.B., Chan,S.M., Moore,A.N., Ganellin,C.R., and Schwartz,J.C. (1996). Characterization and inhibition of a cholecystokinin-inactivating serine peptidase. Nature *380*, 403-409.

Rubin,D.M., Glickman,M.H., Larsen,C.N., Dhruvakumar,S., and Finley,D. (1998). Active site mutants in the six regulatory particle ATPases reveal multiple roles for ATP in the proteasome. EMBO J. *17*, 4909-4919.

Rudensky,A.Y., Preston-Hurlburt,P., Hong,S.C., Barlow,A., and Janeway,C.A., Jr. (1991). Sequence analysis of peptides bound to MHC class II molecules. Nature *353*, 622-627.

Saric,T., Beninga,J., Graef,C.I., Akopian,T.N., Rock,K.L., and Goldberg,A.L. (2001). Major histocompatibility complex class I-presented antigenic peptides are degraded in cytosolic extracts primarily by thimet oligopeptidase. J. Biol. Chem. *276*, 36474-36481.

Saric,T., Chang,S.C., Hattori,A., York,I.A., Markant,S., Rock,K.L., Tsujimoto,M., and Goldberg,A.L. (2002). An IFN-gamma-induced aminopeptidase in the ER, ERAP1, trims precursors to MHC class I-presented peptides. Nat. Immunol. *3*, 1169-1176.

Saric,T., Graef,C.I., and Goldberg,A.L. (2004). Pathway for degradation of peptides generated by proteasomes: a key role for thimet oligopeptidase and other metallopeptidases. J. Biol. Chem. *279*, 46723-46732.

Saveanu,L., Carroll,O., Lindo,V., Del,V.M., Lopez,D., Lepelletier,Y., Greer,F., Schomburg,L., Fruci,D., Niedermann,G., and van Endert,P.M. (2005). Concerted peptide trimming by human ERAP1 and ERAP2 aminopeptidase complexes in the endoplasmic reticulum. Nat. Immunol. *6*, 689-697.

Savory,P.J., Djaballah,H., Angliker,H., Shaw,E., and Rivett,A.J. (1993). Reaction of proteasomes with peptidylchloromethanes and peptidyldiazomethanes. Biochem. J. *296 (Pt 3)*, 601-605.

Schmidt,M., Hanna,J., Elsasser,S., and Finley,D. (2005). Proteasome-associated proteins: regulation of a proteolytic machine. Biol. Chem. *386*, 725-737.

Schmidtke,G., Kraft,R., Kostka,S., Henklein,P., Frommel,C., Lowe,J., Huber,R., Kloetzel,P.M., and Schmidt,M. (1996). Analysis of mammalian 20S proteasome biogenesis: the maturation of beta-subunits is an ordered two-step mechanism involving autocatalysis. EMBO J. *15*, 6887-6898.

Schmidtke,G., Schmidt,M., and Kloetzel,P.M. (1997). Maturation of mammalian 20 S proteasome: purification and characterization of 13 S and 16 S proteasome precursor complexes. J. Mol. Biol. *268*, 95-106.

Schomburg,L., Kollmus,H., Friedrichsen,S., and Bauer,K. (2000). Molecular characterization of a puromycin-insensitive leucyl-specific aminopeptidase, PILS-AP. Eur. J. Biochem. *267*, 3198-3207.

Schubert,U., Anton,L.C., Gibbs,J., Norbury,C.C., Yewdell,J.W., and Bennink,J.R. (2000). Rapid degradation of a large fraction of newly synthesized proteins by proteasomes. Nature *404*, 770-774.

Sebti,S.M., DeLeon,J.C., Ma,L.T., Hecht,S.M., and Lazo,J.S. (1989a). Substrate specificity of bleomycin hydrolase. Biochem. Pharmacol. *38*, 141-147.

Sebti,S.M., Mignano,J.E., Jani,J.P., Srimatkandada,S., and Lazo,J.S. (1989b). Bleomycin hydrolase: molecular cloning, sequencing, and biochemical studies reveal membership in the cysteine proteinase family. Biochemistry *28*, 6544-6548.

Seemuller,E., Lupas,A., and Baumeister,W. (1996). Autocatalytic processing of the 20S proteasome. Nature *382*, 468-471.

Seifert,U., Maranon,C., Shmueli,A., Desoutter,J.F., Wesoloski,L., Janek,K., Henklein,P., Diescher,S., Andrieu,M., de la,S.H., Weinschenk,T., Schild,H., Laderach,D., Galy,A., Haas,G., Kloetzel,P.M., Reiss,Y., and Hosmalin,A. (2003). An essential role for tripeptidyl peptidase in the generation of an MHC class I epitope. Nat. Immunol. *4*, 375-379.

Semple,J.W., Ellis,J., and Delovitch,T.L. (1989). Processing and presentation of insulin. II. Evidence for intracellular, plasma membrane-associated and extracellular degradation of human insulin by antigen-presenting B cells. J. Immunol. *142*, 4184-4193.

Serwold,T., Gonzalez,F., Kim,J., Jacob,R., and Shastri,N. (2002). ERAAP customizes peptides for MHC class I molecules in the endoplasmic reticulum. Nature *419*, 480-483.

Seta,K.A. and Roth,R.A. (1997). Overexpression of insulin degrading enzyme: cellular localization and effects on insulin signaling. Biochem. Biophys. Res. Commun. *231*, 167-171.

Sette,A., Lamont,A., Buus,S., Colon,S.M., Miles,C., and Grey,H.M. (1989). Effect of conformational propensity of peptide antigens in their interaction with MHC class II molecules. Failure to document the importance of regular secondary structures. J. Immunol. *143*, 1268-1273.

Sette,A., Vitiello,A., Reherman,B., Fowler,P., Nayersina,R., Kast,W.M., Melief,C.J., Oseroff,C., Yuan,L., Ruppert,J., Sidney,J., del Guercio,M.F., Southwood,S., Kubo,R.T., Chesnut,R.W., Grey,H.M., and Chisari,F.V. (1994). The relationship between class I binding affinity and immunogenicity of potential cytotoxic T cell epitopes. J. Immunol. *153*, 5586-5592.

Shi,G.P., Webb,A.C., Foster,K.E., Knoll,J.H., Lemere,C.A., Munger,J.S., and Chapman,H.A. (1994). Human cathepsin S: chromosomal localization, gene structure, and tissue distribution. J. Biol. Chem. *269*, 11530-11536.

Silva,C.L., Portaro,F.C., Bonato,V.L., de Camargo,A.C., and Ferro,E.S. (1999). Thimet oligopeptidase (EC 3.4.24.15), a novel protein on the route of MHC class I antigen presentation. Biochem. Biophys. Res. Commun. *255*, 591-595.

Silver,M.L., Parker,K.C., and Wiley,D.C. (1991). Reconstitution by MHC-restricted peptides of HLA-A2 heavy chain with beta 2-microglobulin, in vitro. Nature *350*, 619-622.

Slansky,J.E., Rattis,F.M., Boyd,L.F., Fahmy,T., Jaffee,E.M., Schneck,J.P., Margulies,D.H., and Pardoll,D.M. (2000). Enhanced antigen-specific antitumor immunity with altered peptide ligands that stabilize the MHC-peptide-TCR complex. Immunity. *13*, 529-538.

Slingluff,C.L., Jr., Engelhard,V.H., and Ferrone,S. (2006). Peptide and dendritic cell vaccines. Clin. Cancer Res. *12*, 2342s-2345s.

Smith,C.K., Baker,T.A., and Sauer,R.T. (1999). Lon and Clp family proteases and chaperones share homologous substrate-recognition domains. Proc. Natl. Acad. Sci. U. S. A *96*, 6678-6682.

Spee,P. and Neefjes,J. (1997). TAP-translocated peptides specifically bind proteins in the endoplasmic reticulum, including gp96, protein disulfide isomerase and calreticulin. Eur. J. Immunol. *27*, 2441-2449.

Srivastava,P. (2002a). Interaction of heat shock proteins with peptides and antigen presenting cells: chaperoning of the innate and adaptive immune responses. Annu. Rev. Immunol. *20*, 395-425.

Srivastava,P. (2002b). Roles of heat-shock proteins in innate and adaptive immunity. Nat. Rev. Immunol. *2*, 185-194.

Stoltze,L., Dick,T.P., Deeg,M., Pommerl,B., Rammensee,H.G., and Schild,H. (1998). Generation of the vesicular stomatitis virus nucleoprotein cytotoxic T lymphocyte epitope requires proteasome-dependent and -independent proteolytic activities. Eur. J. Immunol. *28*, 4029-4036.

Stoltze,L., Schirle,M., Schwarz,G., Schroter,C., Thompson,M.W., Hersh,L.B., Kalbacher,H., Stevanovic,S., Rammensee,H.G., and Schild,H. (2000). Two new proteases in the MHC class I processing pathway. Nat. Immunol. *1*, 413-418.

Stoppelli,M.P., Garcia,J.V., Decker,S.J., and Rosner,M.R. (1988). Developmental regulation of an insulin-degrading enzyme from Drosophila melanogaster. Proc. Natl. Acad. Sci. U. S. A *85*, 3469-3473.

Sudoh,S., Frosch,M.P., and Wolf,B.A. (2002). Differential effects of proteases involved in intracellular degradation of amyloid beta-protein between detergent-soluble and -insoluble pools in CHO-695 cells. Biochemistry *41*, 1091-1099.

Tenzer, S. (2004). The cleavage specificity of the 20S proteasome: from in vitro analysis to in silico modelling. Ref. type: Doctoral thesis.

Trowsdale,J., Hanson,I., Mockridge,I., Beck,S., Townsend,A., and Kelly,A. (1990). Sequences encoded in the class II region of the MHC related to the 'ABC' superfamily of transporters. Nature *348*, 741-744.

Tsilibaris,V., Maenhaut-Michel,G., and Van Melderen,L. (2006). Biological roles of the Lon ATP-dependent protease. Research in Microbiology.

Turner,G.C. and Varshavsky,A. (2000). Detecting and measuring cotranslational protein degradation in vivo. Science *289*, 2117-2120.

Tynan,F.E., Reid,H.H., Kjer-Nielsen,L., Miles,J.J., Wilce,M.C., Kostenko,L., Borg,N.A., Williamson,N.A., Beddoe,T., Purcell,A.W., Burrows,S.R., McCluskey,J., and Rossjohn,J. (2007). A T cell receptor flattens a bulged antigenic peptide presented by a major histocompatibility complex class I molecule. Nat. Immunol. *8*, 268-276.

Uebel,S., Kraas,W., Kienle,S., Wiesmuller,K.H., Jung,G., and Tampe,R. (1997). Recognition principle of the TAP transporter disclosed by combinatorial peptide libraries. Proc. Natl. Acad. Sci. U. S. A *94*, 8976-8981.

Uebel,S., Meyer,T.H., Kraas,W., Kienle,S., Jung,G., Wiesmuller,K.H., and Tampe,R. (1995). Requirements for peptide binding to the human transporter associated with antigen processing revealed by peptide scans and complex peptide libraries. J. Biol. Chem. *270*, 18512-18516.

Uebel,S. and Tampe,R. (1999). Specificity of the proteasome and the TAP transporter. Curr. Opin. Immunol. *11*, 203-208.

Ustrell,V., Hoffman,L., Pratt,G., and Rechsteiner,M. (2002). PA200, a nuclear proteasome activator involved in DNA repair. EMBO J. *21*, 3516-3525.

van Endert,P.M., Tampe,R., Meyer,T.H., Tisch,R., Bach,J.F., and McDevitt,H.O. (1994). A sequential model for peptide binding and transport by the transporters associated with antigen processing. Immunity. *1*, 491-500.

Van,M.L., Thi,M.H., Lecchi,P., Gottesman,S., Couturier,M., and Maurizi,M.R. (1996). ATP-dependent degradation of CcdA by Lon protease. Effects of secondary structure and heterologous subunit interactions. J. Biol. Chem. *271*, 27730-27738.

Vekrellis,K., Ye,Z., Qiu,W.Q., Walsh,D., Hartley,D., Chesneau,V., Rosner,M.R., and Selkoe,D.J. (2000). Neurons regulate extracellular levels of amyloid beta-protein via proteolysis by insulin-degrading enzyme. J. Neurosci. *20*, 1657-1665.

Velarde,G., Ford,R.C., Rosenberg,M.F., and Powis,S.J. (2001). Three-dimensional structure of transporter associated with antigen processing (TAP) obtained by single Particle image analysis. J. Biol. Chem. *276*, 46054-46063.

Verma,R., Chen,S., Feldman,R., Schieltz,D., Yates,J., Dohmen,J., and Deshaies,R.J. (2000). Proteasomal proteomics: identification of nucleotide-sensitive proteasome-interacting proteins by mass spectrometric analysis of affinity-purified proteasomes. Mol. Biol. Cell *11*, 3425-3439.

Vinitsky,A., Cardozo,C., Sepp-Lorenzino,L., Michaud,C., and Orlowski,M. (1994). Inhibition of the proteolytic activity of the multicatalytic proteinase complex (proteasome) by substrate-related peptidyl aldehydes. J. Biol. Chem. *269*, 29860-29866.

Voges,D., Zwickl,P., and Baumeister,W. (1999). The 26S proteasome: a molecular machine designed for controlled proteolysis. Annu. Rev. Biochem. *68*, 1015-1068.

Wang,E.W., Kessler,B.M., Borodovsky,A., Cravatt,B.F., Bogyo,M., Ploegh,H.L., and Glas,R. (2000). Integration of the ubiquitin-proteasome pathway with a cytosolic oligopeptidase activity. Proc. Natl. Acad. Sci. U. S. A *97*, 9990-9995.

Wang,X., Chen,C.-F., Baker,P.R., Chen,P., Kaiser,P., and Huang,L. (2006). Mass Spectrometric Characterization of the Affinity-Purified Human 26S Proteasome Complex. American Chemical Society.

Warburton,M.J. and Bernardini,F. (2002). Tripeptidyl peptidase-I is essential for the degradation of sulphated cholecystokinin-8 (CCK-8S) by mouse brain lysosomes. Neurosci. Lett. *331*, 99-102.

Watts,C. (2004). The exogenous pathway for antigen presentation on major histocompatibility complex class II and CD1 molecules. Nat. Immunol. *5*, 685-692.

Webb,A.I., Dunstone,M.A., Williamson,N.A., Price,J.D., de,K.A., Chen,W., Oakley,A., Perlmutter,P., McCluskey,J., Aguilar,M.I., Rossjohn,J., and Purcell,A.W. (2005). T cell determinants incorporating beta-amino acid residues are protease resistant and remain immunogenic in vivo. J. Immunol. *175*, 3810-3818.

Werner,E.D., Brodsky,J.L., and McCracken,A.A. (1996). Proteasome-dependent endoplasmic reticulum-associated protein degradation: an unconventional route to a familiar fate. Proc. Natl. Acad. Sci. U. S. A *93*, 13797-13801.

Wherry,E.J., Golovina,T.N., Morrison,S.E., Sinnathamby,G., McElhaugh,M.J., Shockey,D.C., and Eisenlohr,L.C. (2006). Re-evaluating the generation of a "proteasome-independent" MHC class I-restricted CD8 T cell epitope. J. Immunol. *176*, 2249-2261.

Wickner,S., Maurizi,M.R., and Gottesman,S. (1999). Posttranslational quality control: folding, refolding, and degrading proteins. Science *286*, 1888-1893.

Wilkinson,K.D., Deshpande,S., and Larsen,C.N. (1992). Comparisons of neuronal (PGP 9.5) and non-neuronal ubiquitin C-terminal hydrolases. Biochem. Soc. Trans. *20*, 631-637.

Williams,A.P., Peh,C.A., Purcell,A.W., McCluskey,J., and Elliott,T. (2002). Optimization of the MHC class I peptide cargo is dependent on tapasin. Immunity. *16*, 509-520.

Yewdell,J.W. (2005). The seven dirty little secrets of major histocompatibility complex class I antigen processing. Immunol. Rev. *207*, 8-18.

Yewdell,J.W. and Bennink,J.R. (1999). Immunodominance in major histocompatibility complex class I-restricted T lymphocyte responses. Annu. Rev. Immunol. *17*, 51-88.

Yewdell,J.W. and Princiotta,M.F. (2004). Proteasomes get by with lots of help from their friends. Immunity. *20*, 362-363.

Yewdell,J.W., Reits,E., and Neefjes,J. (2003). Making sense of mass destruction: quantitating MHC class I antigen presentation. Nat. Rev. Immunol. *3*, 952-961.

York,I.A., Chang,S.C., Saric,T., Keys,J.A., Favreau,J.M., Goldberg,A.L., and Rock,K.L. (2002). The ER aminopeptidase ERAP1 enhances or limits antigen presentation by trimming epitopes to 8-9 residues. Nat. Immunol. *3*, 1177-1184.

York,I.A., Mo,A.X., Lemerise,K., Zeng,W., Shen,Y., Abraham,C.R., Saric,T., Goldberg,A.L., and Rock,K.L. (2003). The cytosolic endopeptidase, thimet oligopeptidase, destroys antigenic peptides and limits the extent of MHC class I antigen presentation. Immunity. *18*, 429-440.

York,I.A. and Rock,K.L. (1996). Antigen processing and presentation by the class I major histocompatibility complex. Annu. Rev. Immunol. *14*, 369-396.

Young,P., Deveraux,Q., Beal,R.E., Pickart,C.M., and Rechsteiner,M. (1998). Characterization of two polyubiquitin binding sites in the 26 S protease subunit 5a. J. Biol. Chem. *273*, 5461-5467.

Zarling,A.L., Luckey,C.J., Marto,J.A., White,F.M., Brame,C.J., Evans,A.M., Lehner,P.J., Cresswell,P., Shabanowitz,J., Hunt,D.F., and Engelhard,V.H. (2003). Tapasin is a facilitator, not an editor, of class I MHC peptide binding. J. Immunol. *171*, 5287-5295.

Zhang,G.L., Bozic,I., Kwoh,C.K., August,J.T., and Brusic,V. (2007). Prediction of supertype-specific HLA class I binding peptides using support vector machines. J. Immunol. Methods *320*, 143-154.

7 Abbreviations

aa	amino acid
AAA	ATPases associated with different cellular activities
ABC	ATP-binding Cassette
AcN	Acetonitril
AEP	Legumain or asparagin endopeptidase
AMC	7-Aminomethylcoumarin
Amp	Ampicillin
APC	Antigen Presenting Cell
ATP	Adenosin Triphosphat
BH	Bleomycin Hydrolase
BSA	Rinderserumalbumin
Butab	Butabindide oxalate
Epox	Epoxomicin
C-	Carboxy-
Cpp-AAF-pAb	N-[(RS)-1-Carboxy-3-phenyl-propyl]-Ala-Ala-Phe-4-Abz-OH
CLIP	class II–associated Ii-derived peptide ()
CMK	Chloromethylketon
CMV	Cytomegalovirus
CTL	Cytotoxic T Lymphocyte
Da	Dalton
DEAE	Diethylaminoethyl-
DEPC	Diethylpyrocarbonate
DMEM	Dulbecco´s Modified Eagles Medium
DMSO	Dimethylsulfoxid
DNA	Desoxy-Ribonucleic Acid
dNTPs	2`-Desoxynucleosid-5`-Triphosphate
DRiPs	defective ribosomal products
DTT	Dithiothreitol
EDTA	Ethylendiamintetraactetat
EF1a	Elongation Factor 1-alpha
EGFP	Enhanced Green Fluorescence Protein
ER	ER associated Degradation

ERAP1	ER aminopeptidase 1
ERAP2	ER aminopeptidase 2
FACS	Fluorescence Activated Cell Scanning/Sorting
FCS	Fetal Calf Serum
FRT	Flip Recombinase Target
FSC	Forward Scatter
HC	MHC class I heavy chain
HEPES	4-(2-hydroxyethyl)-1-piperazineethanesulfonic acid
HIV	Human Immunodeficiency Virus
HLA	Human Leukocyte Antigen
HPLC	High Performance Liquid Chromatography
Hyg	Hygromycin
IFN	Interferon
IRES	Internal Ribosome Entry Site
LAP	Leucin Aminopepdidase
LB	Luria Broth
LC	Lactacystin
LMP	Low Molecular Weight Protein
mAb	Monoclonal Antibody
MIIC	Endosomal compartment for MHC class II molecules peptide loading
MCS	Multiple Cloning Site
MHC	Major Histocompatibility Complex
MØ	Monocytes
mRNA	messenger-RNA
MW	Molecular weight
N-	Amino
pA	Polyadenylierungssignalsequenz
PAGE	Polyacrylamid-Gelelektrophorese
PAProC	Prediction Algorithm for Proteasomal Cleavages
PBS	Phosphat-buffered Saline
PCR	Polymerase Chain Reaktion
PDI	Protein Disulfide Isomerase
PLC	Peptide loading complex
PSA	Puromycin sensitive Aminopeptidase

RFU	Real Fluorescence Units
RT	Room temperature
SC	Scramble Control
SDS	Sodium Dodecyl Sulphate, Natriumlaurylsulfate
siRNA	small inhibitory RNA
SSC	Sideward Scatter
suc	Succinyl-
TAP	Transporter Associated with Antigen Presentation
TEMED	Tetramethylethylenediamine
TCR	T-cell Receptor
TFA	Trifluoressigsäure
TOF	Time of Flight
ThOP1	Thimet Oligopeptidase (also, TOP)
TPPII	Tripeptidyl Peptidase II
Ub	Ubiquitine
UV	Ultraviolett